GUIDED ACOUSTIC WAVE'S PHASE AND GROUP VELOCITY AT LOW FREQUENCIES IN FLUID FILLED ELASTIC PIPES

Ignacio David López Miguel

Supervisor: Sebastian Wöckel

Magdeburg 2015

Bachelor's Thesis

ifak - Institut für Automation und Kommunikation e.V. Magdeburg

Department of Measurement Technology and Power Electronics

To Ita

Dedicado a la Ita

Acknowledgement

Do you ever dream, Forrest, about who you're gonna be?
Who I'm gonna be?
Yeah.
Aren't I going to be me?

Forrest Gump, 1994

I take this quote from my favorite film Forrest Gump so as to thank all the people who supported me from the very first moment of my life, they always loved me the way I am and never tried to change me in a different person. Thank you specially to my family, who laid down the step stones on my path during all my life. Thank you to all my friends, who were always there for me in both the good and bad moments. Thank you to the people who let me do this thesis in Ifak since it has been a remarkable experience.

Agradecimientos

Forrest, ¿alguna vez sueñas con quién vas a ser?
¿Quién voy a ser?
Sí.
¿Es que no voy a ser yo?

Forrest Gump, 1994

Tomo esta cita de mi película favorita Forrest Gump para dar las gracias a todas las personas que me han apoyado desde el primer momento de mi vida, que siempre me han querido tal y como soy y que nunca han intentado convertirme en otra persona. Le doy las gracias especialmente a mi familia, quienes fueron dejando las piedras sobre las que pisar para que fuese siguiendo un buen camino durante toda mi vida. Le doy las gracias también a mis amigos, quienes siempre han estado ahí tanto en los momentos buenos como en los malos. También quiero dar las gracias a las personas que me permitieron realizar este proyecto en Ifak, ya que ha sido una experiencia muy gratificante.

Abstract

The industrial process monitoring with acoustic waves is a common and interesting technique especially when a non-invasive clamp-on configuration (by mounting the sensor on the outer surface of a pipe wall) can be realised, because of its non-destructive nature and easy handling. Since a pipe is a closed system no free bulk wave can be assumed and the vessel acts as a complex waveguide. For "low" frequencies the propagation of an acoustic wave within a simple cylindrical pipe depends on the mechanical impedance or elasticity of the boundary (pipe wall) and the particular filling medium. For "higher" frequencies the pipe acts as a waveguide and additional wave modes will occur depending on the measurement frequencyand its geometry.

The tasks of the current thesis are the investigation and empirical verification of the dependency of the sound velocity within the filling fluid – at low frequencies – due to the elastic properties of the pipe wall, the pipes diameter and the bending of the pipe (axial curvilinear shape). The labels "low" and "high" are related to the acoustic cut off frequency f_g (first radial frequency) of the guided waves.

In particular, a feasibility study has to be made to validate the measurability of the guided wave velocities inside the pipe by using a sound source (exciters) placed on the outer pipe wall.

Tasks:

- Literature overview on guided acoustic wave propagation in water filled elastic pipes
- Theoretical description of free and guided acoustic waves
- Understanding for dispersion diagram
- 3D-FEM-Simulation model of water filled elastic pipes
- Parameter study
    o measurement of phase velocities within the pipe by using different sensor points (at least 2) with variable number, spacing in between and to the source
    o influence of pipes diameter and frequency
    o influence of bending and arbitrary pipes shape (phase velocity in front and behind a bending of the pipe)
- Empirical validation of results with a plastic pipe in laboratory

Keywords

Waveguide, elastic pipe, bent pipe, straight pipe, acoustic, sound propagation, phase velocity, group velocity, FEM simulation, measurement

Abstracto

El proceso industrial de monitorización con ondas acústicas es una técnica común e interesante especialmente cuando una configuración no invasiva con abrazaderas montando el sensor en la superficie exterior del tubo puede ser realizada, ya que tiene una naturaleza no destructiva y de fácil manejo. Como un tubo es un sistema cerrado, no se puede asumir una onda de masa libre y el recipiente actúa como una compleja guía de ondas. Para frecuencias bajas, la propagación de una onda acústica dentro de un tubo cilíndrico simple depende de la impedancia mecánica o elasticidad de los límites (pared del tubo) y del medio con el que se haya llenado el mismo. Para frecuencias altas, la tubería actúa como una guía de ondas y otros modos de onda pueden aparecer dependiendo de la frecuencia de medición y de su geometría.

El propósito de este trabajo será la investigación de la dependencia de la velocidad del sonido dentro de una tubería llena con un fluido con el susodicho fluido con el que es llenada a bajas frecuencias y su correspondiente verificación empírica, debido a las propiedades elásticas de la pared de la tubería, el diámetro de la tubería y la curva de la misma (curvilínea axial). Los nombres de baja y alta frecuencia están relacionados con la frecuencia de corte f_g (primera frecuencia radial) de las guías de ondas.

En particular, un estudio de factibilidad será hecho para validar la mensurabilidad de las velocidades en las guías de ondas dentro de tuberías a través de usar fuentes de sonido (excitador) colocadas en la superficie exterior de la pared de la tubería.

Tareas:

- Visión general de la literatura de propagación de ondas acústicas guiadas en tuberías elásticas llenadas con agua
- Descripción teórica de ondas acústicas libres y guiadas
- Entendimiento de los diagramas de dispersión
- Simulación 3D con el método de elementos finitos para modelos de tuberías elásticas llenas con agua
- Estudio paramétrico
    o Medición de las velocidades de fase dentro de tuberías usando diferentes sensores colocados en diferentes posiciones
    o Influencia del diámetro de la tubería y frecuencia de excitación
    o Influencia del cambio de forma de la tubería (velocidad de fase antes y después de la curva)
- Validación empírica de los resultados con una tubería de plástico en el laboratorio

Palabras clave

Guía de onda, tubería elástica, tubería doblada, tubería recta, propagación del sonido, velocidad de fase, velocidad de grupo, simulación de elementos finitos, medición

Table of Contents

List of Figures

List of Tables

List of Symbols and Abbreviations

A	Normalized amplitude
$\boldsymbol{c}$	Speed of sound in the propagation material
$\mathbb{C}$	Complex numbers set
Ch.	Chapter
Eq.	Equation
$\mathcal{F}$	Fourier transform
FFT	Fast Fourier transform
FEM	Finite element method
$\boldsymbol{k}$	Wave vector
k	Wave number
$\mathcal{H}$	Hilbert transform
Hz	Hertz
I_{ref}	Reference sound intensity value of $1 \cdot 10^{-12} W$
I_{rms}	Root-mean square sound intensity
J_n	Bessel function of order n
L_I	Sound intensity
L_p	Sound pressure level
L_u	Particle velocity
m	Meter
n	Refraction index
p	Acoustic pressure
Pa	Pascal
p_{ref}	Reference pressure value of $2 \cdot 10^{-5} Pa$
p_{rms}	Root-mean square pressure
PVC	Polyvinyl chloride
r	Distance to the transmitter center of the wave
$\mathbb{R}$	Real numbers set
$\mathbb{R}^+$	Positive real numbers set
s	Second
$š$	Hilbert transform of the signal s(t)
t	Time
T	Period
$\boldsymbol{u}$	Flow velocity vector
u_{ref}	Reference particle value of $5 \cdot 10^{-8} m/s$
u_{rms}	Root-mean square particle velocity
W	Watt
v_g	Group velocity
v_p	Phase velocity
$\boldsymbol{x}$	Position vector
x	X direction
$\mathbb{Z}$	Integer numbers set
Δp	Pressure variation
θ_i	Incident angle
θ_r	Reflection angle
K	Bulk modulus of the medium
λ	Wavelength

ν Frequency

ρ Density of the fluid

ρ_0 Statistic mass density of the medium

φ Phase of the wave

ω Angular frequency

$\propto$ Proportional

$\in$ Element of

1. Introduction

The use of sounds have been increased over the last few years for different fields, such as medical imaging, detection, and cleaning. It could be said that the most extended application within this field could be the bidimensional-scan of fetus in the womb. Besides, sounds are also used in the measurement technology field for measuring distances, speeds, or vibration frequencies. A really known example in this last field is the use of ultrasounds by bats, which are used in order to navigate in the darkness. [1] [2] [3]

What is different of sound use in measurement technology is that it is possible to measure the aspects we are interested in or to perform a test in a noninvasive way. Normal sensors need to be in touch with the material or the machine that is to be measured, whereas sound sensors just need to be installed outside the material or really close to it, but not in contact with it. This is a really big advantage since the lifetime of the sensor can be longer due to the absence of contact, and the efficiency of the machine that is working does not decrease due to the set of sensors.

Sound could be defined as an oscillating pressure wave with a specific frequency that propagates inside a material, such as water, plastic, or air. It is always necessary to have a material in which the wave can be propagated. [4]

Depending on the frequency of the pressure wave, the sound can be classified as infrasound (lower than what a human hear can detect, lower than about 20Hz), ultrasound (higher than what a human can perceive, higher than about 20kHz), and acoustic (what a human can hear, between 20Hz and 20kHz). A small diagram of this classification can be seen in Image 1.1. [5]
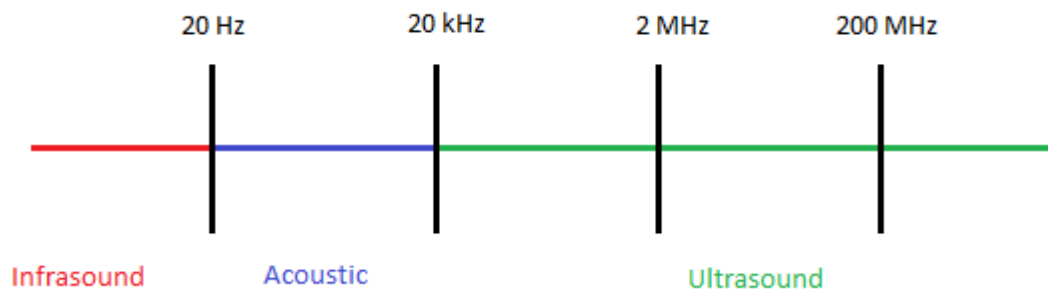
Image 1.1: Classification of sound depending on its frequency.

Ultrasound is the more used sound for technical applications because humans cannot hear it, since it has a frequency higher than the upper limit of the human hearing range, which is approximately 20kHz.

Sound can be propagated in a free way or within a waveguide and the characteristics of its propagation depend on how it does it. In the current thesis the propagation of acoustic waves of low frequencies within a simple cylindrical pipe is going to be investigated. The way it is propagated depends on the characteristics of the pipe and the filling medium, which, in this thesis, will be water.

1.1. Road Map of Thesis

The first thing that is going to be done in this thesis is to give a short explanation of the main theoretical qualitative and mathematical aspects of free acoustics, Ch. 2. , and its most important phenomena that can affect to measurements of pressure waves, Section 2.1.3. After this, a theoretical introduction to waveguides filled with fluid is going to be done in Ch. 3. Besides, there is a short explanation about dispersion diagrams because they will be used in the thesis to represent the phase and group velocities.

The goal of these first two chapters containing theoretical introduction to acoustics is to have a small understanding of how waves are propagated within pipes and so as to be able to interpret the results that will be given later on by measurements. During this theoretical introduction, many references to different authors are given so that the reader can go deeper in this topic if it is wanted. However, in this thesis only the main aspects are presented as an introduction since the main goal of this thesis is not doing an overview of literature concerning acoustics and waveguides, but measuring group and phase velocities.

Therefore, in order to understand what group and phase velocities are, in Ch. 4. a qualitative and mathematical explanation of these concepts is explained. Also, the mathematical concepts are supported with examples so that the reader can better understand them. These examples are given after the theoretical explanation as it is not an easy task to find examples of calculating these velocities in neither on the Internet nor in books. With this chapter concerning group and phase velocities it is wanted to create a guide for future readers who want to know and calculate these velocities in both dispersive and non-dispersive mediums.

At this point, it is possible to start presenting different methods of measuring group and phase velocities, since the theoretical background has been already explained. Thus, in Ch. 5. , a list of different methods to measure these velocities and its mathematical background are discussed, explaining which ones are suitable for which situations. As the signals which are acquired by hydrophones normally have noise, a list of different methods to reduce this noise and how to use them is presented in the sections 5.6. and 5.7.

Now, everything is ready to start simulating a PVC water-filled pipe in order to measure the group and phase velocity at low frequencies. For this reason, a FEM simulation of a straight pipe is performed in 6.1. This simulation is done to have a first overview of how to work with a real system and to compare the results given by simulation to the ones that will be obtained in the laboratory. If both results are similar, it will be possible to say that the simulation was done properly and it can be extended to different kinds of pipes. Therefore, after doing the simulation with a straight pipe of a specific diameter, different properties of it are changed, such as the frequency, the length and the shape. The different shape that is going to be simulated is a pipe with a bending of 90º in the middle of it, section 6.2. This simulation will be also compared with a real PVC water-filled in the laboratory.

In Ch. 7. , an empirical validation in the laboratory with a PVC water-filled pipe of the results obtained in the simulations is done. Besides, in this chapter, different tests and different methods of performing are presented to measure velocities within the pipe for both a straight pipe and a bent pipe. The problems of measuring velocities with different methods is presented and, in the end of every experiment, it is possible to see which method has been chosen in order to calculate properly

the desired velocities avoiding reflections and other issues. These measurements are also explained with MATLAB scripts as an example of how to work with the obtained data by the hydrophones.

In the end, after comparing the simulations and results obtained in the laboratory, there is a comparison among them in order to decide whether the experiments and the simulations have been carried on properly. Finally, in Ch. 8. there is a global conclusion concerning the work done in this thesis and presenting questions and some research lines for further research.

2. Main aspects of free acoustic waves

An acoustic wave is a longitudinal wave which is associated with a sound. If it is propagated in an elastic and continuous medium, it produces a local deviation on the pressure and density, which is transmitted as a spherical periodic or quasi-periodic wave. Mechanically, sound waves are a kind of elastic wave. [6]

Variations of pressure, humidity or medium temperature produce a displacement of the molecules which form it. Every molecule transmits the vibration to the ones that are close to it, producing a chain move.

2.1. Wave propagation

2.1.1 Propagation mode

The sound is formed by longitudinal elastic mechanical waves or compression waves in a medium. Therefore, it means that: [7] [8]

- In order to propagate, they need a material medium, such as air, water, or a solid body, that transmits the perturbation. It travels faster in solids than in liquids, and faster in liquids than in air. Sound waves cannot be propagated in vacuum. The medium is the one which produces and propitiate the wave propagation with its compression and expansion. The medium needs to be elastic so as to compress and expand, since a rigid body does not allow vibration to propagate. Therefore, without elastic mediums, sound would not exist, as it does not propagate in vacuum.
- Besides, fluids can also transmit undulatory moves in which the particle vibration is given in the parallel direction to the propagation velocity along the propagation direction. Thus, the pressure gradients of the sound wave propagation are produced in the same direction of the propagation wave. Therefore, this waves are a kind of longitudinal waves (in solids, transversal waves can be also propagated).

2.1.2 Propagation in mediums

An acoustic wave needs a medium in which it can be propagated, such as air, water, etc. The propagation of sound waves can be modeled by an equation of continuity (conservation of mass) and an equation of motion (conservation of momentum). These two equations can be given as follows: [9]

$$\frac{\partial p}{\partial t}(\boldsymbol{x}, t) + \mathrm{K}\nabla \cdot \boldsymbol{u}(\boldsymbol{x}, t) = \mathbf{0}$$

Eq. 2.1

$$\rho_0 \frac{\partial \boldsymbol{u}}{\partial t}(\boldsymbol{x}, t) + \nabla p(\boldsymbol{x}, t) = \mathbf{0}$$

Eq. 2.2

Where Eq. 2.1 is the mass balance and Eq. 2.2 is the momentum balance. $p(x,t)$ is the acoustic pressure, $u(x,t)$ is the flow velocity vector, which gives the velocity of an element of a fluid at a position $x = (x, y, z)$ and time t, K is the bulk modulus of the medium, and ρ_0 is the statistic mass density of the medium.

Richard Feynman derives the wave equation that describes the behavior of sound in matter in one dimension as [10]:

$$\frac{\partial^2 p}{\partial x^2} - \frac{1}{c^2}\frac{\partial^2 p}{\partial t^2} = 0,$$

<div align="right">**Eq. 2.3**</div>

Where c is the speed of sound in the propagation material.

Sound waves travel in three dimensions and their wavefronts are, in isotropic mediums, concentric spheres which have their center in the perturbation focus. The pressure changes that happen in a three-dimension wave with frequency ν and wavelength λ in an isotropic medium in repose are given by the differential equation:

$$\frac{1}{r^2}\frac{\partial}{\partial r}\left(r^2 \frac{\partial p(r,t)}{\partial r}\right) - \frac{1}{c^2}\frac{\partial^2 p(r,t)}{\partial t^2} = 0$$

<div align="right">**Eq. 2.4**</div>

Where r is the distance to the transmitter center of the wave and c is the propagation wave velocity in the medium. For a wave which has its period well defined, it is verified that $c = \lambda\nu$, and in this case, the solution to the equation for distances far away from the transmitter center can be written as [11]:

$$p(r,t) = p_0 + \frac{\Delta p}{r}\sin\left(2\pi\nu t - 2\pi\frac{r}{\lambda} + \varphi_0\right)$$

<div align="right">**Eq. 2.5**</div>

Where p_0 is the initial sound pressure of the fluid and Δp is the maximum overpressure that is produced by the pass of the wave.

In the case of ordinary sound waves, they are produced by the superposition of waves of different frequency and different wavelengths, which produce a finite pulse. For these waves, the phase velocity is not the same than the group velocity or pulse propagation velocity. The phase velocity is different for every frequency and depends on the relation $c = \lambda\nu$. The general solution to Eq. 2.4 can be expressed as:

$$p(r,t) = p_0 + \frac{\Delta p}{r}\int_{\mathbb{R}^3} A(k)\sin\left(\omega t - \|k\|r\right)d^3 k$$

<div align="right">**Eq. 2.6**</div>

Where $A(k)$ is the normalized amplitude for the component k, k is the wave vector, and $\omega = c\|k\|$ is the angular frequency.

2.1.3 Phenomena

Acoustic waves exhibit phenomena like diffraction, reflection, and interference. However, they do not have polarization, as they oscillate along the same direction as they move.

2.1.3.1 Diffraction

Diffraction occurs when a propagating wave encounters an obstacle or a slit that is comparable in size to its wavelength. The sound wave is dispersed after finding this obstacle or slit. Huygens [12] explained that every point which a luminous disturbance reaches becomes a source of spherical wave and the sum of these secondary waves determines the form of the wave at any subsequent time. Besides, according to Huygens, this secondary waves travel only in the "forward" direction, which means that they do not come back. In Image 2.1 (created by Arne Nordmann, published in Wikipedia, and with license CC BY-SA 3.0) it is possible to appreciate this phenomenon, where the blue wave is the original wave, the yellow dots indicate notional origins of new waves, the gray waves are the secondary ones conforming the green wave. [13]
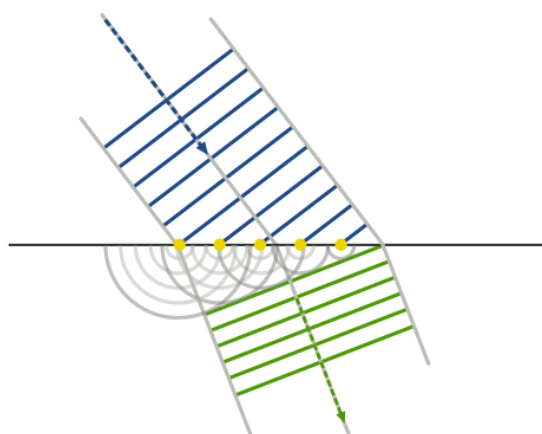
Image 2.1: Wave refraction in the manner of Huygens.
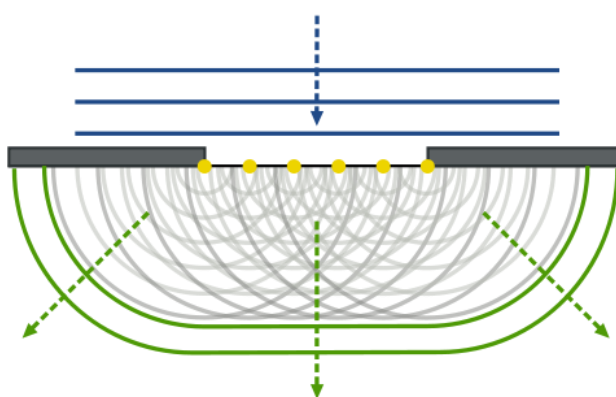
Image 2.2: Wave diffraction in the manner of Huygens and Fresnel.

As Huygens was not able to explain why these waves only travel in the "forward" direction, Fresnel [14] explained using his principle of interference and Huygens' principle this phenomenon and establishes that every point in a wavefront is susceptible of becoming a new transmitter focus like the one which generated this wavefront with a rectilinear propagation. Therefore, when a wave

finds an obstacle or an aperture that prevents its propagation, all the points that are on this plane become secondary sources of waves, transmitting new waves that are called diffracted waves. In Image 2.2 (created by Arne Nordmann, published in Wikipedia, and with license CC BY-SA 3.0) the phenomenon described by Huygens-Fresnel is shown, where the colors represent the same things than in Image 2.1.

Diffraction occurs with all waves, including sound waves, water waves, and electromagnetic waves, and can be seen as a consequence of the isotropy of space, which means that all the directions in space are equal. Isotropy of space is fundamental to quantum electrodynamics, where the wave function of any object propagates along all available unobstructed paths [15].

2.1.3.2 Reflection

Reflection is referred to the phenomenon that explains the reason why a wave is absorbed or it returns. When a wave finds an object in its way that cannot cross nor encircle, it crashes with the object and it is reflected, going back again in the direction of the main transmitting focus. If the obstacle is small in relation to its wavelength, the sound wave will surround it (diffraction), whereas if it is big, the sound wave will be reflected [16]. In Image 2.3 (created by Johan Arvelius on 26.09.2005, published in Wikipedia, and with license CC BY-SA 3.0) a diagram of a wave reflecting on a mirror (or a barrier) is displayed. It is important to notice that the angle in which the original wave incises on the mirror is the same than the angle with which it is reflected, that is to say, $\theta_i = \theta_r$. This phenomenon is going to be important in the research of this thesis because inside pipes, the sound is reflected many times and it is going to influence the obtained results.
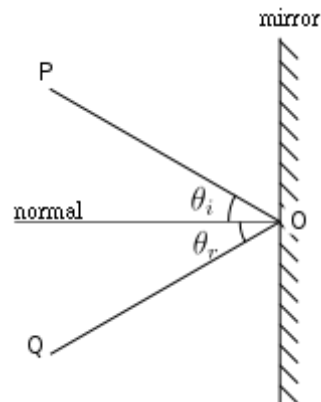
Image 2.3: Diagram of a wave reflecting.

2.1.3.3 Refraction

Refraction is the change in direction of propagation of a wave due to a change in its transmission medium. This phenomenon was explained by Ibn Sahl [17] and later Willebroad Snellius (1580–1626) stated his law saying that the ratio of the sine of the angles of incidence and refraction is equivalent to the ratio of phase velocities in the two media, or equivalent to the reciprocal of the ratio of the indices of refraction:

$$\frac{sin\theta_1}{sin\theta_2} = \frac{v_{p1}}{v_{p2}} = \frac{n_2}{n_1}$$

Eq. 2.7

where θ is the angle measured from the normal of the boundary, v_p is the phase velocity, and n is the refractive index, respectively in each medium. When the incident waves reaches a critical angle, there is no refracted wave and there is only reflected wave. In Image 2.4 (created by Josell7 on 21.09.2012, published in Wikipedia, and with license CC BY-SA 3.0) it is possible to see a diagram of this phenomenon with different incident angles.
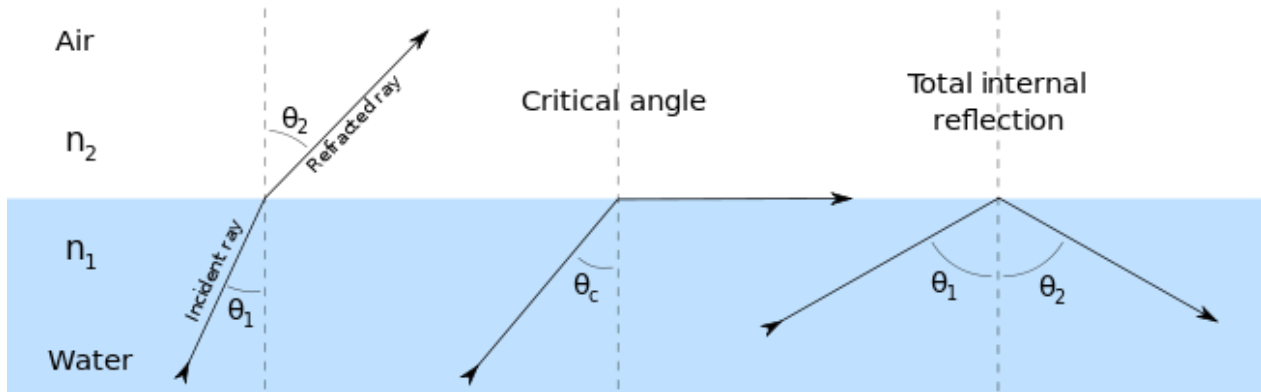
Image 2.4: Optical reflection: critical angle and total internal reflection.

2.2. Measurement

Sound pressure can be measured using a microphone, which converts air pressure variations into electrical signals.

It is not the same the sound pressure, the particle velocity and the sound intensity. The quantities are normally measured as a level in decibels relative to a certain quantity.

The sound pressure level is normally given by:

$$L_p = 10 \cdot \log_{10}\left(\frac{p_{rms}^2}{p_{ref}^2}\right) = 20 \cdot \log_{10}\left(\frac{p_{rms}}{p_{ref}}\right),$$

Eq. 2.8

Where p_{rms} is the root-mean square pressure in Pa and p_{ref} is the reference pressure value of $2 \cdot 10^{-5} Pa$.

The particle velocity is given by:

$$L_u = 10 \cdot \log_{10}\left(\frac{u_{rms}^2}{u_{ref}^2}\right) = 20 \cdot \log_{10}\left(\frac{u_{rms}}{u_{ref}}\right),$$

Eq. 2.9

Where u_{rms} is the root-mean square particle velocity in m/s and u_{ref} is the reference particle velocity value of $5 \cdot 10^{-8} m/s$.

The sound intensity is given by:

$$L_I = 10 \cdot \log_{10}\left(\frac{I_{rms}}{I_{ref}}\right),$$

Eq. 2.10

Where I_{rms} is the root-mean square sound intensity in W and I_{ref} is the reference sound intensity value of $1 \cdot 10^{-12} W$.

3. Main aspects of guided acoustic waves in fluid-filled pipes

A waveguide is a structure that guides waves, such as electromagnetic waves or pressure waves. There are different types of waveguides for each type of wave. The one that is going to be used in the end of this work for guiding pressure waves in water is a PVC pipe.

However, it is also common to use a hollow conductive metal pipe to carry high frequency radio waves. It is becoming more popular to use optical fiber to transmit light and signals for long distances and with high signal rate.

Waves propagate in open space in every direction behaving as spherical waves. Nevertheless, when a waveguide is used, waves can only propagate within the guide and, therefore, not in every direction, but just in one.

3.1. Propagation of sound waves in cylindrical tubes

Depending on what fluid the sound is propagating, its propagation speed changes according to the following expression:

$$c_{fluid} = \sqrt{\frac{K}{\rho}},$$

Eq. 3.1

where ρ is the density of the fluid and K its bulk modulus, which is given by:

$$K = -V\frac{dP}{dV},$$

Eq. 3.2

where dP/dV denotes the derivative of pressure on density.

The approximate bulk modulus for water is $K = 2{,}2 \cdot 10^9 \, Pa$. Besides, its density is $\rho = 1000 \, kg/m^3$. Therefore, speed of sound in water is approximately:

$$c_{water} = \sqrt{\frac{2{,}2 \cdot 10^9}{1000}} = 1480 \, m/s$$

Eq. 3.3

Note that this speed change depending on the deepness (pressure), quantity of salt and other components, and temperature, since all this parameters affect to both bulk modulus and density of water.

3.2. Propagation modes

The solution of the equation for propagating waves along a tube in cylindrical coordinates is [18]:

$$u(r,\theta,z,t) = [A \cdot \sin(k_\theta\theta) + B\sin(k_\theta\theta)]J_n(k_c r)e^{i(k_z z - \omega t)}$$

$$k_c^2 = k^2 - k_z^2$$

$$\omega = k \cdot c$$

where A and B are constants, k is the wave number in each spatial direction, and J_n is the Bessel function of order n.
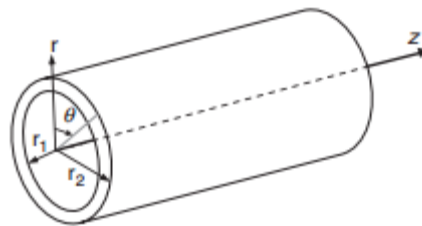
Image 3.1: Parameters of the pipe

The solution of the waveguide equation provides three types of propagation modes: longitudinal, torsional, and flexural mode. For all of these modes, it exists an infinite number of individual modes, which are distinguished by their cut-off frequency, phase velocity and attenuation. Longitudinal wave, which is displayed in Image 3.2, has a displacement in the radial, r, and axial, z, direction. Torsional mode, which can be seen in Image 3.3, however, have only a displacement in θ direction. Both modes are axially symmetric, which means that the displacement in a certain distance to the source is constant over the circumference. The flexural modes, which are shown in Image 3.4, are not axially symmetric and have a negligible displacement component in the axial direction.

A longitudinal mode group is normally expressed as $L(m,n)$, a torsional mode group as $T(m,n)$ and a flexural mode group as $F(m,n)$, where the integer m denotes the circumferential order of a mode and the integer n represents the group order of a mode. An axisymmetric mode has the circumferential number $m = 0$.
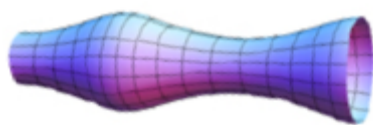
Image 3.2: Longitudinal mode
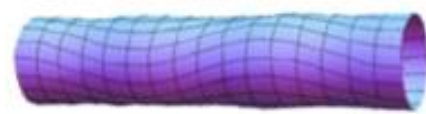
Image 3.3: Torsional mode
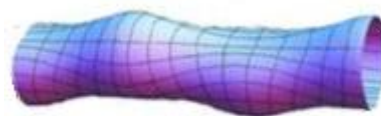
Image 3.4: Flexural mode

In Image 3.5, the phase velocity depending on the time for the different modes in a pipe filled with water and air is shown.
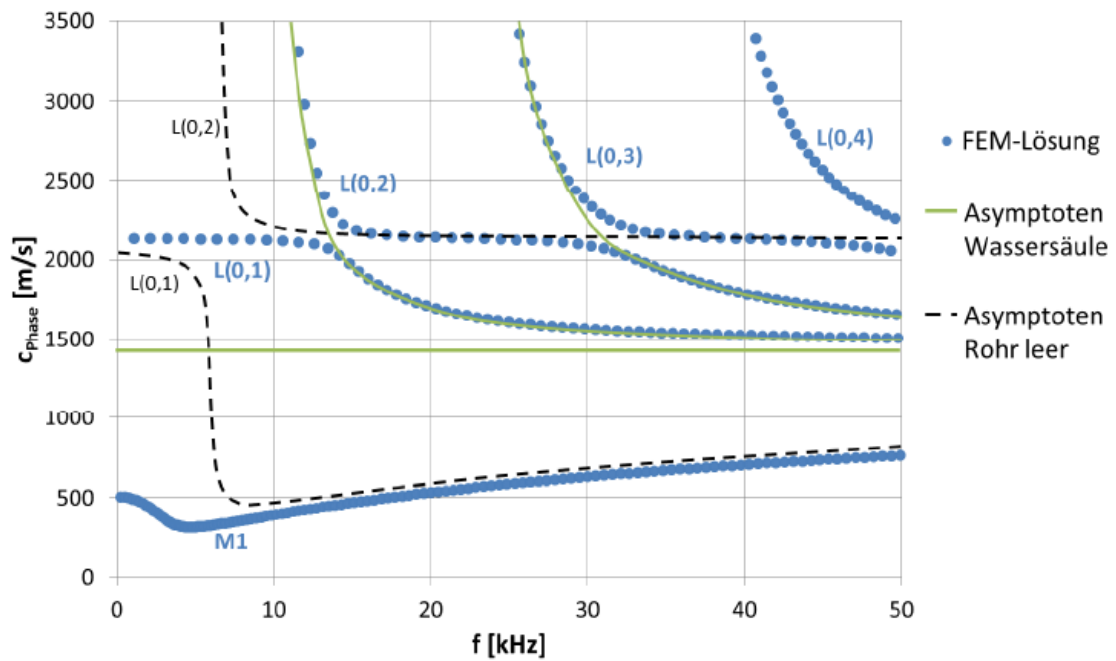
Image 3.5: Dispersion diagram for the phase velocity on frequency dependency for a pipe filled with water and air.

4. Group and phase velocities

Let us consider a wave travelling in the x direction, with constant maximum amplitude A, with constant velocity v independent of wavelength and also independent of amplitude. This wave can described by D'Alambert's formula:

$$u(x, t) = F(x - vt) + G(x + vt),$$

<div align="right">**Eq. 4.1**</div>

where F and G represent two waveforms travelling through the medium in opposite direction.

We can distinguish between continuous waves, which have constant maximum amplitude, and modulated waves, in which their amplitude vary with time and/or position.

A modulated wave can be mathematically described as follows:

$$u(x, t) = A(x, t) \cos(\omega t - kx + \varphi),$$

<div align="right">**Eq. 4.2**</div>

where

- $A(x, t)$ represents the change of the maximum amplitude depending with the position and the time, that is to say, the amplitude envelope of the wave
- k is the wave number, which is the spatial frequency of a wave, which means the number of wavelengths per unit distance or the number of cycles per wavelength
- ω is the angular velocity, which is related to the wave frequency by $\omega = 2\pi f$
- φ is the phase of the wave

There are two velocities that are associated with waves: phase velocity and group velocity.

4.1. Phase velocity

The phase velocity of a wave is the rate at which the phase of a wave propagates in space. Its value is given by the following expression:

$$v_p = \frac{\lambda}{T},$$

<div align="right">**Eq. 4.3**</div>

where λ is the wavelength and T is the period.

It can also be written in terms of the angular frequency and the wave number by:

$$v_p = \frac{\omega}{k},$$

<div align="right">**Eq. 4.4**</div>

In order to understand what phase velocity is, let us assume a continuous wave as:

$$u(x, t) = A \sin(kx - \omega t + \varphi),$$

<div align="right">**Eq. 4.5**</div>

in which the amplitude is constant and it does not depend on the timer nor the position.

Let us have two different points in the positive x direction, x_1 and x_2, with $x_2 > x_1$. Thus, the phase velocity will be defined by:

$$v_p = \frac{x_2 - x_1}{t_{21}}$$

<div align="right">**Eq. 4.6**</div>

where t_{12} is the time elapse between the time t_1 in which the size of the wave is given by $u(x_1, t_1)$ and the time t_2 in which the size of the wave is given by $u(x_2, t_2)$, taking into account that $u(x_1, t_1) = u(x_2, t_2) = u_o$.

Therefore:

$$A \cos(\omega t_1 - kx_1 + \varphi) = A \cos(\omega t_2 - kx_2 + \varphi)$$

<div align="right">**Eq. 4.7**</div>

Simplifying:

$$\cos(\omega t_1 - kx_1 + \varphi) = \cos(\omega t_2 - kx_2 + \varphi)$$

<div align="right">**Eq. 4.8**</div>

Both arguments must be the same:

$$\omega t_1 - kx_1 = \omega t_2 - kx_2$$

<div align="right">**Eq. 4.9**</div>

$$t_{12} = t_1 - t_2 = \frac{k}{\omega}(x_1 - x_2)$$

<div align="right">**Eq. 4.10**</div>

$$v_p = \frac{x_2 - x_1}{t_2 - t_1} = \frac{x_2 - x_1}{\frac{k}{\omega}(x_2 - x_1)} = \frac{\omega}{k}$$

<div align="right">**Eq. 4.11**</div>

So it is proven that it is possible to measure the phase velocity by measuring the size of the wave in two different positions.

4.1.1 Example

For instance, let us have a sinusoidal wave such as:

$$u(x, t) = \cos(10x - t + \pi)$$

<div align="right">**Eq. 4.12**</div>

In the Image 4.1 in blue it is shown the wave in $t_1 = 10$ and in red in $t_2 = 13$. Two points are selected, $x_1 = 1{,}627$ and $x_2 = 1{,}927$. In these points, the wave reaches the same size in 10 and 20, respectively. Therefore, it is possible to apply Eq. 4.6:

$$v_p = \frac{x_2 - x_1}{t_2 - t_1} = \frac{1{,}927 - 1{,}627}{13 - 10} = 0{,}1,$$

<div align="right">**Eq. 4.13**</div>

which is the same result than using Eq. 4.4:

Eq. 4.14

$$v_p = \frac{\omega}{k} = \frac{1}{10} = 0,1$$
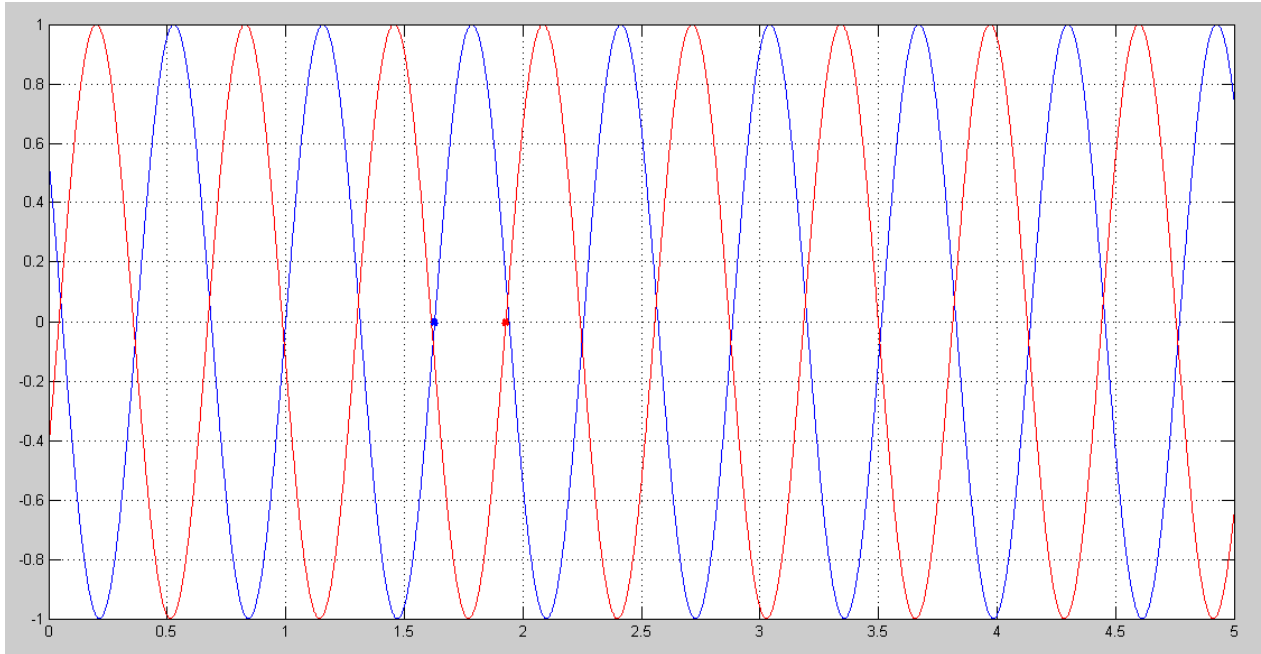
Image 4.1: Two points in the distance selected to calculate the phase velocity.
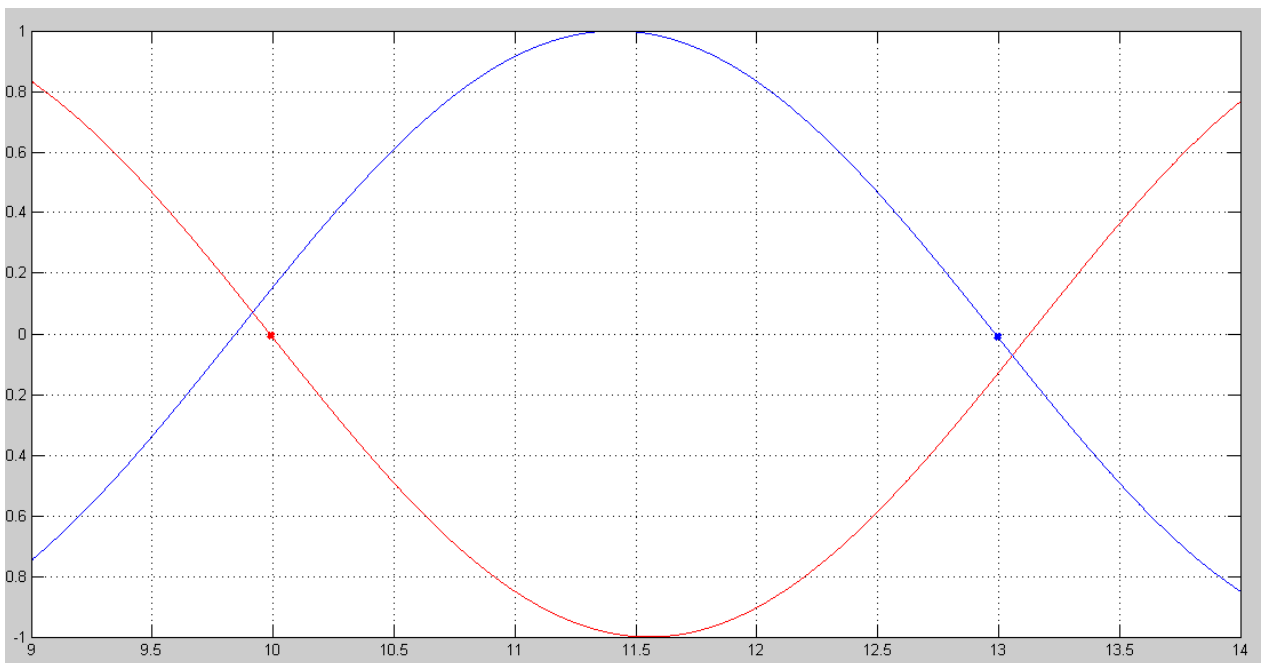
Image 4.2: Two points in the time selected to calculate the phase velocity.

So it is possible to measure the phase velocity by knowing the time elapse and measuring the distance. Furthermore, it is also possible to get the same result by knowing the distance between these two points and measuring the time elapse. This second way of performing is shown in Image

4.2 with the same wave as in Image 4.1, in red it is shown the wave in position $x_1 = 1,627$ and in blue the position $x_2 = 1,927$, in a time range from 9 to 14.

The same result as in the last performance is obtained:

$$v_p = \frac{x_2 - x_1}{t_2 - t_1} = \frac{1,927 - 1,627}{13 - 10} = 0,1 \qquad \text{Eq. 4.15}$$

Thus, it is possible to measure the phase velocity of a wave by knowing either the time elapse and measuring the distance between the two sensors, or the distance between them and measuring the time elapse.

4.2. Group velocity

The group velocity is also known as modulation or envelope of the wave, and it is the velocity which the overall shape of the waves' amplitudes propagates through space. It is defined by:

$$v_g = \frac{\partial \omega}{\partial k} \qquad \text{Eq. 4.16}$$

It is clear that if $\omega \propto k$, then the group velocity and the phase velocity would be the same, since:

$$v_g = \frac{\partial \omega}{\partial k} = \frac{\omega}{k} = v_p \qquad \text{Eq. 4.17}$$

In general, in the rest of the cases, phase velocity and group velocity will be different.

For instance, let us have two continuous waves:

$$u_1(x, t) = A_1 \cos(\omega_1 t - k_1 x + \varphi_1) \qquad \text{Eq. 4.18}$$

$$u_2(x, t) = A_2 \cos(\omega_2 t - k_2 x + \varphi_2) \qquad \text{Eq. 4.19}$$

And let us have a wave formed by the superposition of the two previous waves:

$$u(x, t) = A_1 \cos(\omega_1 t - k_1 x + \varphi_1) + A_2 \cos(\omega_2 t - k_2 x + \varphi_2) =$$

$$= A_1 \left[\cos(\omega_1 t - k_1 x + \varphi_1) + \left(1 + \frac{A_2 - A_1}{A_1} \right) \cos(\omega_2 t - k_2 x + \varphi_2) \right] = \qquad \text{Eq. 4.20}$$

$$= A_1 \left[2 \cos \frac{\omega_1 t - k_1 x + \varphi_1 + \omega_2 t - k_2 x + \varphi_2}{2} \cos \frac{\omega_1 t - k_1 x + \varphi_1 - \omega_2 t + k_2 x - \varphi_2}{2} \right.$$
$$\left. + \frac{A_2 - A_1}{A_1} \cos(\omega_2 t - k_2 x + \varphi_2) \right]$$

Let us set the following average values:

$$\omega_P = \frac{\omega_1 + \omega_2}{2}; k_P = \frac{k_1 + k_2}{2}; \omega_M = \frac{\omega_1 - \omega_2}{2}; k_M = \frac{k_1 - k_2}{2}$$

Eq. 4.21

Using the values of Eq. 4.21 in Eq. 4.20:

$$u(x,t) = A_1 \left[2 \cos(\omega_p t - k_p x + \varphi_p) \cos(\omega_m t - k_m x + \varphi_m) \right.$$
$$\left. + \frac{A_2 - A_1}{A_1} \cos(\omega_2 t - k_2 x + \varphi_2) \right]$$

Eq. 4.22

Note that if the amplitude of the two waves is the same, the result wave is:

$$u(x,t) = 2A \cos(\omega_M t - k_M x) \cos(\omega_P t - k_p x)$$

Eq. 4.23

4.2.1 Example

For instance, let us have the two following waves, which will be superposed:

$$u_1(x,t) = 2 \cos(8t - x)$$

Eq. 4.24

$$u_2(x,t) = 2 \cos\left(7{,}5t - \frac{15}{16}x\right)$$

The average values are:

$$\omega_P = 7{,}75 s^{-1}; k_P = \frac{31}{32} m^{-1}; \omega_M = 0{,}25 s^{-1}; k_M = \frac{1}{32} m^{-1}$$

Eq. 4.25

Then, the resulting wave is:

$$u(x,t) = 2 \cdot 2 \cos\left(0{,}25t - \frac{1}{32}x\right) \cos\left(7{,}75t - \frac{31}{32}x\right)$$

Eq. 4.26

It is possible to see the result of this wave depending of the time and the position by using the script of MATLAB shown in the appendix A. 1. Propagation of a wave in a non-dispersive medium.
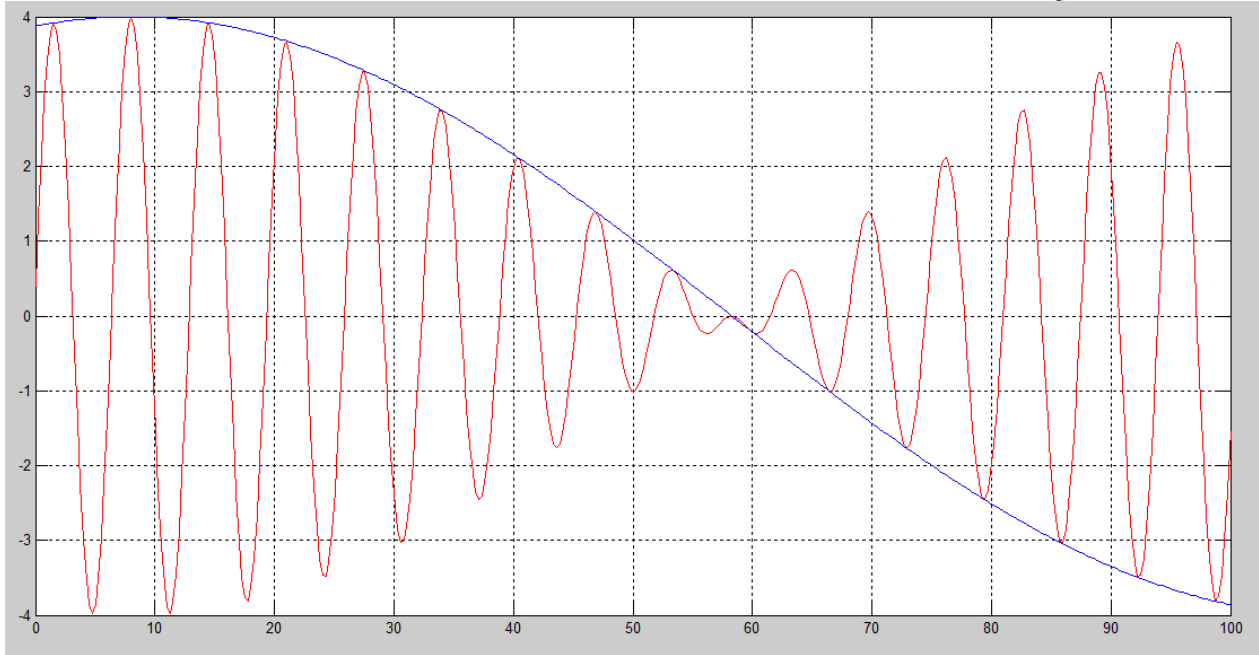
Image 4.3: Envelope wave of two waves superposed propagating in the positive x direction in a non dispersive medium.

In Image 4.3 it is possible to see the wave at $t = 1$ and in a space between 0 and 100, whose MATLAB script is also shown in appendix A. 1. Propagation of a wave in a non-dispersive medium. A envelope wave is possible to be appreciated, which is propagating in the positive x direction. The wavelength of the envelope wave is:

$$\lambda_M = \frac{2\pi}{k_M} = \frac{2\pi}{1/16} = 100{,}5 \; m$$

Eq. 4.27

Inside this envelope wave, there are a group of small waves which have a wavelength of:

$$\lambda_M = \frac{2\pi}{k_p} = \frac{2\pi}{31/32} = 6{,}4 \; m$$

Eq. 4.28

It is also possible to calculate the phase velocity and the group velocity:

$$v_g = \frac{\omega_p}{k_p} = \frac{7{,}75}{31/32} = 8 \; m/s$$

Eq. 4.29

$$v_M = \frac{\omega_M}{k_M} = \frac{0{,}25}{1/32} = 8 \; m/s$$

Eq. 4.30

Phase velocity and group velocity are the same due to the fact that in this example a non dispersive medium has been chosen since the velocities of the waves that are superposed are the same (note that in non superposed waves phase velocity and group velocity are the same):

$$v_1 = \frac{\omega_1}{k_1} = \frac{8}{1} = 8\frac{m}{s} = v_1 = \frac{\omega_2}{k_2} = \frac{7{,}5}{15/16} = 8\frac{m}{s}$$

<div align="right">Eq. 4.31</div>

In a non dispersive medium, it is fulfilled:

$$v_p = \frac{\omega_1}{k_1} = \frac{\omega_2}{k_2}$$

<div align="right">Eq. 4.32</div>

However, in a dispersive medium, velocities for different frequencies are different. Let us have now these two waves that are going to be superposed:

$$u_1(x,t) = 2\cos(8t - x)$$

<div align="right">Eq. 4.33</div>

$$u_2(x,t) = 2\cos\left(7{,}5t - \frac{14{,}5}{16{,}5}x\right)$$

The average values will be:

$$\omega_P = 7{,}75\,s^{-1}; k_P = \frac{31}{33}m^{-1}; \omega_M = 0{,}25\,s^{-1}; k_M = \frac{2}{33}m^{-1}$$

<div align="right">Eq. 4.34</div>

Then, the resulting wave is:

$$u(x,t) = 2 \cdot 2\cos\left(0{,}25t - \frac{2}{33}x\right)\cos\left(7{,}75t - \frac{31}{33}x\right)$$

<div align="right">Eq. 4.35</div>
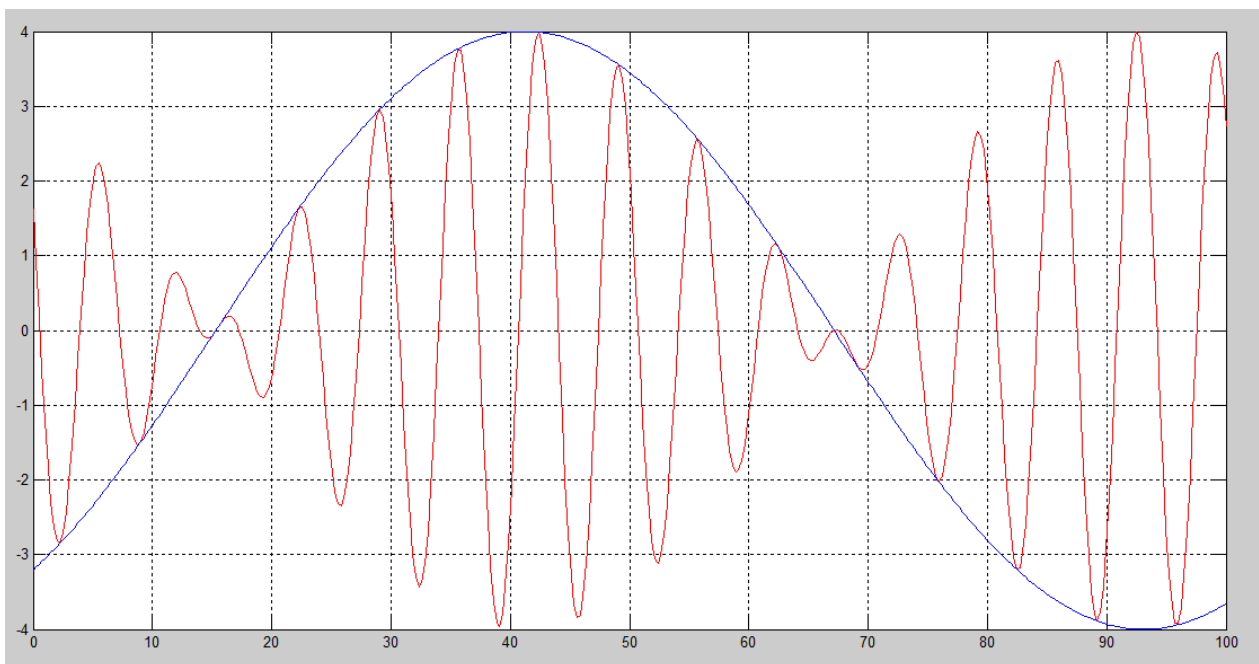
Image 4.4: Envelope wave of a superposition of two waves propagating in the positive x direction in a dispersive medium.

In Image 4.4, it is possible to see the wave at $t = 1$ and in a space between 0 and 100. A envelope wave is possible to be appreciated, which is propagating in the positive x direction. The wavelength of the envelope wave is:

$$\lambda_M = \frac{2\pi}{k_M} = \frac{2\pi}{2/33} = 103{,}7 \; m$$

<div align="right">Eq. 4.36</div>

Inside this envelope wave, there are a group of small waves which have a wavelength of:

$$\lambda_M = \frac{2\pi}{k_p} = \frac{2\pi}{31/33} = 6{,}69 \; m$$

<div align="right">Eq. 4.37</div>

It is also possible to calculate the phase velocity and the group velocity:

$$v_p = \frac{\omega_p}{k_p} = \frac{7{,}75}{31/33} = 8{,}25 \; m/s$$

<div align="right">Eq. 4.38</div>

$$v_g = \frac{\omega_M}{k_M} = \frac{0{,}25}{2/33} = 4{,}13 \; m/s$$

<div align="right">Eq. 4.39</div>

Phase velocity and group velocity are not the same due to the fact that in this example a dispersive medium has been chosen and the velocities of the waves that are superposed are not the same:

$$v_1 = \frac{\omega_1}{k_1} = \frac{8}{1} = 8\,\frac{m}{s} \neq v_2 = \frac{\omega_2}{k_2} = \frac{7{,}5}{14{,}5/16{,}5} = 8{,}53\,\frac{m}{s}$$

<div align="right">Eq. 4.40</div>

Thus, it is clear that in general phase and group velocity are different. Actually, just with a little chance in one of the waves that is to be superposed -as in the last example-, group velocity can vary considerably.

4.3. Dispersion diagram

The phase and group velocity have a relation with the frequency of the source wave. It means that if we have a pipe filled with water and we stimulate the water with a sinusoidal wave, the phase and group velocity change depending on the frequency of this sinusoidal wave. This statement is easy to confirm by the definition of phase and group velocity, since they both depend on the frequency ω of the wave, as it is shown in Eq. 4.4 and in Eq. 4.16: $v_g = \frac{\partial \omega}{\partial k}$; $v_p = \frac{\omega}{k}$.

In order to show the relation between the phase and group velocities and the frequency of the source wave, a dispersion diagram can be built, as it is shown in Image 4.5, where the dispersion diagram of a water-filled PVC straight pipe of 2 meters for low frequencies is shown.

When the frequency is increased, the dispersion diagram changes and it looks like the one in Image 3.5.

Dispersion diagram water-filled PVC pipe
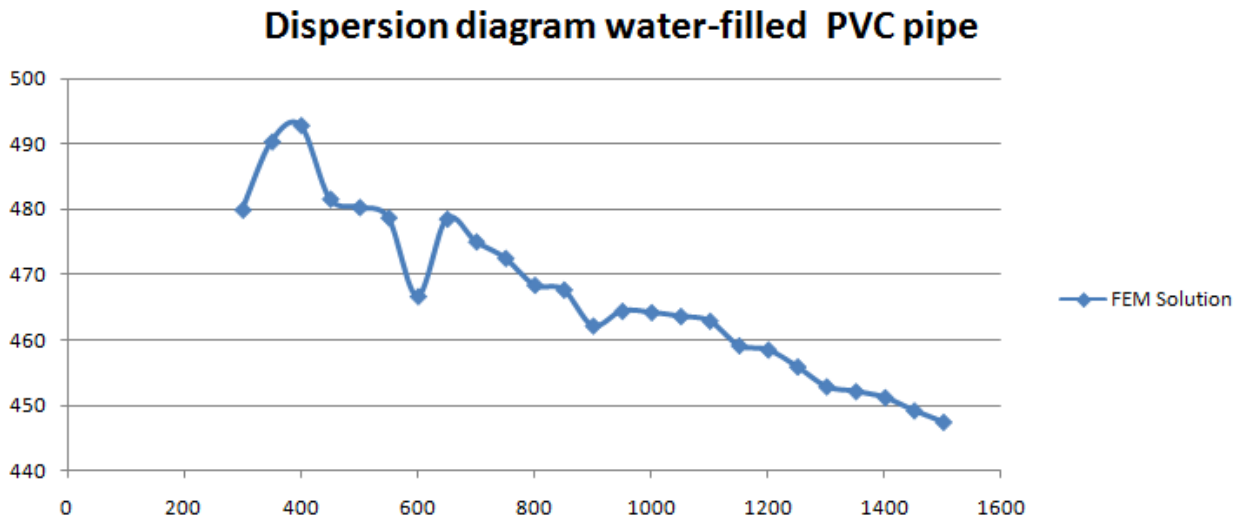
Image 4.5: Phase velocity on the space of the frequency of a water-filled PVC pipe.

5. Measurement methods to measure the phase and group velocity of dispersive sound waves

5.1. Phase velocity by zero crossing time delay

It could be a possibility to measure the phase velocity of a wave by measuring when the size of the wave in two different points and, then, measuring the time elapse between when the wave changes from positive to negative in the first point and in the second, or vice versa.

It is easy to show this method in an example with two waves like these:

$$x(t) = \cos(\omega t)$$
Eq. 5.1

$$y(t) = \cos(\omega t + \varphi)$$
Eq. 5.2

$x(t)$ will change from positive to negative in $t_x = \left(\frac{\pi}{2} + 2\pi \cdot k\right)/\omega$, where $k \in \mathbb{Z}$. Besides, $y(t)$ will do it in $t_y = \left(\frac{\pi}{2} + 2\pi \cdot k\right)/\omega - \varphi$, where $k \in \mathbb{Z}$. Therefore, for a given $k \in \mathbb{Z}$, the time elapse will be:

$$\Delta t = t_x - t_y = \frac{\left(\frac{\pi}{2} + 2\pi \cdot k\right)}{\omega} - \frac{\left(\frac{\pi}{2} + 2\pi \cdot k\right)}{\omega} + \varphi = \varphi$$
Eq. 5.3

Calculated this time, it is now possible to obtain the value of the phase velocity by:

$$v_p = \frac{s}{\Delta t},$$
Eq. 5.4

where s is the space between the two points in which the wave is measured.

For example, if the following two waves are obtained by two points separated $s = 0,1m$ by measuring a wave propagating:

$$x(t) = \cos(10t)$$
Eq. 5.5

$$y(t) = \cos(10t + 5)$$
Eq. 5.6

The shapes of the waves and the time elapse are shown in Image 5.1. Then, the phase velocity of this wave can be calculated as:

$$v_p = \frac{s}{\Delta t} = \frac{0,1}{0,9137 - 0,7854} = 0,779 \text{ m/s},$$
Eq. 5.7
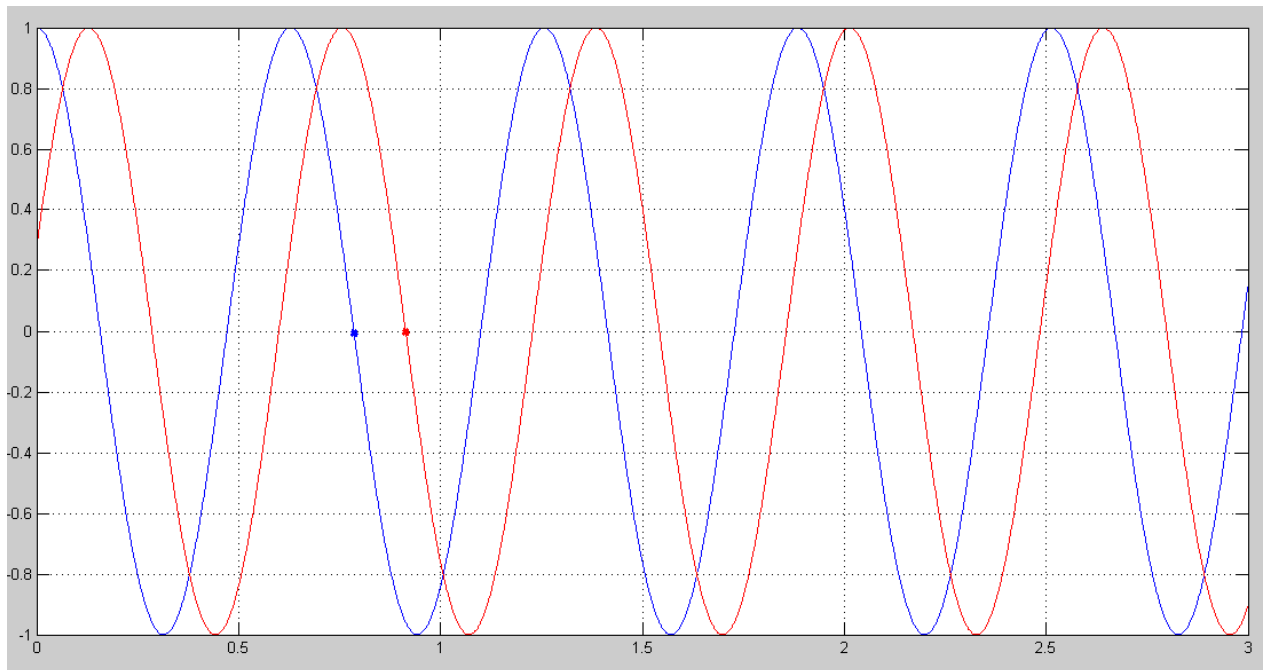
Image 5.1: Two points selected to calculate the phase velocity with the method of zero crossing.

Note that this method is not good for noisy signals because there could be noise in points close to zero, producing a lot of changes in the sign of the wave and, therefore, making this method unusable. This problem is clearly observed in Image 5.2 when adding a gaussian noise to the waves shown in Eq. 5.5 and Eq. 5.6. A zoom has been performed in Image 5.3 in order to better appreciate this problem. It is clear that is not possible to use this method with noisy signals unless a filter is used.
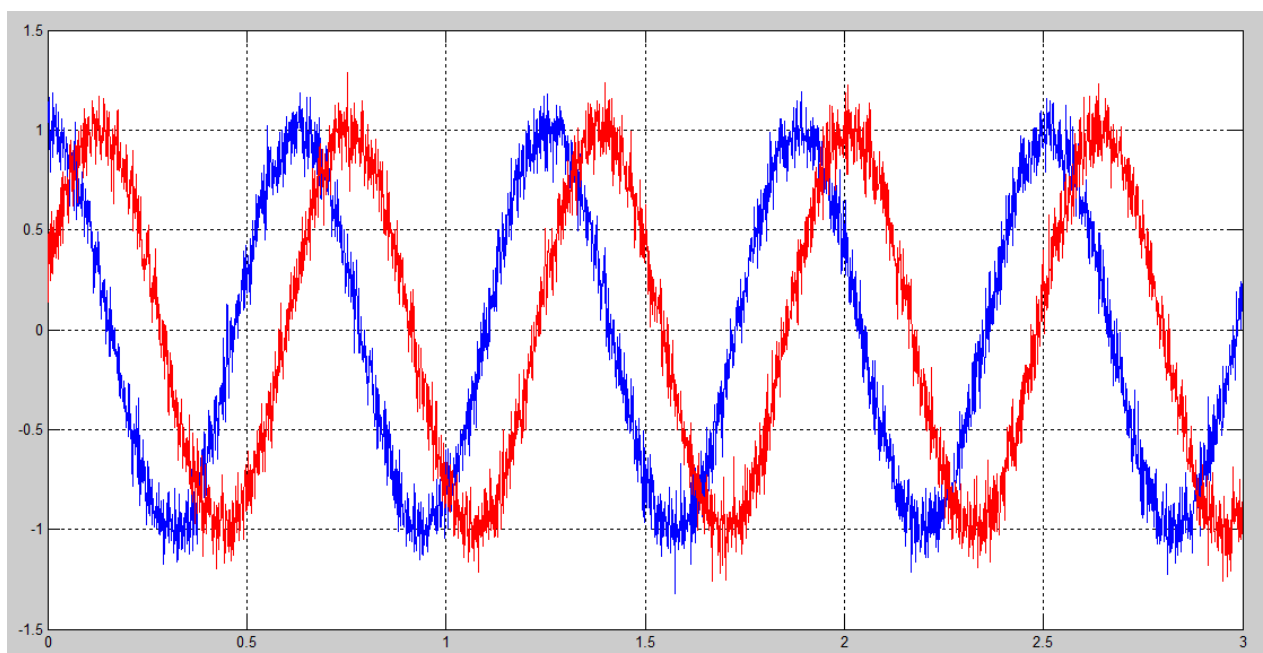
Image 5.2: Two noisy waves that makes unusable the method of zero crossing without using filters.

The MATLAB script that has been used to emulate the noise can be seen in the appendix A. 3. Noisy waves with which is not possible use the zero-crossing method.
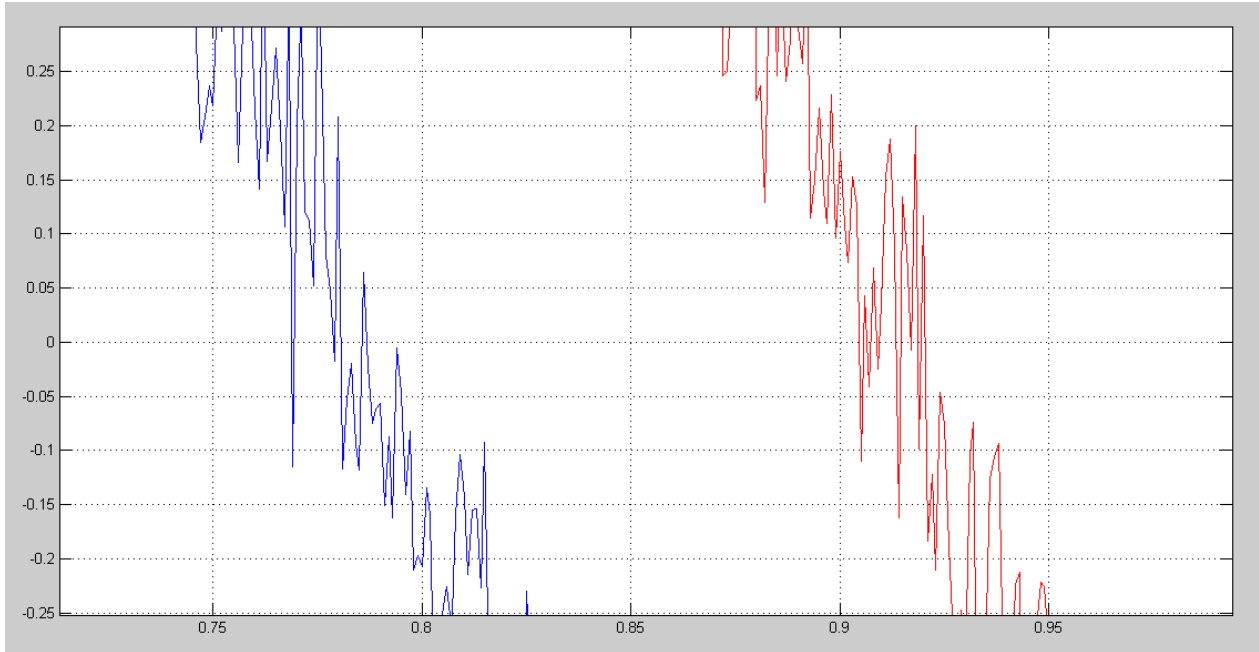
Image 5.3: Zoom of two noisy waves that make unusable the method of zero crossing.

5.2. Phase velocity in frequency domain by phase shift

In order to calculate the phase velocity it is also possible to obtain the Fourier transform of the signal measured in two different points and measure the phase shift between the two transforms.

Fourier transform $\mathcal{F}\{f\}$ of a function f is given by [19]:

$$\mathcal{F}\{f\}(\omega) = \int_{-\infty}^{\infty} f(x)e^{-ix\omega}\, dx,$$

Eq. 5.8

where $f \in L^1(\mathbb{R})$, where $L^1(\mathbb{R})$ is defined by the group of functions $f: \mathbb{R} \to \mathbb{C}$ such that f verifies that:

$$\int_{-\infty}^{\infty} |f(x)|dx < \infty$$

Eq. 5.9

However, we are interested in discrete signals, which are acquired by the sensors that receive them. For this reason, it is also possible to define a discrete Fourier transform as:

Eq. 5.10

$$\mathcal{F}\{x_k\} = X_k = \sum_{n=0}^{N-1} x_n\, e^{-\frac{2\pi i}{N}kn}\ , \qquad k = 0, \dots, N-1$$

As the result is a serial of complex numbers, the amplitude A_k and phase φ_k of every sample can be calculated as:

$$A_k = |X_k| = \sqrt{Re(X_k)^2 + Im(X_k)^2}$$

<div align="right">**Eq. 5.11**</div>

$$\varphi_k = \arg(X_k) = atan2[Im(X_k), Re(X_k)],$$

<div align="right">**Eq. 5.12**</div>

where atan2 is the arctangent function with two arguments that returns the value of the arctangent in the correct quadrant.

An example to better understand the result that is given by the discrete Fourier, let us have the following serial:

$$x_k = 2^k, \qquad k = 0,1,2$$

<div align="right">**Eq. 5.13**</div>

Applying the definition of the Fourier transform to Eq. 5.13:

$$F\{x_k\} = X_k = \sum_{n=0}^{2} 2^n\, e^{-\frac{2\pi i}{N}kn} =$$

<div align="right">**Eq. 5.14**</div>

$$= 2^0 e^0 + 2^1 e^{-\frac{2\pi i}{2}k\cdot 1} + 2^2 e^{-\frac{2\pi i}{2}k\cdot 2} =$$

<div align="right">**Eq. 5.15**</div>

$$= 1 + 2e^{-\pi i k} + 4e^{-2\pi i k}, \qquad k = 0,1,2$$

<div align="right">**Eq. 5.16**</div>

Therefore:

$$x_0 = 7\,; x_1 = 1 + 2e^{-\pi i} + 4e^{-2\pi i}; x_2 = 1 + 2e^{-2\pi i} + 4e^{-4\pi i}$$

<div align="right">**Eq. 5.17**</div>

If it is expressed as complex numbers:

$$x_0 = 7\,; x_1 = -2 + \sqrt{3}\cdot i; x_2 = -2 - \sqrt{3}\cdot i$$

<div align="right">**Eq. 5.18**</div>

And then expressed in the polar form:

$$x_0 = 7_{0\,rad}$$

<div align="right">**Eq. 5.19**</div>

$$x_1 = \sqrt{7}_{atan\,2(-2,\sqrt{3})} \approx 2{,}6458_{-0{,}8571\,rad}$$

$$x_2 = \sqrt{7}_{atan\,2(-2,-\sqrt{3})} \approx 2{,}6458_{-2{,}2845\,rad}$$

If the phase shift between two signals is wanted to be known in order to measure the phase velocity, it is necessary to perform a discrete Fourier transform and compare the graphs obtained for the two signals.

So now suppose that the two following signals are acquired in two sensors separated a distance $d = 0{,}1m$:

$$x_k = \cos(2\pi \cdot 10k/1000), \qquad k = 1, \dots, 201$$

<div align="right">**Eq. 5.20**</div>

$$y_k = \cos(2\pi \cdot 10k/1000 + 1{,}5), \quad k = 1, \dots, 201$$

Eq. 5.21

Where $F_s = 1000\ Hz$ is the sample frequency. Calculating their discrete Fourier transform:

$$X_k = \sum_{n=1}^{201} \cos(2\pi \cdot 10k/1000)\, e^{-\frac{2\pi i}{N}kn}, \qquad k = 1, \dots, 201$$

Eq. 5.22

$$Y_k = \sum_{n=1}^{201} \cos(2\pi \cdot 10k/1000 + 1{,}5)\, e^{-\frac{2\pi i}{N}kn}, \qquad k = 1, \dots, 201$$

Eq. 5.23

The calculation of the Fourier transform done with MATLAB step by step is shown in appendix A. 4. Fourier transform. MATLAB also has a function that calculates the Fourier transform in a fast way (Fast Fourier Transform, FFT) first discussed by Cooley and Tukey [20] .

Calculating the value of X_k and Y_k for $k = 3$, as $(3-1) \cdot \frac{Fs}{N} = (3-1) \cdot \frac{1000}{201} \approx 10\ Hz$, the values obtained are:

$$X_{100} = \ 100{,}7342_{1{,}7910º}$$

Eq. 5.24

$$Y_{100} = 100{,}2352_{87{,}7145º}$$

Eq. 5.25

The phase shift is then:

$$\varphi = 87{,}7145 - 1{,}7910 = 85{,}9234 \cdot \frac{\pi}{180} \frac{rad}{º} = 1{,}4996 \approx 1{,}5\ rad,$$

Eq. 5.26

which is the phase delay of the two signals. Therefore, if the distance between the two points is known, it is possible to calculate the phase velocity:

$$v_p = 0{,}1m / \frac{1{,}5 rad}{2\pi \cdot 10 \frac{rad}{s}} = 4{,}189 m/s$$

Eq. 5.27
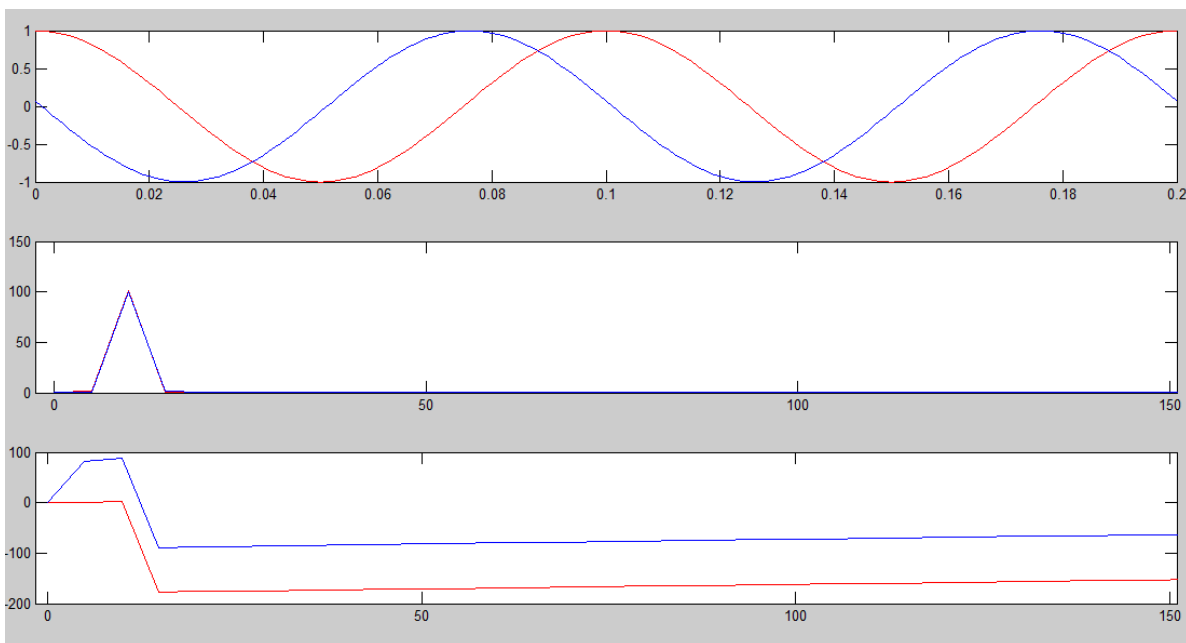
Image 5.4: Fourier transform of two ideal waves.

39

To show how this could be done with MATLAB, in appendix A. 5. Phase velocity with the method of phase shift, a script is written which calculates the Fourier transform of the previous two serials (or waves) and displays this information. In Image 5.4 the original waves, the absolute value of the Fourier transform, and the phase shift of the Fourier transform are shown. Measuring the difference between the two curves in the phase shift diagram in the main frequency ($f = 10Hz$), the result is $\varphi = 87,27^\circ$, which is almost the same value than the one obtained analytically before.
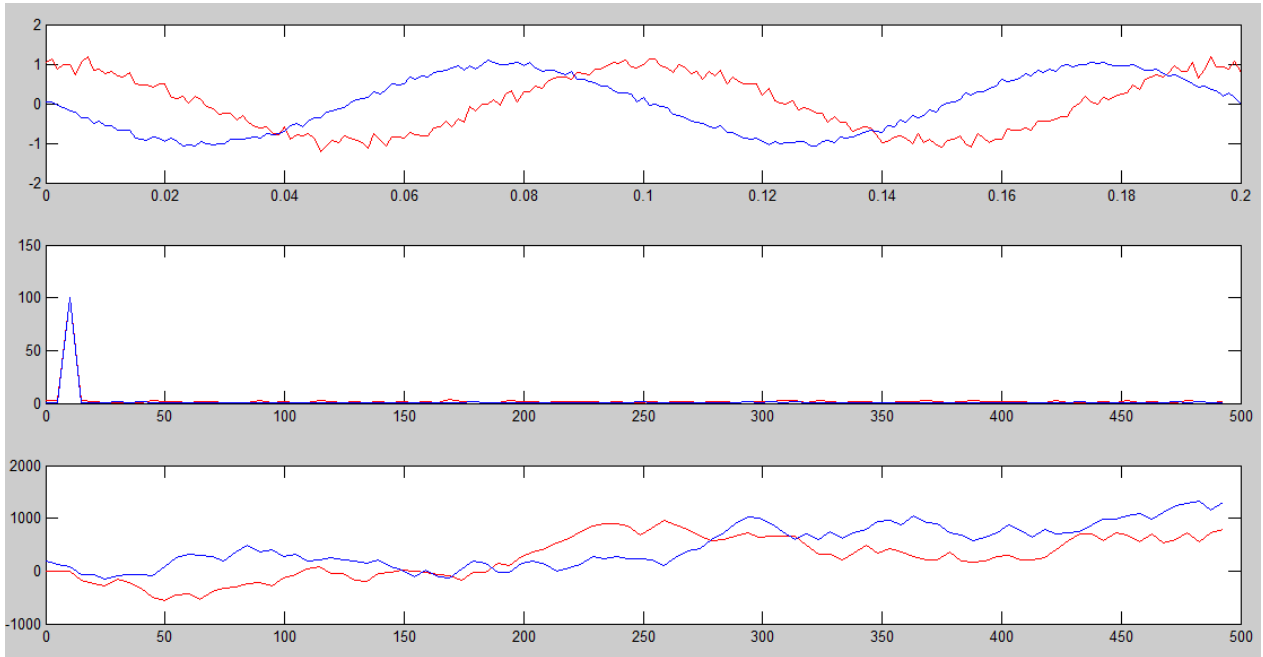
Image 5.5: Fourier transform of two noisy waves.
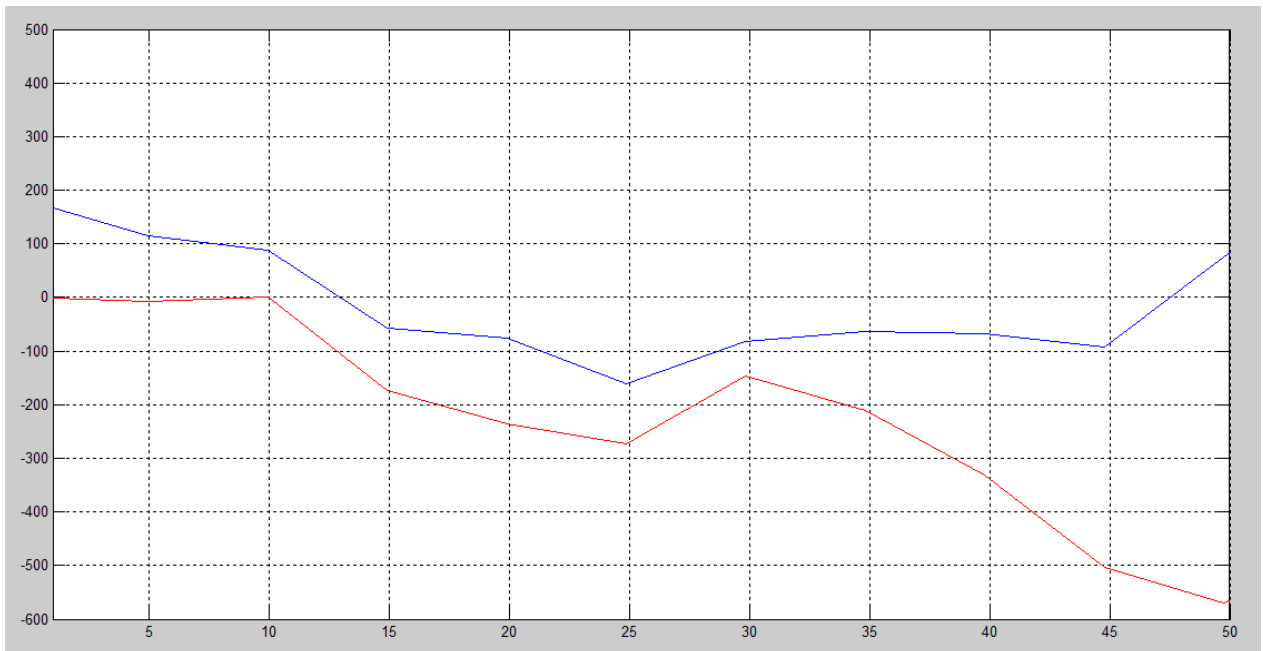
Image 5.6: Zoom of the angle of the Fourier transform of two noisy waves.

However, when some noise is introduced, even though the phase diagram is completely deformed, it is possible to measure the phase velocity, since the phase values in the interesting

frequency is not deformed. For instance, adding small gaussian noise the phase diagrams is shown in Image 5.5 the big deformation of it, and in Image 5.6 a zoom in which it is appreciated that the phase shift is still the same. The way to add this gaussian noise is the same than the one used in the section 5.1. Phase velocity by zero crossing time delay.

5.3. Group velocity by time delay of maximum of envelope wave

One of the ways of measuring the group velocity of a wave is by calculating its envelope and measuring it in two different points. Then, it is possible to determine at what time the envelope reaches its maximum value and measure the time elapse between the time in which the first point acquires the maximum value of the envelope and the time in which the second point does it.

In Image 5.7 the wave of Eq. 4.35 is shown in the points $x_1 = 1m$ and $x_2 = 10m$ in time dependency. The maximum values of the envelope are reached in $t_1 = 0,2425s$ and $t_2 = 2,424s$, making the group velocity be:

$$v_g = \frac{s}{\Delta t} = \frac{9}{2,424 - 0,2425} = 4,1256 \approx 4,13 \text{ m/s} \,, \qquad \text{Eq. 5.28}$$

which is the same result that was calculated in Eq. 4.39.

However, let us have gaussian noise in the signals as it is shown in Image 5.8. Now it is more difficult to calculate the envelope wave because it is necessary to apply a filter so as to reduce the noise.
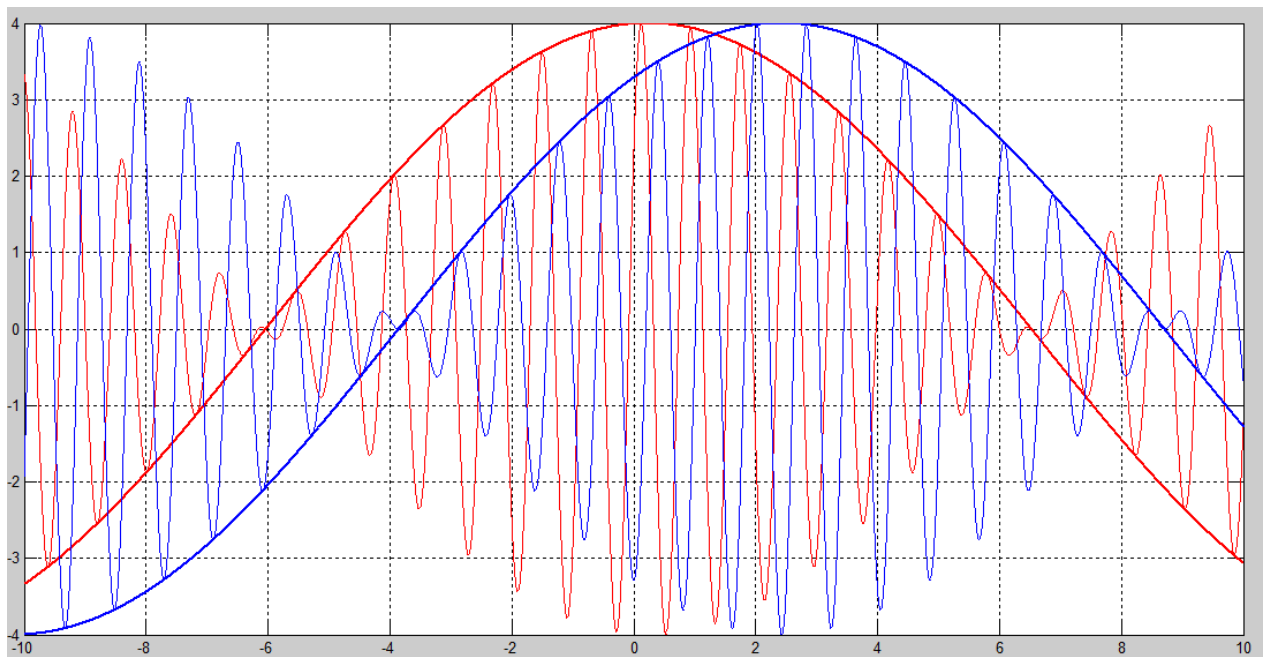
Image 5.7: Envelope waves of two waves formed by the superposition of two waves to calculate the group velocity.
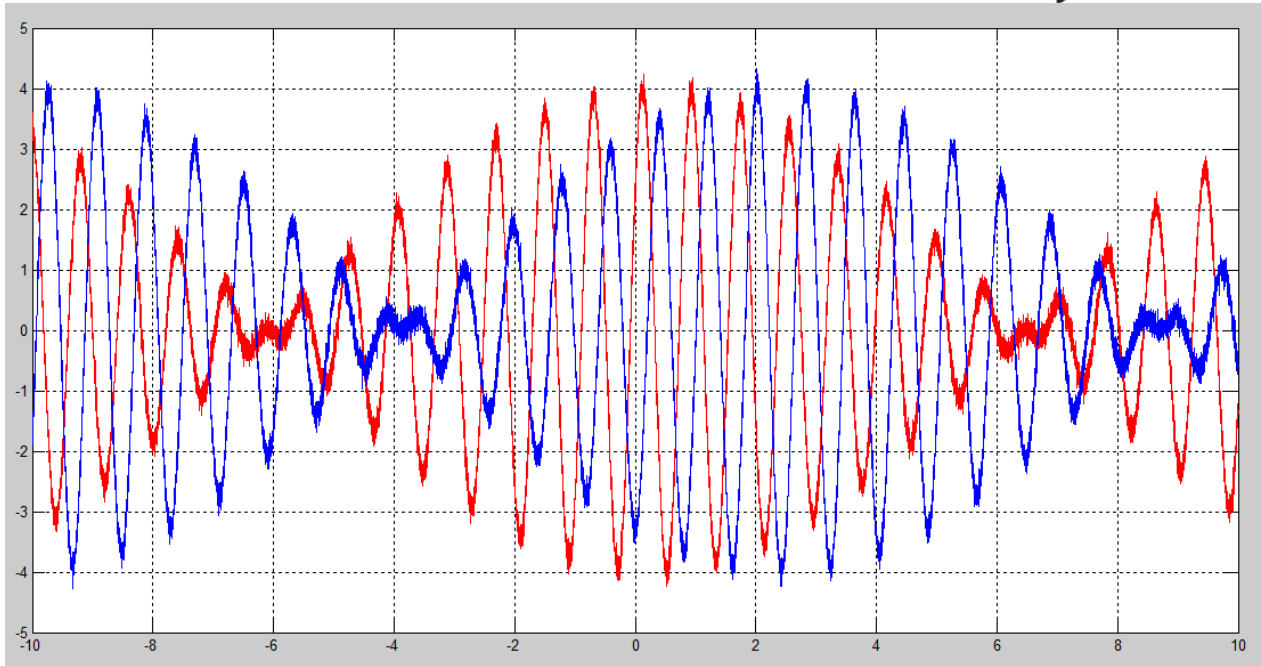
Image 5.8: Two noisy waves that make difficult to calculate the envelope waves without applying filters.

5.3.1 Calculation of the envelope wave by the Hilbert transform

When a modulated wave is obtained by the probes and its envelope is wanted to be calculated so as to measure the group velocity, a first approximation can be done by calculating its Hilbert transform.

Hilbert transform of a real function $s(t)$ is obtained by the convolution of the signal itself and $1/\pi t$. Then, it can be interpreted as the output of a LTI system with input $s(t)$ and impulse response of $1/\pi t$ as it is schematized in Image 5.9. Mathematically, it is defined by [21]:

$$\check{s}(t) = \mathcal{H}\{s\}(t) = (h * s)(t) = \frac{1}{\pi} \int_{-\infty}^{\infty} \frac{s(\tau)}{t - \tau} d\tau ,$$

Eq. 5.29

where $h(t) = 1/\pi t$.
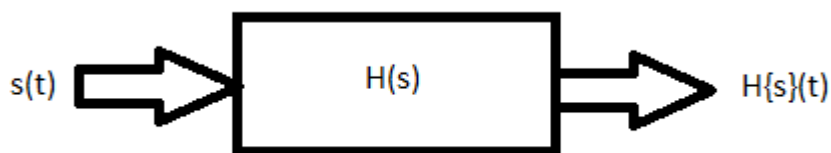
Image 5.9: LTI system for calculating the Hilbert transform.

Using $\check{s}(t)$ it is possible to build the analytical signal of $s(t)$ as:

$$s_a(t) = s(t) + i\check{s}(t)$$

Eq. 5.30

Hilbert transform frequency response is given by the Fourier transform by:

$$\mathcal{H}(\omega) = \mathcal{F}\{h\}(\omega) = \begin{cases} +i, & \text{if } \omega < 0 \\ -i, & \text{if } \omega > 0 \end{cases} \qquad \text{Eq. 5.31}$$

or, equivalently:

$$\mathcal{H}(\omega) = \mathcal{F}\{h\}(\omega) = -i \cdot \text{sgn}(\omega) \qquad \text{Eq. 5.32}$$

And, due to the fact that:

$$\mathcal{F}\{\breve{s}\}(\omega) = \mathcal{H}(\omega) \cdot \mathcal{F}\{s\}(\omega) \qquad \text{Eq. 5.33}$$

Therefore, Hilbert transform produces a displacement in negative frequencies of s(t) of $+90º$ and for the positive ones, $-90º$.

It is also interesting to notice that it is possible to obtain the original signal s(t) when the Hilbert transform is calculated by taking into account that:

$$\mathcal{H}^2(\omega) = -1 \qquad \text{Eq. 5.34}$$

Thus, multiplying Eq. 5.33 by $-\mathcal{H}(\omega)$:

$$\mathcal{F}\{s\}(\omega) = -\mathcal{H}(\omega) \cdot \mathcal{F}\{\breve{s}\}(\omega) \qquad \text{Eq. 5.35}$$

So the original signal is given by:

$$s(t) = -(h * \breve{s})(t) = -\mathcal{H}\{\breve{s}\}(t) \qquad \text{Eq. 5.36}$$

As we are dealing with discrete signals, the definition of the Hilbert transform given in Eq. 5.29 is not usable because it works only for continuous signals. In the case of discrete signal s_k with $k = 0,1,\dots,N-1$ Hilbert transform is given by [22]:

$$\breve{s}_k = h\{s\}_k = \begin{cases} \dfrac{2}{\pi} \displaystyle\sum_{n \text{ odd}} \dfrac{s_n}{k-n}, & k \text{ even} \\[2em] \dfrac{2}{\pi} \displaystyle\sum_{n \text{ even}} \dfrac{s_n}{k-n}, & k \text{ odd} \end{cases} \qquad \text{Eq. 5.37}$$

Discrete Hilbert transform can be calculated by a four-step algorithm [23], which is the method that MATLAB uses when the function *hilbert* is called:

     1. Calculating the Fast Fourier Transform of the input sequence, storing the result in a vector x.

     2. Creating a vector h whose elements h(i) have the values:

- 1 for i = 1, (n/2)+1
- 2 for i = 2, 3, … , (n/2)
- 0 for i = (n/2)+2, … , n

     3. Calculating the element-wise product of x and h.

     4. Calculating the inverse Fast Fourier Transform of the sequence obtained in step 3 and giving the first n elements of the result.

5.4. Group velocity by time delay of cross-correlation

In order to compare two discrete signals $\{x_n\}_{n \in A}$ and $\{y_n\}_{n \in A}$ where A is the subspace of N real numbers which contains the time values in which the samples are been taken, it is possible to use the cross-correlation defined as:

$$c_{xy} = \sum_{i=1}^{N} x_i \cdot y_i$$

Eq. 5.38

If the value of c_{xy} is positive, it means that when an increment in x_n is associated to a decrement of y_n, and vice versa. Besides, the bigger c_{xy} is, the bigger the similarity between the two signals is. Note that this definition depends on the number of samples N. Thus, it is also possible to define the cross-correlation independently of N by:

$$c_{xy} = \frac{1}{N} \sum_{i=1}^{N} x_i \cdot y_i$$

Eq. 5.39

	1	2	3	4	5	6	7	8	9
x	4	2	-1	3	-2	-6	-5	4	5
y	-4	1	3	7	4	-2	-8	-2	1
xi*yi	-16	2	-3	21	-8	12	40	-8	5

Table 5.1: Values of two signals of which cross-correlation is going to be calculated

For instance, the cross-correlation between two signals with values shown in Table 5.1 can be calculated by Eq. 5.39 as shown in Eq. 5.40.

$$c_{xy} = \frac{1}{9}[4 \cdot (-4) + 2 \cdot 1 - 3 \cdot 1 + 3 \cdot 7 - 2 \cdot 4 - 6 \cdot (-2) - 5 \cdot (-8) + 4 \cdot (-2)$$
$$+ 5 \cdot 1] = \frac{1}{9} \cdot 45 = 5$$

Eq. 5.40

However, this Eq. for the cross-correlation does not give a good result when two signals has the same frequency but different phase. For this reason, it is reasonable to think about moving one of the series to right or the left (advance or delay) a time delay k in order to equal both phases. Then, the Eq. for the cross-correlation will be:

$$c_{xy}(k) = \sum_{i=1}^{N} x_i \cdot y_{i+k} \,,$$

Eq. 5.41

where $(i + k) \in A$ and it means a displacement of the series $\{y_n\}_{n \in A}$ to the left or the right.

The purpose of this method is to find the value of k that maximizes the value of $c_{xy}(k)$. When this value of k is found, both phases are equaled and, thus, the time delay between the two signals is k. By doing so it is possible to find the time delay k between the two given signals and, therefore, calculate the group velocity of the propagating wave.

For example, if we have the two following general expressions that represent two waves in N sample points:

$$x_n = \cos(\omega \cdot n)$$

Eq. 5.42

$$y_n = \cos(\omega \cdot n + \varphi)$$

Eq. 5.43

Then, the cross-correlation will be:

$$c_{xy}(k) = \sum_{i=1}^{N} \cos(\omega \cdot i) \cdot \cos(\omega \cdot i + \varphi + k)$$

Eq. 5.44

In order to calculate the value of k that maximizes c_{xy}, we are going to consider two continuous signals:

$$x(t) = \cos(\omega t)$$

Eq. 5.45

$$y(t) = \cos(\omega t + \varphi)$$

Eq. 5.46

Therefore, the cross-correlation is now:

$$c_{xy}(k) = \int_0^T \cos(\omega t) \cdot \cos(\omega t + \varphi + k)\, dt, \qquad T \in \mathbb{R}^+$$

Eq. 5.47

In order to maximize c_{xy}, we differentiate it in k:

$$\frac{d}{dk} c_{xy}(k) = \frac{d}{dk}\left[\int_0^T \cos(\omega t) \cdot \cos(\omega t + \varphi + k)\, dt\right]$$

Eq. 5.48

$$= \frac{d}{dk}\left[\int_0^T \frac{\cos(2\omega t + \varphi + k) + \cos(\varphi + k)}{2}\, dt\right]$$

Eq. 5.49

$$= \frac{1}{2}\frac{d}{dk}\left[\int_0^T \cos(2\omega t + \varphi + k)\,dt + \int_0^T \cos(\varphi + k)dt\right]$$

<div align="right">Eq. 5.50</div>

$$= \frac{1}{2}\frac{d}{dk}\int_0^T \cos(2\omega t + \varphi + k)\,dt + \frac{1}{2}\frac{d}{dk}\cos(\varphi + k)T$$

<div align="right">Eq. 5.51</div>

$$= \frac{1}{2}\frac{d}{dk}\left[\frac{-\sin(2\omega t + \varphi + k)}{2\omega}\right]_0^T - \frac{1}{2}T\sin(\varphi + k)$$

<div align="right">Eq. 5.52</div>

$$= \frac{1}{4\omega}\frac{d}{dk}\left[-\sin(2\omega T + \varphi + k) + \sin(\varphi + k)\right] - \frac{1}{2}T\sin(\varphi + k)$$

<div align="right">Eq. 5.53</div>

$$= \frac{1}{4\omega}\left[-cos(2\omega T + \varphi + k) + \cos(\varphi + k)\right] - \frac{1}{2}T\sin(\varphi + k)$$

<div align="right">Eq. 5.54</div>

Making it equal to 0:

$$\cos(\varphi + k) - cos(2\omega T + \varphi + k) - 2\omega T\sin(\varphi + k) = 0 \rightarrow$$

<div align="right">Eq. 5.55</div>

$$\rightarrow 2\sin(\omega T + \varphi + k)\sin(2\omega T) = 2\omega T\sin(\varphi + k)$$

<div align="right">Eq. 5.56</div>

Now if $k = -\varphi$:

$$2\sin(\omega T)\sin(2\omega T) = 0$$

<div align="right">Eq. 5.57</div>

Then either $\sin(\omega T)$ or $\sin(2\omega T)$ has to be equal to 0. Then:

$$\omega T = \frac{\pi}{2}m, \qquad m \in \mathbb{Z}$$

<div align="right">Eq. 5.58</div>

Therefore, when Eq. 5.58 is verified, it exists a maximum or minimum in $k = -\varphi$. In order to see whether it is a maximum or minimum, the second differentiate is going to be performed:

$$\frac{d^2 c_{xy}(k)}{dk^2} = \frac{d}{dk}\frac{d}{dk}\frac{1}{4\omega}\left[-cos(\pi m + \varphi + k) + \cos(\varphi + k)\right] - \frac{d}{dk}\frac{1}{2}T\sin(\varphi + k) =$$

<div align="right">Eq. 5.59</div>

$$= \frac{1}{4\omega}\left[\sin(\pi m + \varphi + k) - \sin(\varphi + k)\right] - \frac{1}{2}T\cos(\varphi + k)$$

<div align="right">Eq. 5.60</div>

Making $k = -\varphi$:

$$\left.\frac{d^2 c_{xy}(k)}{dk^2}\right|_{k=-\varphi} = -\frac{1}{2}T < 0$$

<div align="right">Eq. 5.61</div>

Thus, there is a maximum in $k = -\varphi$ when $T = \frac{\pi}{2}m,\ m \in \mathbb{Z}$.

This result can be exported to a discrete wave as long as the sample frequency is big enough. Then, the maximum value of the cross-correlation will be reached in $k = -\varphi$. So, when the two wave signals acquired by the two sensors, an iteration process will be performed in order to find the maximum value of the cross correlation by changing the parameter k. When this maximum value is

reached, the value of k with which it is reached is the value of $-\varphi$ and, thus, it will be possible to determine the group velocity.

Let us now measure the signal of Eq. 4.35 by this method. In Image 5.10 the result of the cross-correlation for different values is shown. A maximum is reached in $k = 5{,}74\,rad \rightarrow \varphi = -5{,}74\,rad + 2\pi = 0{,}5432\,rad$.

$$v_g = \frac{(10-1)\text{m}}{0{,}5432\text{rad}/(0{,}25\text{rad/s})} = 4{,}14\text{m/s},$$

<div align="right">Eq. 5.62</div>

which is the same result obtained by measuring the time difference in the maximum of the envelope.

The script used to obtain these results is displayed in the appendix A. 7. Group velocity with cross-correlation.

5.5. Phase velocity by comparing two same points in two waves

Let us have the superposition of two waves that forms an amplitude-modulated wave:

$$u(x,t) = A_1 \left[2\cos\left(\omega_p t - k_p x + \varphi_p\right)\cos\left(\omega_m t - k_m x + \varphi_m\right) + \frac{A_2 - A_1}{A_1}\cos\left(\omega_2 t - k_2 x + \varphi_2\right) \right]$$

<div align="right">Eq. 5.63</div>
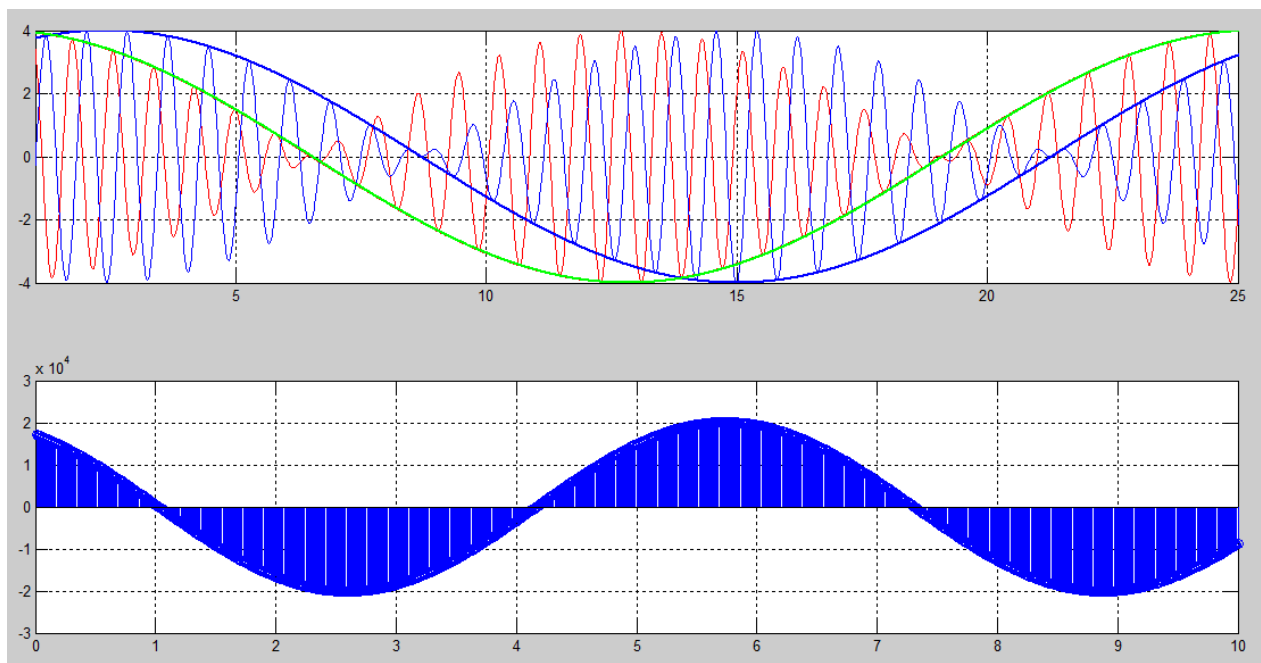
Image 5.10: Envelope for the k that makes the cross-correlation reaches a maximum and cross-correlation of two waves for different values of k

We will try to compare two points with the same characteristics in the two waves, so let us choose when the waves reach their maximums. So as to find the maximum values of the wave, it is necessary to differentiate in time:

$$u(t) = A_1 \left[2\cos(\omega_p t + \varphi_p)\cos(\omega_m t + \varphi_m) + \frac{A_2 - A_1}{A_1}\cos(\omega_2 t + \varphi_2) \right]$$

Eq. 5.64

$$\frac{du(t)}{dt} = -A_1\,\omega_1\sin(\omega_1 t + \varphi_1) - A_2\omega_2\sin(\omega_2 t + \varphi_2) = 0$$

Eq. 5.65

$$A_1\omega_1\left[\sin(\omega_1 t + \varphi_1) + \sin(\omega_2 t + \varphi_2) + \frac{A_2\omega_2 - A_1\omega_1}{A_1\omega_1}\sin(\omega_2 t + \varphi_2)\right] = 0$$

Eq. 5.66

$$2\sin\left[\frac{(\omega_1 + \omega_2)t + \varphi_1 + \varphi_2}{2}\right]\cos\left[\frac{(\omega_1 - \omega_2)t + \varphi_1 - \varphi_2}{2}\right] + \frac{A_2\omega_2 - A_1\omega_1}{A_1\omega_1}\sin(\omega_2 t + \varphi_2) = 0$$

Eq. 5.67

When it is verified that $A_1\omega_1 = A_2\omega_2$:

$$\sin(\omega_p t + \varphi_p)\,\cos(\omega_m t + \varphi_m) = 0$$

Eq. 5.68

So the solution is when either the sine or the cosine (or both) is zero:

$$\omega_p t + \varphi_p = \pi \cdot m, \qquad m \in \mathbb{Z}$$

Eq. 5.69

$$t = \frac{\pi \cdot m - \varphi_p}{\omega_p}, \qquad m \in \mathbb{Z}$$

Eq. 5.70

$$\omega_m t + \varphi_m = \frac{\pi}{2}\cdot p, \qquad p \in \mathbb{Z}$$

Eq. 5.71

$$t = \frac{\frac{\pi}{2}\cdot p - \varphi_m}{\omega_m}, \qquad p \in \mathbb{Z}$$

Eq. 5.72

So when a maximum or minimum is found when $A_1\omega_1 = A_2\omega_2$ is:

$$t_0 = \left\{ \frac{\pi \cdot m - \varphi_p}{\omega_p}, \frac{\frac{\pi}{2}\cdot p - \varphi_m}{\omega_m} \right\}, \qquad m, p \in \mathbb{Z}$$

Eq. 5.73

To see if it is a maximum or minimum, the second differentiate is performed and evaluated in t_0:

$$\frac{d^2u(t)}{dt^2}\Big|_{t_0} = \frac{d}{dt}\big[2A_1\omega_1\sin(\omega_p t + \varphi_p)\,\cos(\omega_m t + \varphi_m)\big]\Big|_{t_0} = \quad\quad\text{Eq. 5.74}$$

$$= 2A_1\omega_1\big[\omega_p\cos(\omega_p t + \varphi_p)\,\cos(\omega_m t + \varphi_m) \\ - \omega_m\sin(\omega_p t + \varphi_p)\sin(\omega_m t + \varphi_m)\big]\Big|_{t_0} \quad\quad\text{Eq. 5.75}$$

Therefore, if t_0 has the form of $\frac{\pi \cdot m - \varphi_p}{\omega_p}$:

$$\frac{d^2u(t)}{dt^2}\Big|_{t_0=\frac{\pi\cdot m-\varphi_p}{\omega_p}} = 2A_1\omega_1\left[\omega_p\cos(\pi\cdot m)\,\cos\left(\frac{\omega_m\pi\cdot m}{\omega_p} + \frac{\omega_p\varphi_m - \omega_m\varphi_p}{\omega_p}\right)\right] \quad\text{Eq. 5.76}$$

So $\cos(\pi\cdot m) > 0$ when $m = 2q$, $q\in\mathbb{Z}$, and $\cos(\pi\cdot m) < 0$ when $m = 1 + 2q$, $q\in\mathbb{Z}$.

The other part of the equation has to be negative when $\cos(\pi \cdot m)$ is positive so as the global equation is negative and, therefore, there is a maximum in t_0, or the other part of the equation positive when $\cos(\pi \cdot m)$ is negative. Let us find when the other part of the equation is negative:

$$\frac{\pi}{2} + 2\pi r < \frac{\omega_m\pi\cdot m}{\omega_p} + \frac{\omega_p\varphi_m - \omega_m\varphi_p}{\omega_p} < \frac{3\pi}{2} + 2\pi r, \quad\quad r\in\mathbb{Z} \quad\quad\text{Eq. 5.77}$$

Solving:

$$\frac{\omega_m\varphi_p + \omega_p\left(2\pi r - \varphi_m + \frac{\pi}{2}\right)}{\omega_m\pi} < m < \frac{\omega_m\varphi_p + \omega_p\left(2\pi r - \varphi_m + \frac{3\pi}{2}\right)}{\omega_m\pi}, r\in\mathbb{Z} \quad\text{Eq. 5.78}$$

Therefore, when t_0 is with the form of $\frac{\pi \cdot m - \varphi_p}{\omega_p}$, $m = 2q$, $q\in\mathbb{Z}$ and Eq. 5.78 is verified, it implies that $\frac{d^2u(t)}{dt^2}\Big|_{t_0=\frac{\pi\cdot m-\varphi_p}{\omega_p}} < 0$ and, thus, there is a maximum in t_0.

Similarly, if t_0 is with the form of $\frac{\frac{\pi}{2}\cdot p - \varphi_m}{\omega_m}$, $m = 1 + 2q$, $q\in\mathbb{Z}$ and Eq. 5.79 is verified, it implies that $\frac{d^2u(t)}{dt^2}\Big|_{t_0=\frac{\pi\cdot m-\varphi_p}{\omega_p}} < 0$ and, thus, there is a maximum in t_0.

$$\frac{\omega_m\varphi_p + \omega_p\left(2\pi r - \varphi_m + \frac{\pi}{2}\right)}{\omega_m\pi} > m > \frac{\omega_m\varphi_p + \omega_p\left(2\pi r - \varphi_m + \frac{3\pi}{2}\right)}{\omega_m\pi}, r\in\mathbb{Z} \quad\text{Eq. 5.79}$$

In order to find the maximum of the original wave with $A_1\omega_1 \neq A_2\omega_2$ it is necessary to use numerical methods or use graphs. However, when $A_1\omega_1 \neq A_2\omega_2$, the solution will be close to the one found before if $A_1\omega_1 \approx A_2\omega_2$.

For example, let us have these two waves that are going to form a superposed wave:

$$u_1(x,t) = 2\cos(8t - 1)$$

<div align="right">Eq. 5.80</div>

$$u_2(x,t) = 2,2\cos\left(\frac{8}{1,1}t - \frac{15}{16}\right)$$

It verifies that $A_1\omega_1 = A_2\omega_2 \rightarrow 2 \cdot 8 = 16 = 2,2 \cdot \frac{8}{1,1} = 16$. Therefore, the method can be applied.

$$\omega_P = 7,63636\text{s}^{-1}; \varphi_p = -0,96875\text{rad}; \omega_M = 0,363636\text{s}^{-1}; \varphi_m = -0,03125\text{rad}$$

<div align="right">Eq. 5.81</div>

$$\frac{-0,96875 \cdot 0,363636 \cdot +7,63636\left(2\pi r + 0,03125 + \frac{\pi}{2}\right)}{0,363636 \cdot \pi} < m <$$
$$< \frac{-0,96875 \cdot 0,363636 \cdot +7,63636\left(2\pi r + 0,03125 + \frac{3\pi}{2}\right)}{0,363636 \cdot \pi}, r \in \mathbb{Z}$$

<div align="right">Eq. 5.82</div>

If $r = 0$:

$$10,4005 < m < 31,4005 \rightarrow m = \{11,12,\dots,31\}$$

<div align="right">Eq. 5.83</div>

If $m = 21$:

$$t_0 = 8,76624\text{s}$$

<div align="right">Eq. 5.84</div>

Doing the same for the two following waves:

$$u_1(x,t) = 2\cos(8t - 2)$$

<div align="right">Eq. 5.85</div>

$$u_2(x,t) = 2,2\cos\left(\frac{8}{1,1}t - \frac{30}{16}\right)$$

$$7,1180 < m < 28,1180 \rightarrow m = \{8,9,\dots,28\}$$

<div align="right">Eq. 5.86</div>

The result for $r = 0$ and $m = 21$ is:

$$t_0 = 8,89310s$$

So now $it\ is$ possible to calculate the phase velocity:

$$v_p = \frac{1}{8,89310 - 8,76624} = 7,8827\text{m/s}$$
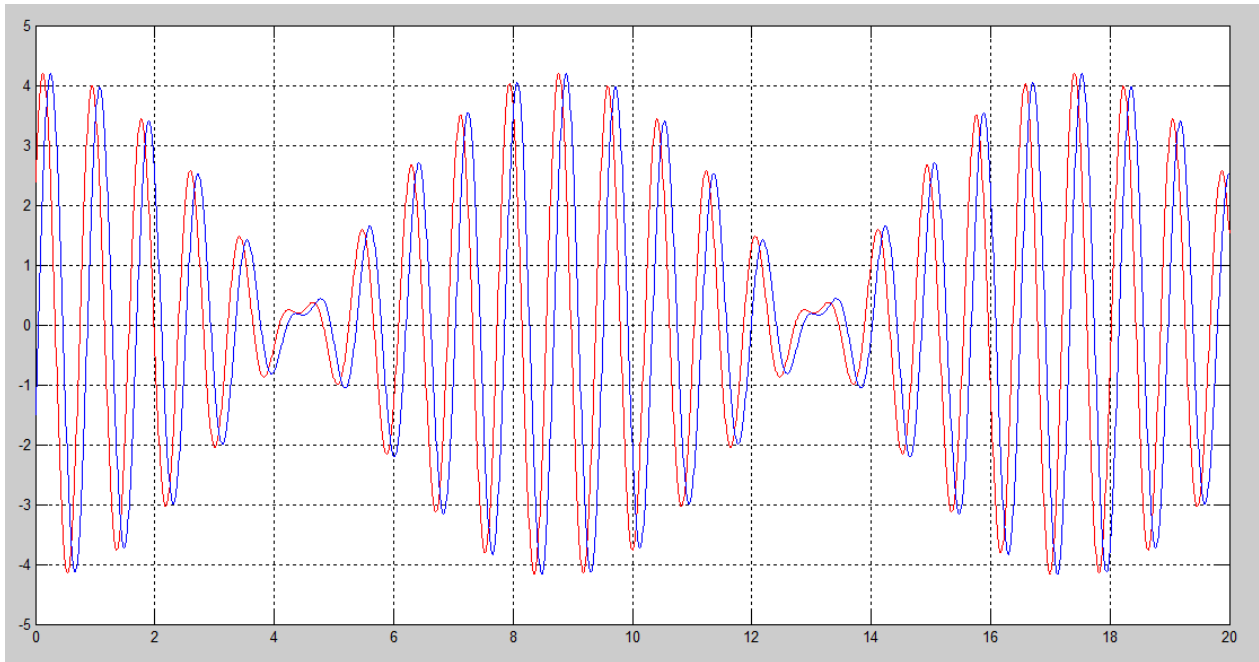
Image 5.11: Two waves whose phase velocity is going to be calculated.
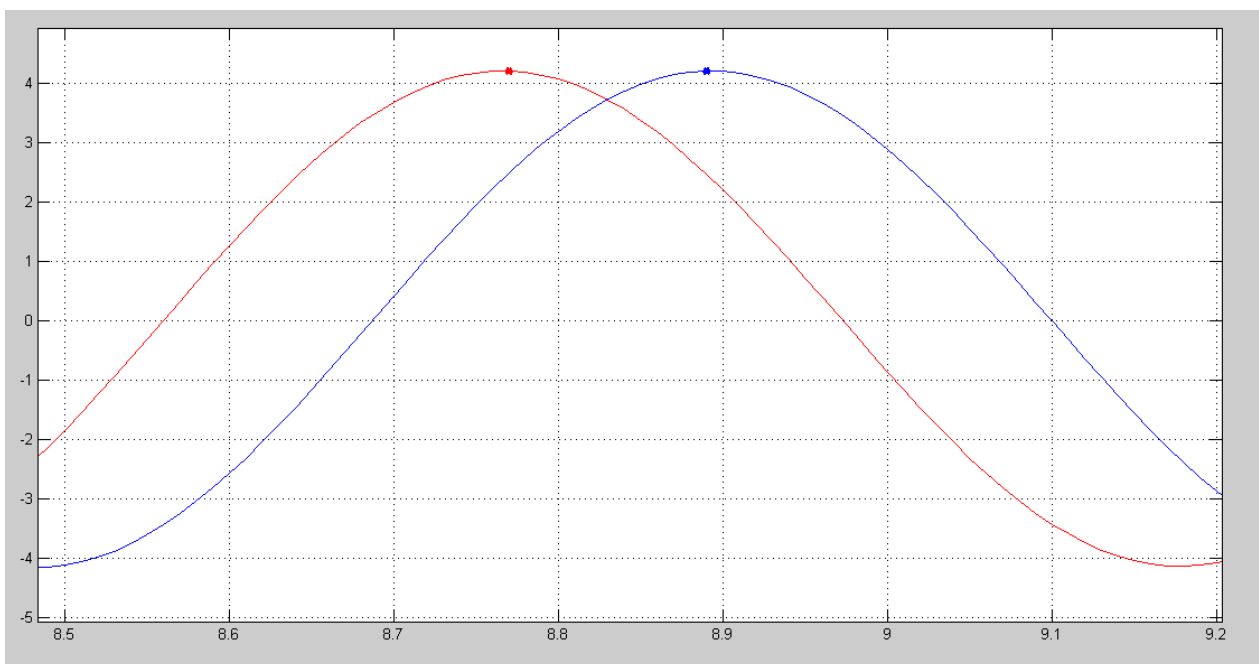
Image 5.12: Zoom of the points selected to calculate the phase velocity.

Now let us have these two other waves:

$$u_1(x, t) = 2\cos(8t - x)$$

$$u_2(x, t) = 2\cos\left(7{,}5t - \frac{15}{16}x\right)$$

The result of superposing them is:

$$u(x, t) = 4\cos\left(0{,}25t - \frac{2}{33}\right)\cos\left(7{,}75t - \frac{31}{33}\right)$$

Therefore:

$$\omega_P = 7{,}75s^{-1}; \; \varphi_p = -\frac{31}{33}\text{rad}; \; \omega_M = 0{,}25s^{-1}; \; \varphi_m = -\frac{2}{33}\text{rad}$$

$$\frac{-\frac{31}{33}0{,}25 + 7{,}75\left(2\pi r + \frac{2}{33} + \frac{\pi}{2}\right)}{0{,}25 \cdot \pi} > m > \frac{-\frac{31}{33}0{,}25 + 7{,}75\left(2\pi r + \frac{2}{33} + \frac{3\pi}{2}\right)}{0{,}25 \cdot \pi}, r\epsilon\,\mathbb{Z}$$

If $r = 0$:

$$15{,}799 < m < 46{,}799 \rightarrow m = \{16, 17, \dots, 46\}$$

$$t_{0_1} = \left\{\frac{\pi \cdot m + 31/33}{7{,}75}, \frac{\frac{\pi}{2} \cdot p + 2/33}{0{,}25}\right\}, \quad m, p\,\epsilon\,\mathbb{Z}$$

For instance, if $m = 21$:

$$t_{0_1} = \frac{\pi \cdot 21 + 31/33}{7{,}75} = 8{,}6339, \quad m, p\,\epsilon\,\mathbb{Z}$$

It will be a maximum in $t_{0_1} = 8{,}6339$.

Now let us have the following wave:

$$u_2(x, t) = 4\cos\left(0{,}25t - \frac{4}{33}\right)\cos\left(7{,}75t - \frac{62}{33}\right)$$

Therefore:

$$\omega_P = 7{,}75s^{-1}; \; \varphi_p = -\frac{62}{33}\text{rad}; \; \omega_M = 0{,}25s^{-1}; \; \varphi_m = -\frac{4}{33}\text{rad} \qquad \text{Eq. 5.97}$$

Applying the same equations than for the other wave:

$$\frac{-\frac{62}{33}0{,}25 + 7{,}75\left(2\pi r + \frac{4}{33} + \frac{\pi}{2}\right)}{0{,}25 \cdot \pi} < m < \frac{-\frac{62}{33}0{,}25 + 7{,}75\left(2\pi r + \frac{4}{33} + \frac{3\pi}{2}\right)}{0{,}25 \cdot \pi}, r\epsilon\,\mathbb{Z} \qquad \text{Eq. 5.98}$$

If $r = 0$:

$$16{,}098 < m < 47{,}098 \rightarrow m = \{17,18,\dots,46\} \qquad \text{Eq. 5.99}$$

If $m = 21$:

$$t_{0_2} = \frac{\pi \cdot 21 + 62/33}{7{,}75} = 8{,}7551 \qquad \text{Eq. 5.100}$$

5.6. Elimination of the noise by using the method of least squares

The purpose of this method is to obtain a wave without noise with which it is possible to measure the phase and group velocities easily. In order to use this method, it is necessary to know the shape of the wave a priori, as the theoretical wave and the obtained wave in the simulation/measurements are going to be compared.

Let us assume that the function $u(x, t, \beta_0)$ that best adjust to the serial of values $\{w_k\}_{k\in\mathbb{N}}$ obtained in simulation/measurement is wanted to be calculated. The value of the square difference for every k has to be minimized and so the function $u(x, t, \beta_0)$ is going to be defined as:

$$u(x, t, \boldsymbol{\beta_0}): \; S(\boldsymbol{\beta_0}) = \min[S(\boldsymbol{\beta})] \qquad \text{Eq. 5.101}$$

where

$$S(\boldsymbol{\beta}) = \sum_{k=1}^{N} [w_k - u(x, k \cdot T, \boldsymbol{\beta})]^2, \boldsymbol{\beta}\epsilon\,\mathbb{R}^m, \qquad \text{Eq. 5.102}$$

where N is the number of samples of the serial $\{w_k\}_{k\in\mathbb{N}}$, m is the number of parameters that can be changed in the function $u(x, t, \boldsymbol{\beta})$ and T is the period sample.

For example, suppose a serial of numbers like the ones in the first two columns of Table 5.2 want to be adjust by a sinusoidal wave. What it wants to be minimized is the sum of the quadratic difference between the values that want to be adjusted and the calculated wave for every point. This calculated wave is obtained by iteration by changing the values of the amplitude, the frequency and the phase delay. Therefore:

$$\boldsymbol{\beta} = (A, \omega, \varphi)$$ **Eq. 5.103**

$$u(x, t, \boldsymbol{\beta}) = A \cdot \cos(\omega t + \varphi)$$ **Eq. 5.104**

The points which are solution for this optimization are shown in the third column of Table 5.2.

$t_k = T \cdot k$	w_k	u_k	$(u_k - w_k)^2$
0	0,065	0,0696797	2,19E-05
0,1	-0,45	-0,51948095	0,0048276
0,2	-0,99	-0,90922631	0,00652439
0,3	-0,98	-0,9499432	0,00090341
0,4	-0,61	-0,62600148	0,00025605
0,5	0	-0,06175398	0,00381355
0,6	0,45	0,52619927	0,00580633
0,7	1	0,91215823	0,00771618
0,8	0,88	0,94796325	0,004619
0,9	0,57	0,6198697	0,00248699
1	0,12	0,05382421	0,00437923

Table 5.2: Values used to perform an optimitation by the method of least squares

The solution that best fits to the values is:

$$\boldsymbol{\beta_0} = (0{,}980; 6{,}30; 1{,}50)$$ **Eq. 5.105**

$$u(x, t, \boldsymbol{\beta}) = 0{,}980 \cdot \cos(6{,}30t + 1{,}50)$$ **Eq. 5.106**

These values of the amplitude, frequency and phase delay minimize the sum:

Eq. 5.107

$$S(\boldsymbol{\beta_0}) = \sum_{k=1}^{11} [w_k - u(x, k \cdot T, \boldsymbol{\beta_0})]^2 = 0,04135$$

The solution is shown in Image 5.13
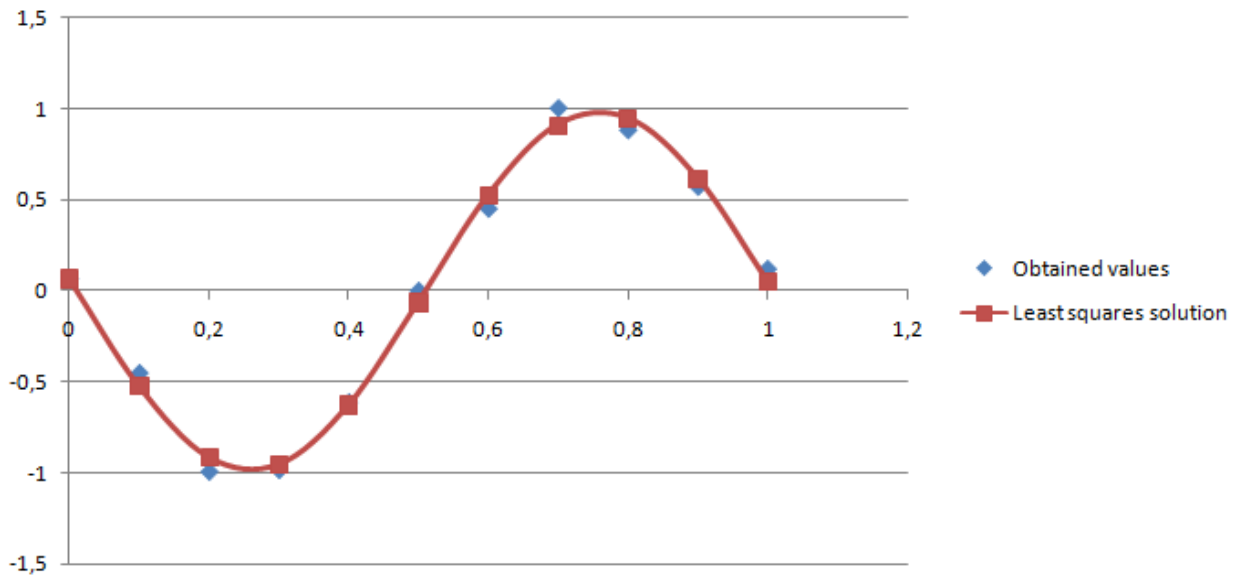
Image 5.13: Approximation of a sample of values to a sinusoidal wave.

This method can be also used for any other kind of signals and it is not affected by the noise. After obtaining the signal that best fits to the values, it is easy to calculate any other parameters concerning this signal.

5.7. Elimination of the noise by using filters

The purpose of this method is to eliminate any other signal or noise that has a frequency different than the one with which the pipe is being stimulated. After removing all the other components of the signal, it is possible to use one of the methods mentioned in this chapter.

The kind of filters that will be used are lowpass filters and bandpass filters. The first one can be used to eliminate noise, since noise has much higher frequencies than the ones with which the pipe is stimulated. Therefore, with a lowpass filter, only the low frequencies are kept and the high frequencies are removed, eliminating the noise and obtaining a clearer signal.

Besides, bandpass filters can be used to keep one range of frequencies and remove the rest ones. It can be used to select a part of the spectrum of a signal, such as a narrow band that includes the frequency with which the pipe is excited. By doing this, only the component with this frequency

will be kept and any other frequency will be removed, avoiding, thus, noise components and, sometimes, reflection components.

For every kind of filter, there are a wide range of possibilities to obtain it. In this thesis, two different ways to obtain filters (FFR and IIR) are going to be used depending on the computing time, the phase shift originated by the applied filter, and the magnitude obtained in the frequency response.[24]

The techniques for designing FIR, Frequency Impulse Response, filters are based on directly approximating the desired frequency response of the discrete-time system. For a FIR filter, Equiripple is the method that is going to be used, whose characteristics can be seen in the appendix B. 1. FIR Equiripple. This method will be used when the computing is not an important factor and the obtained method does not have a lot of coefficients. Therefore, it can be used when a bandpass filter of a wide band is needed or with a lowpass filter. [25] [26]

IIR filter design is based on transformations of continuous-time IIR systems into discrete-time IIR systems. For an IIR filter type, Butterworth and Elliptic are among the better known design methods and will be the ones used in this thesis. Their characteristics can be checked on the appendices B. 2. IIR Butterworth and B. 3. IIR Elliptic. Elliptic method will be selected when the desired phase shift is small. Butterworth will be chosen when the frequencies out of the selected range are wanted to be removed with a really important factor, and when the phase shift that applying this filter originates in the original signal is not an important characteristic. [27] [28]

The advantage of IIR filters compared with FIR ones is that they need smaller coefficients to perform the filter operations, that is to say, their order is lower. Therefore, IIR filters are executed faster and do not need extra memory. Nevertheless, the disadvantage of IIR filters is that their phase response is not lineal and can only be used when this information is not important. However, when applied an IIR Elliptic, its phase response is not lineal but its values are close to zero in the band selected.
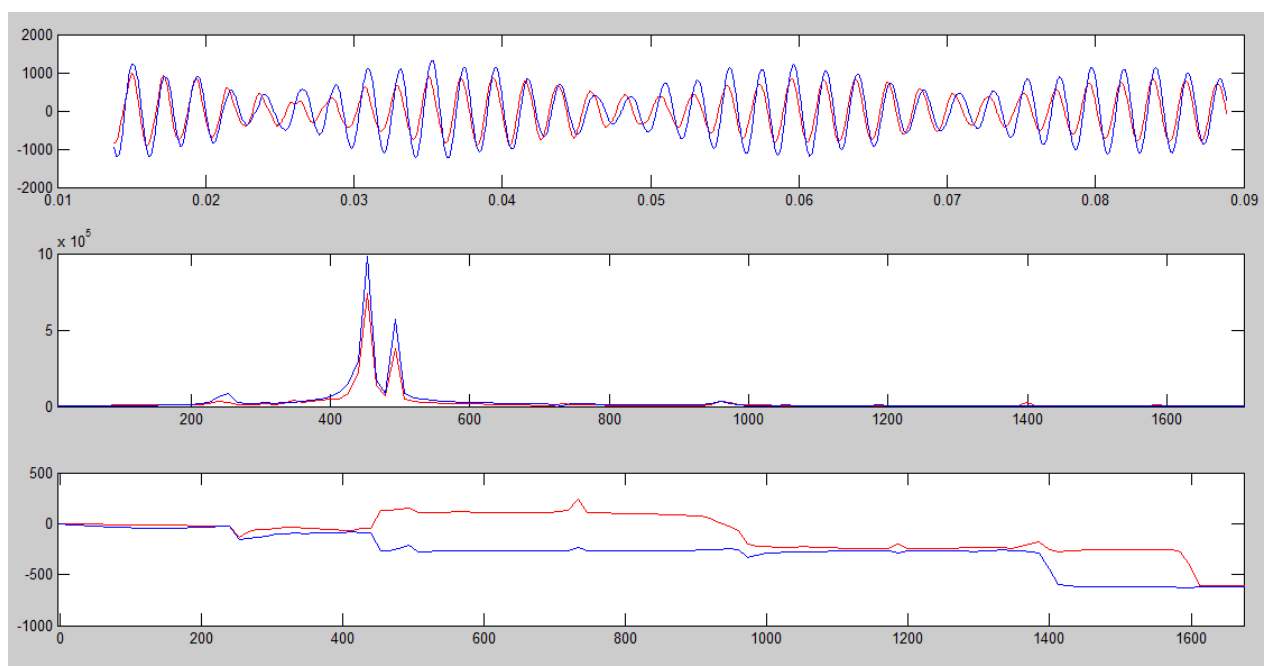
Image 5.14: Fourier transform of two waves without been filtered.

5.7.1 Example of using the filter to calculate the phase velocity with the method of phase shift

To show an example of how this method works with waves formed by the superposition of different waves, the Fourier transform of two waves is going to be performed so as to calculate the phase shift. In Image 5.14, the two obtained waves for two probes are shown. Besides, the Fourier transform is displayed in the same image. It is clear that it is difficult to measure the phase shift with the obtained diagram. However, if the signals are filtered and only the frequency of $f = 450Hz$ is not filtered, the result of the phase shift when performing the Fourier transform is much clearer, as it can be seen in Image 5.15. The phase diagram does not have any noise and both signals follow the same curve but displaced in a finite value.
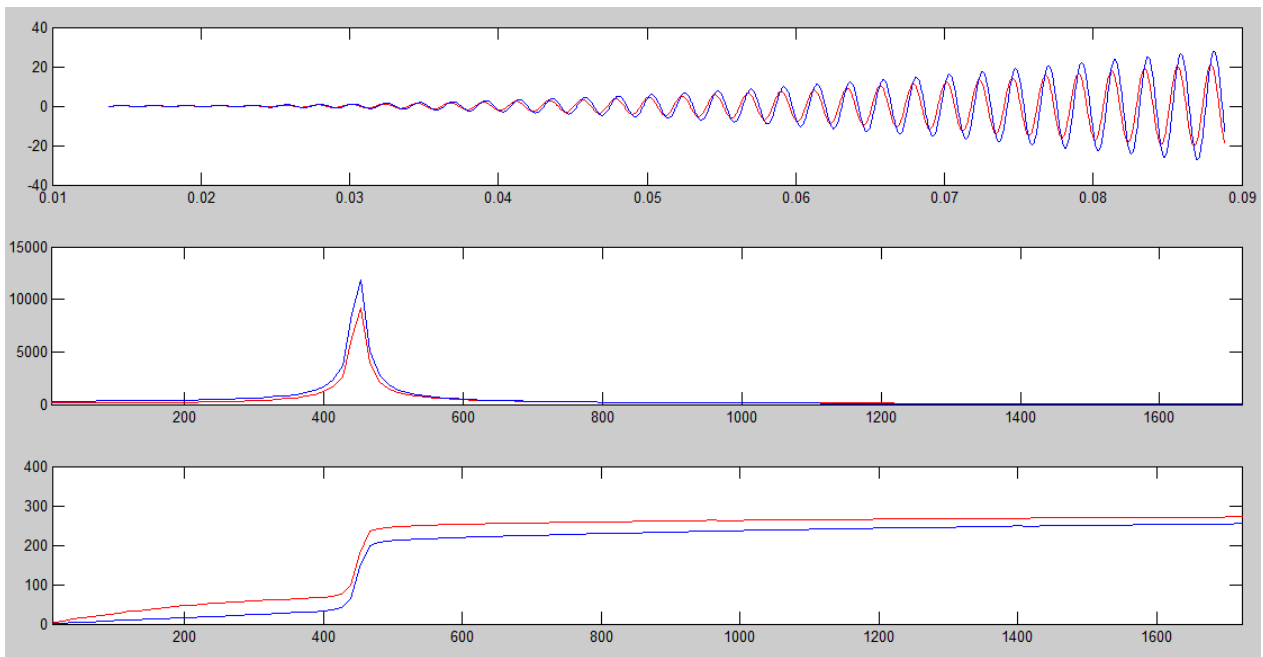
Image 5.15: Fourier transform of two waves after been filtered.
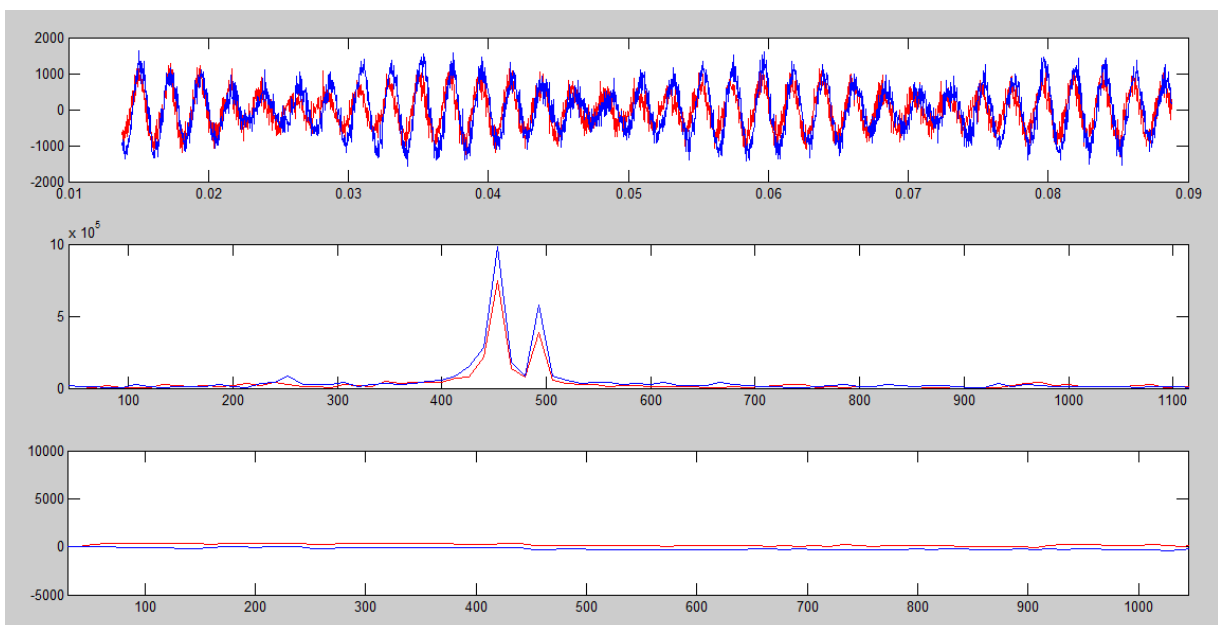
Image 5.16: Fourier transform of two noisy waves without filtering them.

Let us now have two noisy waves like the ones in the previous example, as the ones shown in Image 5.16. If the Fourier transform is applied to these two signals, the result of the phase diagram is not clear at all and make it difficult to measure any phase shifts. However, if a bandpass filter of $f = 450 Hz$ is applied, the two waves become exactly the same than the ones in the example without noise and it is now possible to measure the phase shift, as it can be seen in Image 5.17.
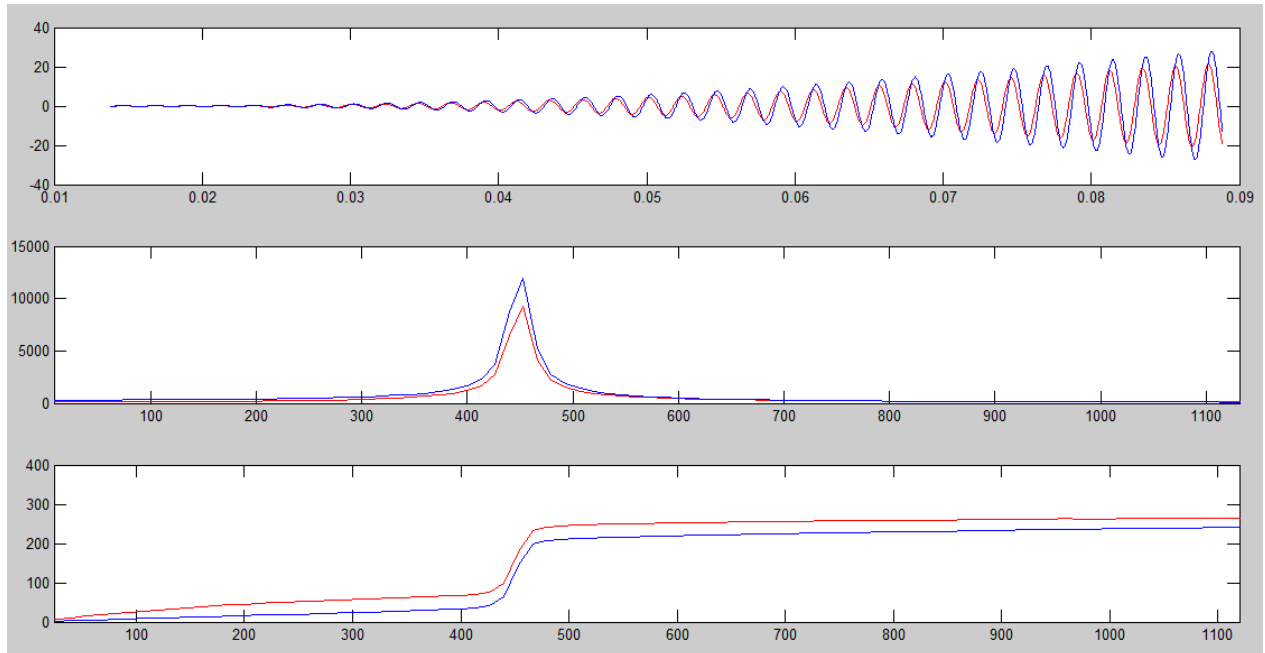
Image 5.17: Fourier transform of two noisy waves after filtering them.

6. Simulations

6.1. Straight pipe stimulated by plane source

It has been simulated a straight elastic PVC pipe of the characteristics shown Table 6.1 with a plane source in one of its extremes. This source produces a sinusoidal wave pressure of a specific frequency, which is propagated through the pipe. The length of the pipe is changing depending on the stimulating frequency in order to avoid reflection effects. For this reason, the length of the pipe is going to verify that:

$$L > 2 \cdot \lambda = 2 \cdot \frac{v_p}{f}$$

Eq. 6.1

As the phase velocity is going to have values about $500 \, m/s$ and the lowest frequency is going to be 300 Hz, the largest length will be:

$$L < 2 \cdot \frac{500}{300} = 3{,}33 \text{m}$$

Eq. 6.2

Density (ρ)	$1380 \dfrac{kg}{m^3}$
Young's modulus (E)	$5{,}787 \cdot 10^9 \, Pa$
Posisson's ratio (ν)	0,3
Coefficient of thermal expansion (α)	$100 \cdot 10^{-6} \, K^{-1}$
Relative permittivity (ε)	2,9
Thermal conductivity (k)	$0{,}1 \dfrac{W}{m \cdot K}$

Table 6.1: Characteristics of the simulated PVC pipe.
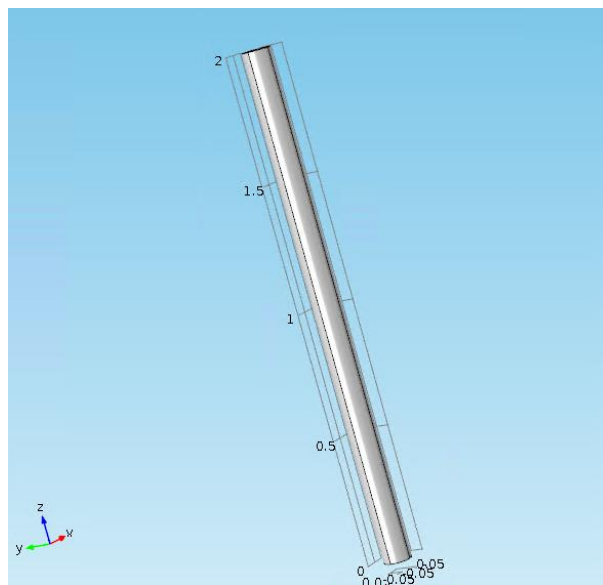
Image 6.1: Diagram of the simulated PVC water-filled pipe.
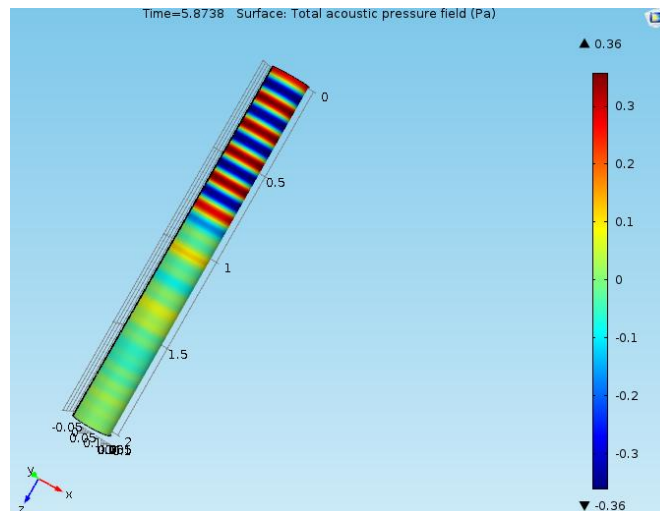
Image 6.2: 3D model result of the propagation of an acoustic pressure wave within a plastic pipe.

However, this length can be reduced in higher frequencies and it will not be a problem if it is reduced in low frequencies because the condition for the length was to be bigger than two times the wavelength and being once bigger is enough. To illustrate how important the reflection effects are, in Image 6.2, it is possible to appreciate the propagation of the sound wave within the modeled pipe in $t = 5{,}8738s$ for a frequency of $f = 1000\text{Hz}$. There are points in which the pressure is positive and other in which it is negative because the wave source is a sinusoidal wave that has positive and negative values. It is also important to mention that the pressure changes not only in the points that the sound wave have reached, but also in the next ones. In this image, the sound wave has not reached the end of the pipe and, therefore, there are not reflection effects.
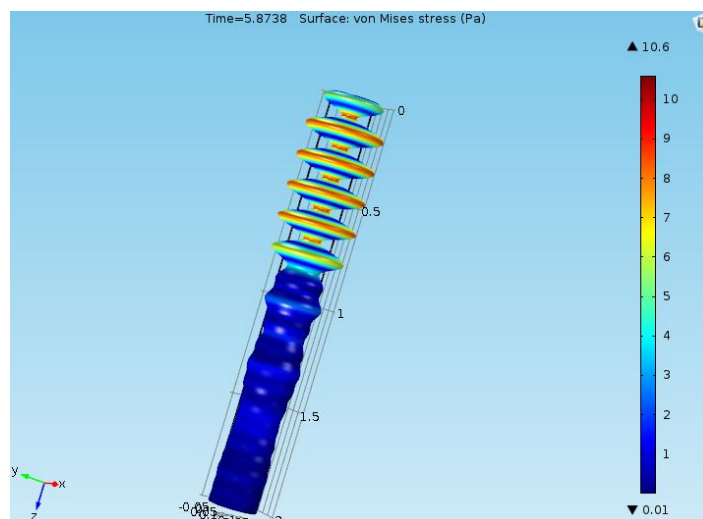
Image 6.3: 3D model of the stress caused by the propagation of an acoustic pressure wave within a plastic pipe.

Besides, in Image 6.3 the stress caused by the propagation of the sound wave is shown. The points which have more stressed correspond to the ones in which the pressure is higher, as it can be seen by comparing this image with Image 6.2. In the points at which the wave has not arrived, the stress is close to zero.
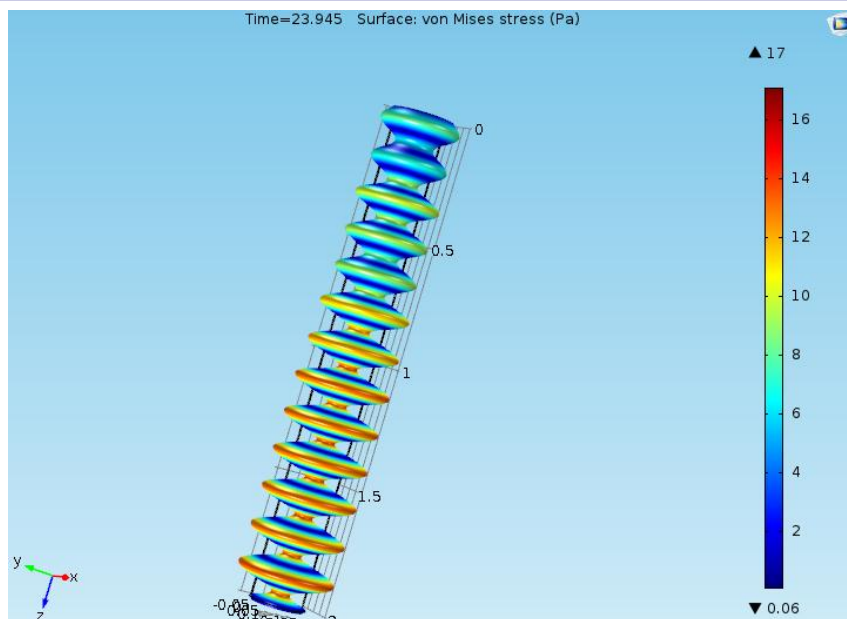
Image 6.4: 3D model of the increase in the stress of a plastic pipe caused by the reflection of an acoustic pressure wave.

Nevertheless, in Image 6.4, the stress in the elastic pipe in $t = 23{,}495 s$ is displayed. At this point of the time, the sound wave has had time to travel along the pipe and be reflected on the ending wall of the pipe. Due to this reflection effect, the stress of the pipe is increased considerably reaching maximum values of $p = 16{,}5\ Pa$, whereas without reflection, the maximum pressure values were $p = 10\ Pa$. The reflection effects can produce measurement errors due to the interferences of different waves and, therefore, increase the values of both the pressure and the stress. For this reason, it is very important to take into account these reflection effects, as the changes in both pressure and stress values change significantly.

Different probes have been set along the pipe in different positions in order to measure the phase velocity of the sound wave at different frequencies and to decide which positions are good to carry out this measurement.

In order to measure the phase velocity of the sound wave, the values that the probes get are saved and adjusted to a sinusoidal wave by method of the least squares in following the next steps:

1.   Select a part of the wave that looks like a sinusoidal wave.

2.   Introduce a sinusoidal wave of the same frequency that the one which has been simulated with a amplitude similar to the one has been simulated.

3.   Calculate the error between this sinusoidal wave and the points obtained in the simulation by the following expression:

Eq. 6.3

$$\varepsilon = \sum_{i=1}^{n} [p_i - s(t_i)]^2$$

4.   Minimize the error calculated by changing the parameters of the sinusoidal wave. This is done by an iterative procedure by the tool Solver of Microsoft Office Excel 2010.

As the distance among proves is known, it is possible to calculate the phase velocity of the sound wave at the simulated frequency as it was explained in the section Phase velocity by measuring the time elapse between the time in which the first probe reaches a certain value, and the time in which the second probe reaches that same value.

The method just explained is going to be developed now with an example.

There is a stimulating sinusoidal wave that produces one wave in every probe, which can be seen in Image 6.6. Afterwards, a time range from these waves is selected so that both waves look quite similar to a sinusoidal wave and, then, they are adjusted to a sinusoidal wave by the method of least squares. The part selected of the two waves and the adjustment is shown in Image 6.6.
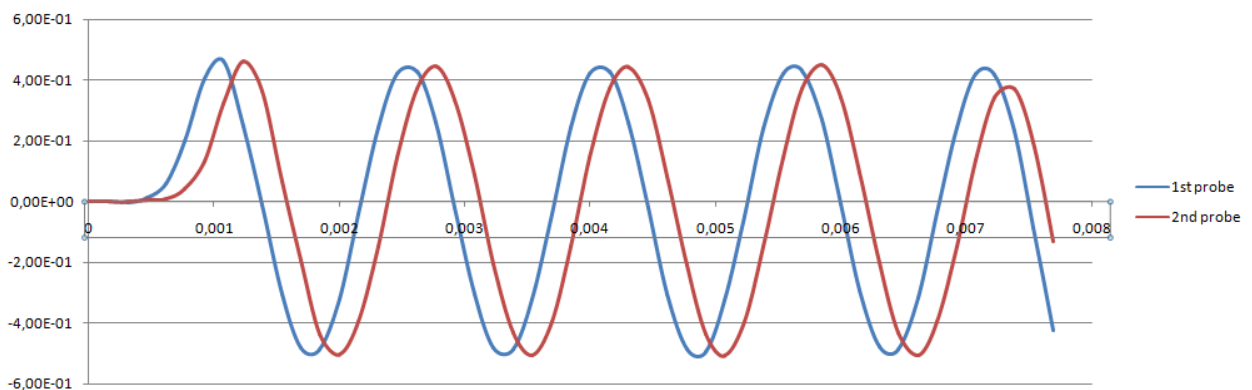
Image 6.5: Obtained values from two different probes.
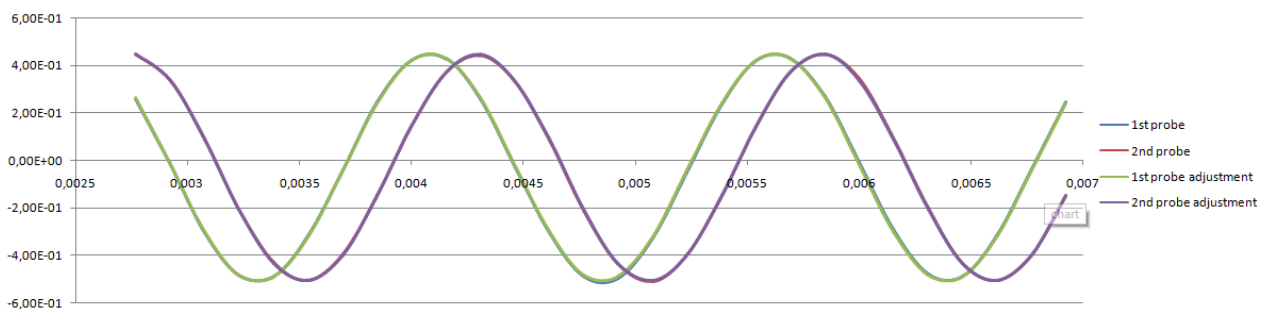
Image 6.6: Approximation of two obtained waves with the method of least squares.

In this case, the two waves obtained with this method are:

$$u_1 = -0,029248 + 0,47983 \sin(2\pi \cdot 650 + 3,7434)$$

Eq. 6.4

$$u_2 = -0,029938 + 0,47701 \sin(2\pi \cdot 650 + 2,8900)$$

Eq. 6.5

Therefore, the phase difference is:

$$\varphi = 3{,}7434 - 2{,}8900 = 0{,}85338 \text{ rad} \qquad \textbf{Eq. 6.6}$$

Thus, the time difference is:

$$t = \frac{\varphi}{2\pi f} = \frac{0{,}85338}{2\pi \cdot 650} = 0{,}20895 \text{ ms} \qquad \textbf{Eq. 6.7}$$

$$v_p = \frac{d}{t} = \frac{0{,}1\text{m}}{0{,}20895 \text{ ms}} = 478{,}58 \text{ m/s} \qquad \textbf{Eq. 6.8}$$
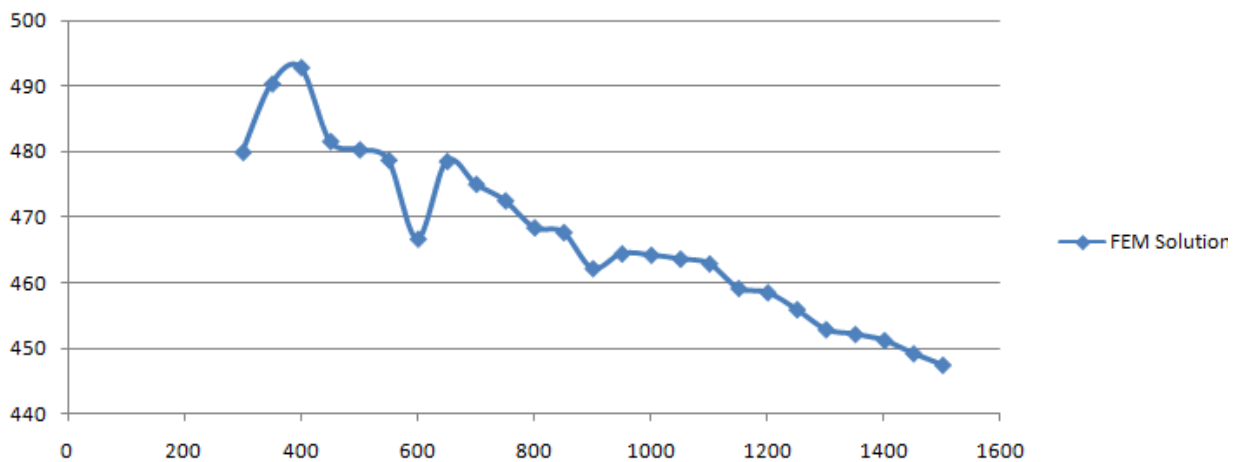
Image 6.7: Phase velocity on frequency dependency obtained with FEM simulation for a water-filled PVC pipe of D=11cm.

Doing this for a wide range of frequencies, the phase velocity for these frequencies is shown in Image 6.7 and the exact values are displayed in Table 6.2.

Frequency (Hz)	Phase velocity (m/s)	Frequency (Hz)	Phase velocity (m/s)
300	479,98	950	464,5
350	490,41	1000	464,29
400	492,89	1050	463,7
450	481,65	1100	462,98
500	480,37	1150	459,22
550	478,78	1200	458,58
600	466,75	1250	455,99
650	478,58	1300	452,95
700	475,11	1350	452,21
750	472,59	1400	451,28
800	468,48	1450	449,28
850	467,76	1500	447,52
900	462,25		

Table 6.2: Values of the phase velocity for different frequncies obtained by FEM simulation of a water-filled PVC pipe of D=11cm.
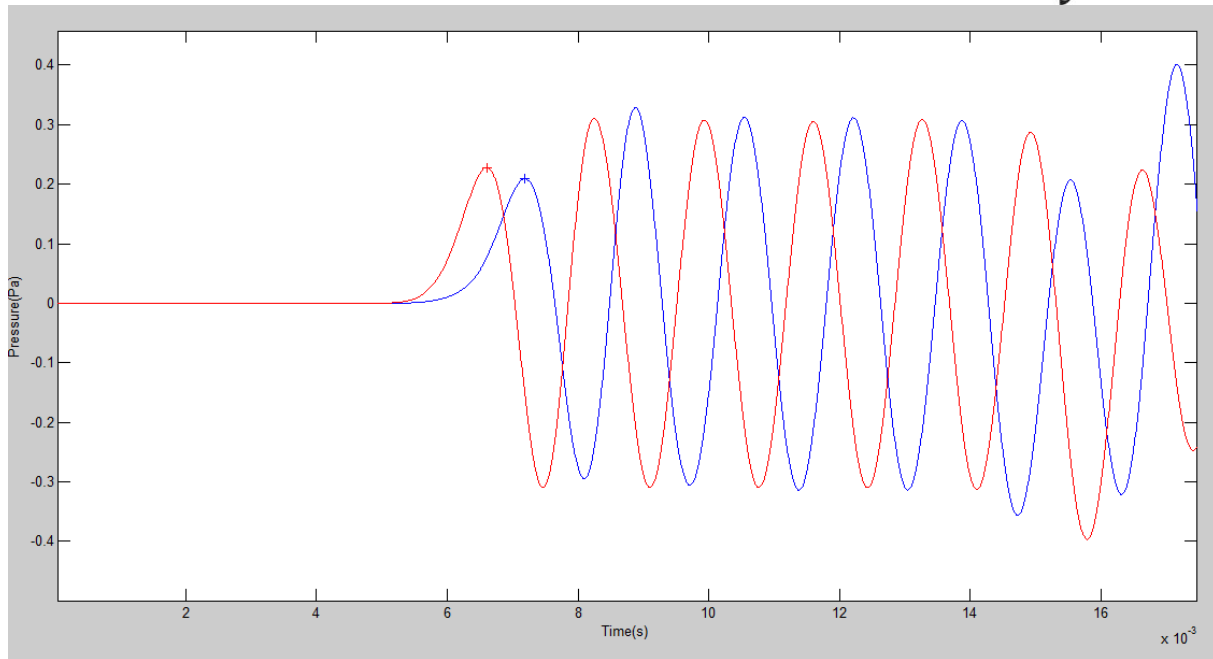
Image 6.8: Obtained signals after filtering the acquired signals for two probes in FEM simulation with 0,2m of distance to each other when a water-filled PVC pipe of 0,22m of diameter is excited with a sinusoidal wave.

In order to see what the result is when a different diameter is set, it has been simulated a pipe with the same characteristics than previously but with a diameter of $D = 0,22\ m$. In this case, the method to calculate the phase velocity was not working properly and it was decided to measure the first peak of the first transient in the probes when the pipe is excited when it is excited with a sinusoidal wave like previously. Nevertheless, the acquired signals have also noise and it has been decided to use an IIR Butterworth lowpass filter so as to reduce it -noise has high frequency- because it does not have too much calculation time, the phase shift produced by it does not affect to the obtained signals because they are long enough, and after the cutoff frequency of the filter the components are reduced significantly. In Image 6.8, the acquired signals for two probes with a distance to each other of $d = 0,2m$ is displayed and the two points which are selected to measure the phase velocity are highlighted. Measuring the time elapse between these two points, it is possible to obtain the phase velocity since the distance is known.

Image 6.9: Phase velocity obtained in FEM simulation for a water-filled PVC pipe of 0,22m of diameter.

In Image 6.9 and in Table 6.3 the obtained values for the phase velocity for a PVC pipe of 0,22m of diameter is displayed. These values are all of them close to $350\ m/s$ with a deviation of

about 5%. It is possible to see that the values are decreasing until the frequency of $1kHz$ but, after it, they start to increase until the end of the range of frequencies simulated.

Frequency(Hz)	Phase velocity(m/s)
300	360,000
350	362,069
400	363,6364
450	360,000
500	357,1429
550	351,0638
600	349,5146
650	348,2143
700	347,1074
750	343,5115
800	340,4255
850	337,7483

Frequency(Hz)	Phase velocity(m/s)
900	335,4037
950	335,2941
1000	337,0787
1050	336,8984
1100	340,2062
1150	341,5842
1200	349,5146
1250	353,7736
1300	361,1111
1350	368,1818
1400	375,000

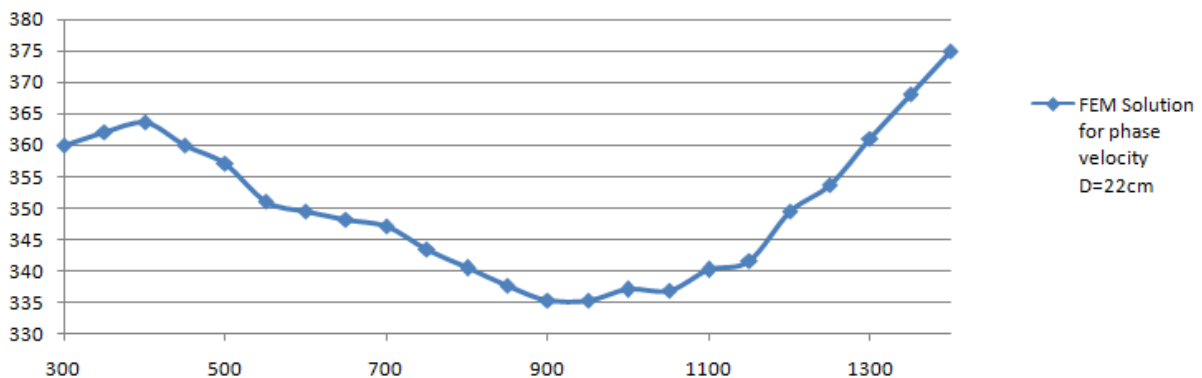Table 6.3: Exact values for phase velocity obtained in FEM simulation for a water-filled PVC pipe of 0,22m of diameter.

Comparing the results obtained for the two different frequencies (Image 6.10), a constant gap of about $120\,m/s$ between them is seen. Besides, the phase velocity for the simulation done with the smaller diameter is always decreasing on frequency dependency, whereas the other is decreasing and then increasing. This could be produced to the existence of a first cutoff frequency for the bigger diameter in $1kHz$. This first cutoff frequency for the smaller diameter must be in higher frequencies and, thus, the phase velocity does not increase on these range of frequencies.
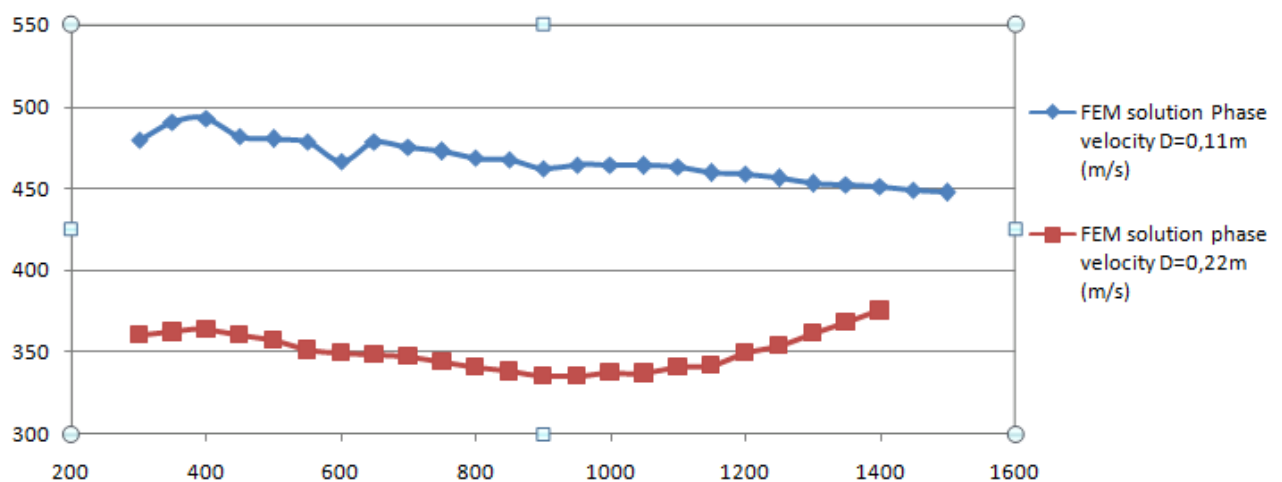
Image 6.10: Phase velocity comparison between the obtained in FEM simulation for a water-filled PVC pipe of D=11cm and one of D=22cm.

6.2. Bent pipe stimulated by plane source

The Image 6.11 shows the model of the pipe that is going to be proved so as to measure the phase velocity of the sound inside it. It has been highlighted in blue the surface that is going to play the role of exciter. This source is going to transmit a continuous sinusoidal wave for a specific time.

By changing the frequency of this wave, we are going to be able to draw the dispersion diagram of the phase velocity depending on the frequency.

A lot of probes have been placed before and after the bending in order to obtain different waves and then choose the ones with which is easier to measure the phase velocity.
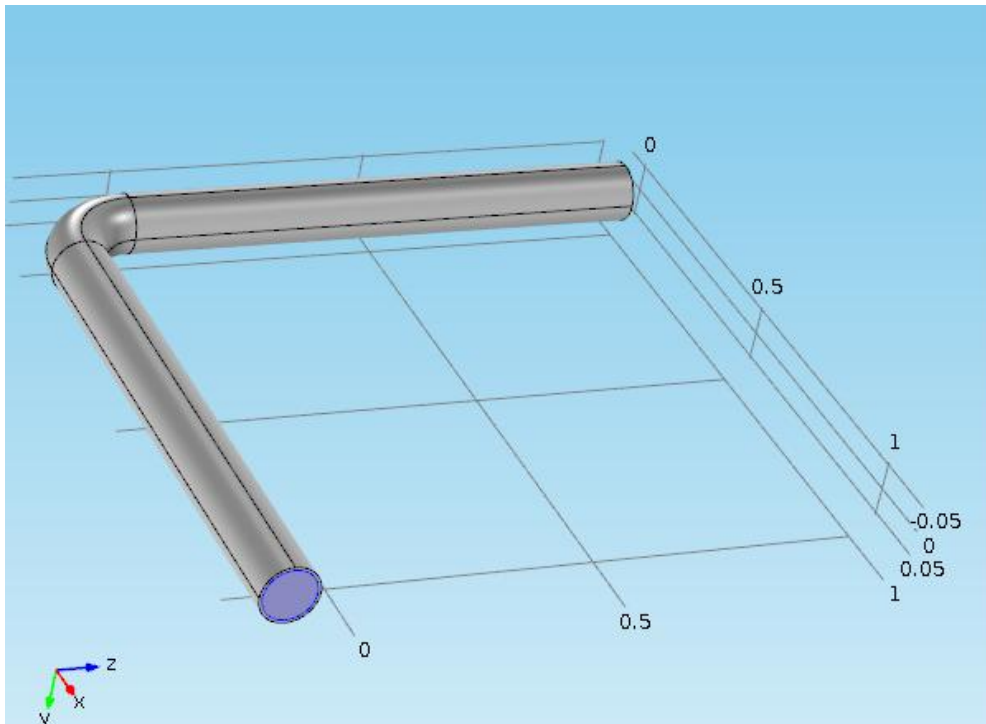
Image 6.11: Model used to simulate a bent pipe.
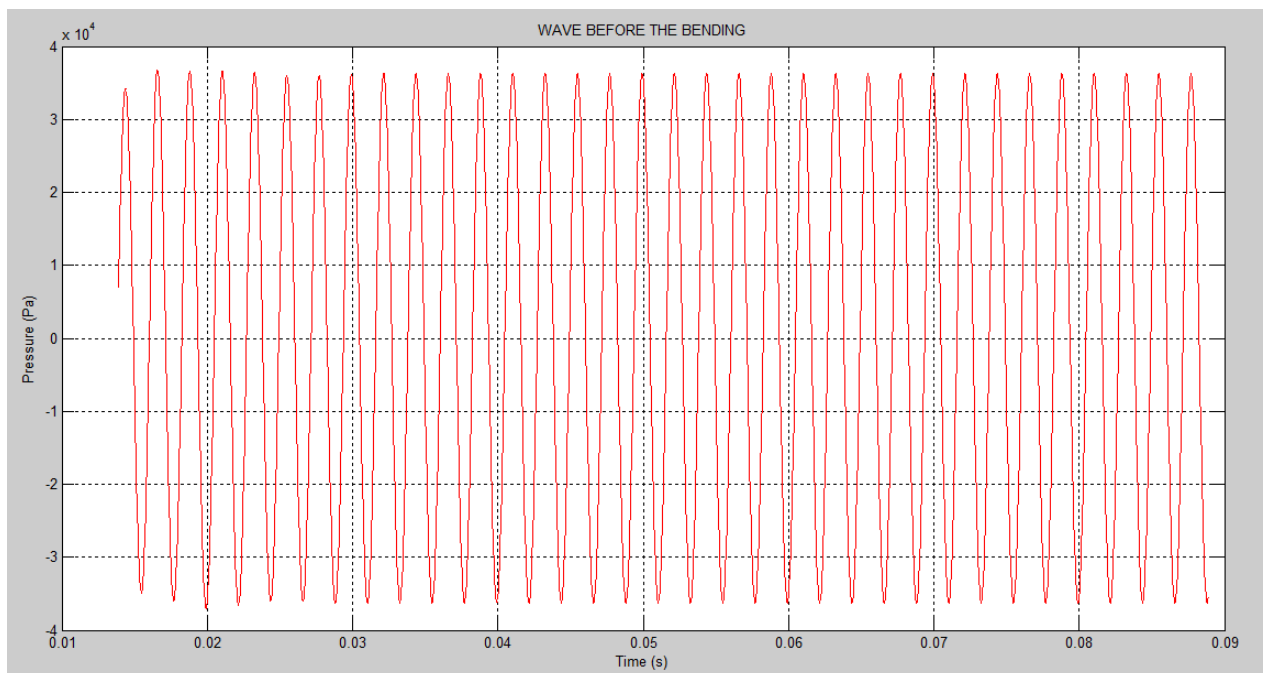
Image 6.12: Obtained wave before the bending.

There is a difference of the shape wave before and after the bending. Before of the bending, the waves obtained by the sensors is clearly a sinusoidal wave, as it can be seen in Image 6.12, where

66

the excitation frequency was $f = 450Hz$ and the length of both sides of the pipe was $L = 1m$. In this case, the phase velocity can be easily calculated as it was done in the simulation section 6.1. by adjusting the two obtained waves (Image 6.15) to two sinusoidal waves resulting a phase velocity of $v_p = 538{,}63 \, m/s$. However, in order to be sure that the reflection is not affected to this result, it is possible to measure the phase difference a t the beginning of the wave, where the wave has not had enough time to travel to the first part of the pipe and reflect on the bending. By doing this, the result of the phase velocity is $v_p = 527{,}25 \, m/s$. Therefore, both results are quite similar and it is possible to say that the reflection effects in this case do not affect considerably to the phase velocity and it is possible to measure the phase velocity as it was done in the section 6.1. The deviation in the second result for the phase velocity can be also produced due to the lack of sample points at the beginning of the signal.
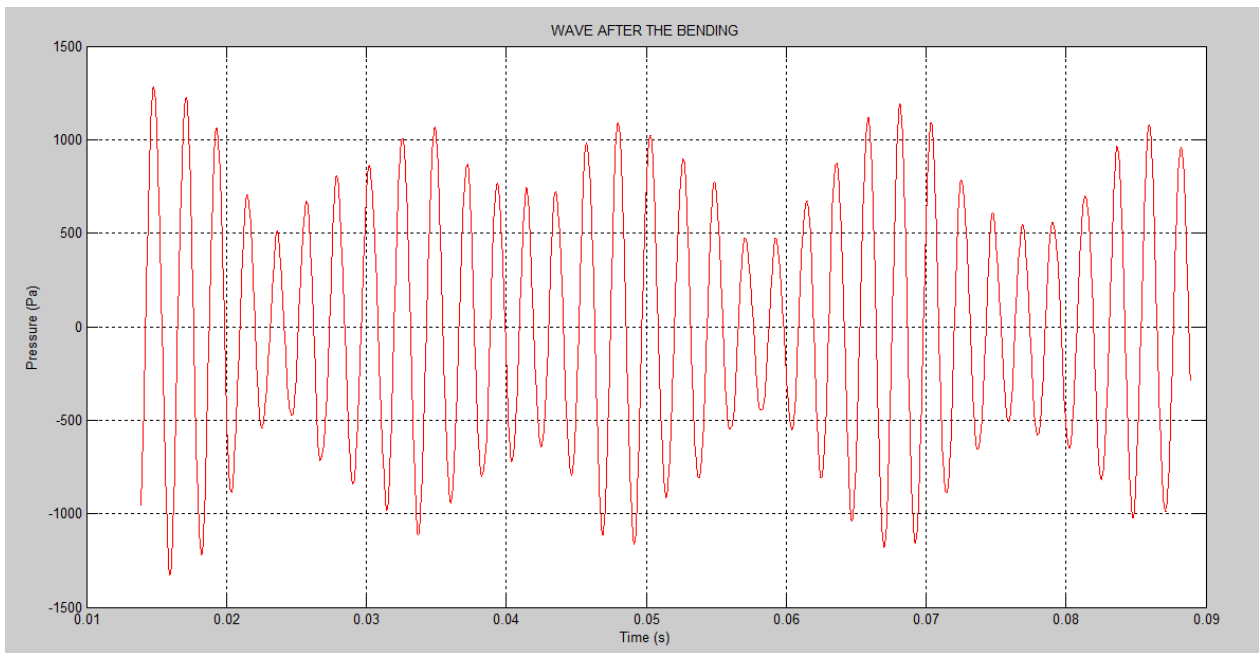
Image 6.13: Obtained wave after the bending.

Continuing measuring the phase velocity for the different lengths, the results that are obtained are shown in Table 6.4 and in Image 6.14. It is possible to appreciate an increase in the phase velocity when the length rises. However, this increase is not really significantly as it is only 1%.

Length (m)	Phase velocity (m/s)
1	538,63
1,5	539,87
2	539,51
2,5	542,23
3	543,79

Table 6.4: Phase velocity before the bending on length dependency.

Nevertheless, if a look is taken after the bending, the wave is now not a sinusoidal wave, but a composition of waves, as it can be seen in Image 6.13. This composition of waves can be written as follows:

$$u(t) = A_1 \cos(\omega_1 t + \varphi_1) + A_2 \cos(\omega_2 t + \varphi_2)$$

Eq. 6.9
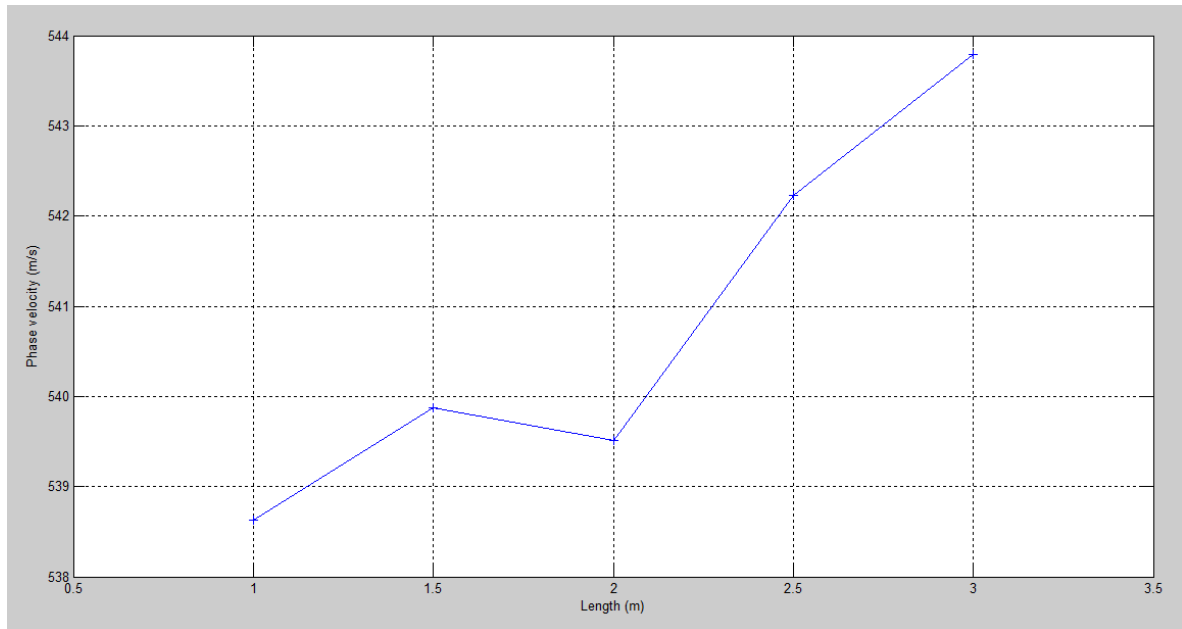
Image 6.14: Phase velocity before the bending on length dependency.
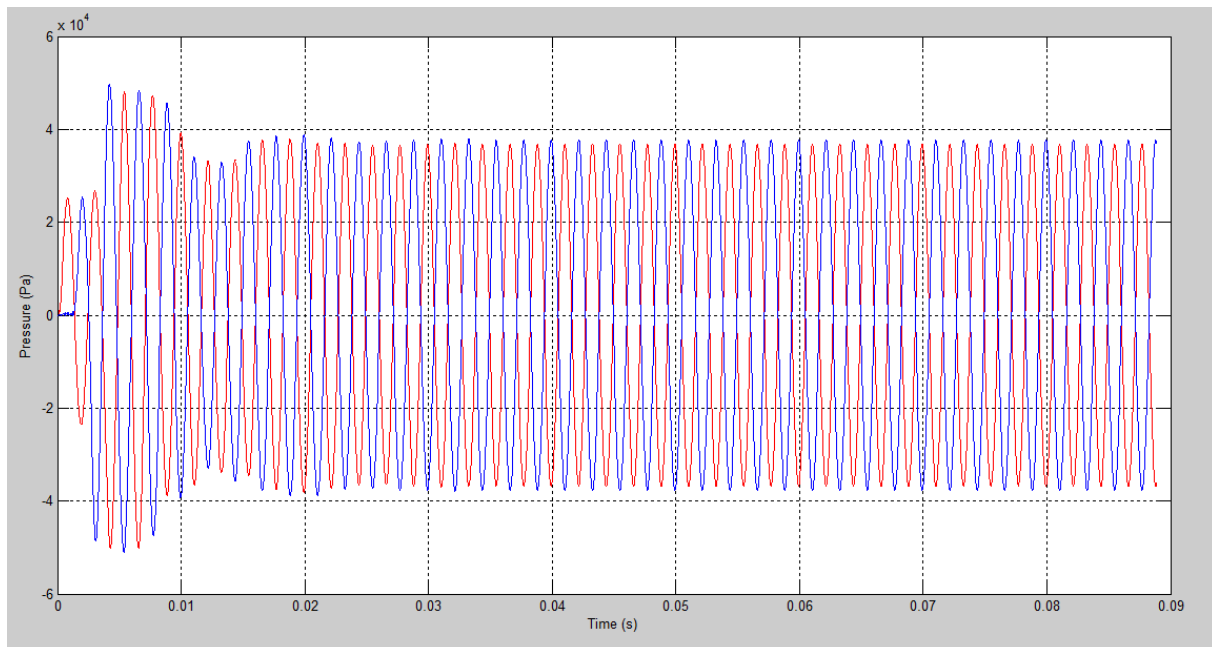
Image 6.15: Signals obtained by two probes before the bending with a distance to each other of d=0,6m.

Therefore, it will be possible to adjust the obtained wave to an addition of two waves with the method of least squares as it has been also done for the other simulations. The first frequency ω_1 is going to be logically the excitation frequency, and the second frequency is unknown and a

68

Image 6.16: Approximation to different waves for different values of the length of the pipe. Graph with the "second" frequency on length dependency.

In Image 6.16 the obtained waves by simulation are displayed in blue, and the adjust waves in red. It is easy to see that the adjustment fits well. In the last graph of this image it is possible to see the "second" frequencies corresponding to the value $\omega_2/2\pi$. This values describe a curve reaching a maximum in the length of $L = 2m$.

Note that the waves are obtained by different probes, but this fact does not affect to the final result as it has been also proved that this "second" frequency does not depend on the place of the probe. This is verified by measuring the "second" frequency for the same length and obtaining the same value in all the probes.

In order to be sure that this "second" frequency is well calculated, a Fourier transform of the original waves is performed. By doing this, it is possible to see the peaks in the frequency spectrum so as to obtain which values of frequency predominate. Of course, there is going to be a peak in $f = 450Hz$ and the second biggest peak will have to be the same value than the obtained by the previous method.

The MATLAB script which is going to be used for this aim is shown in A. 9. Fourier transform for different waves for different lengths.

In Image 6.17, the result of performing the Fourier transform is shown. There is a peak in $f = 450Hz$ as it was expected and other peaks in different frequencies. In the last graph of this image, the frequency of second biggest peak is displayed with the length of the pipe. This graph is almost the same than the one obtained with the other method. The difference can be explained because the analyses of the Fourier transform is not performed with enough frequency values, thus

there are some missing frequencies and some of them are mixing together. Besides, it can also be explained because there can be more than one "second" frequency.
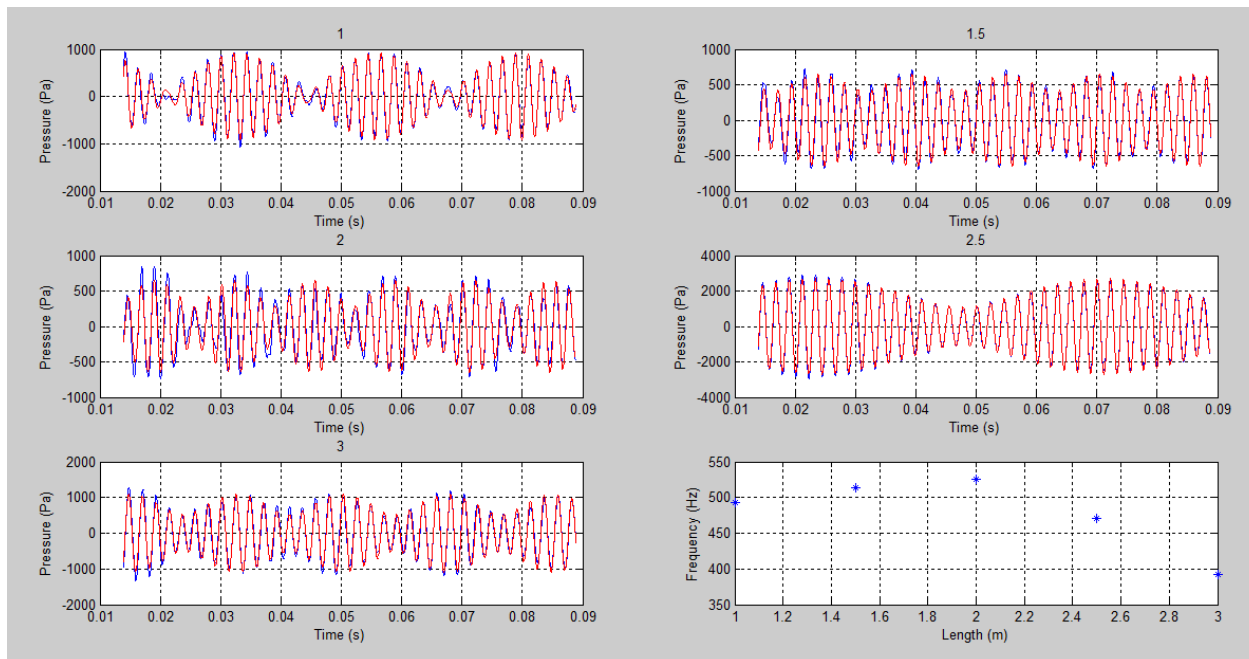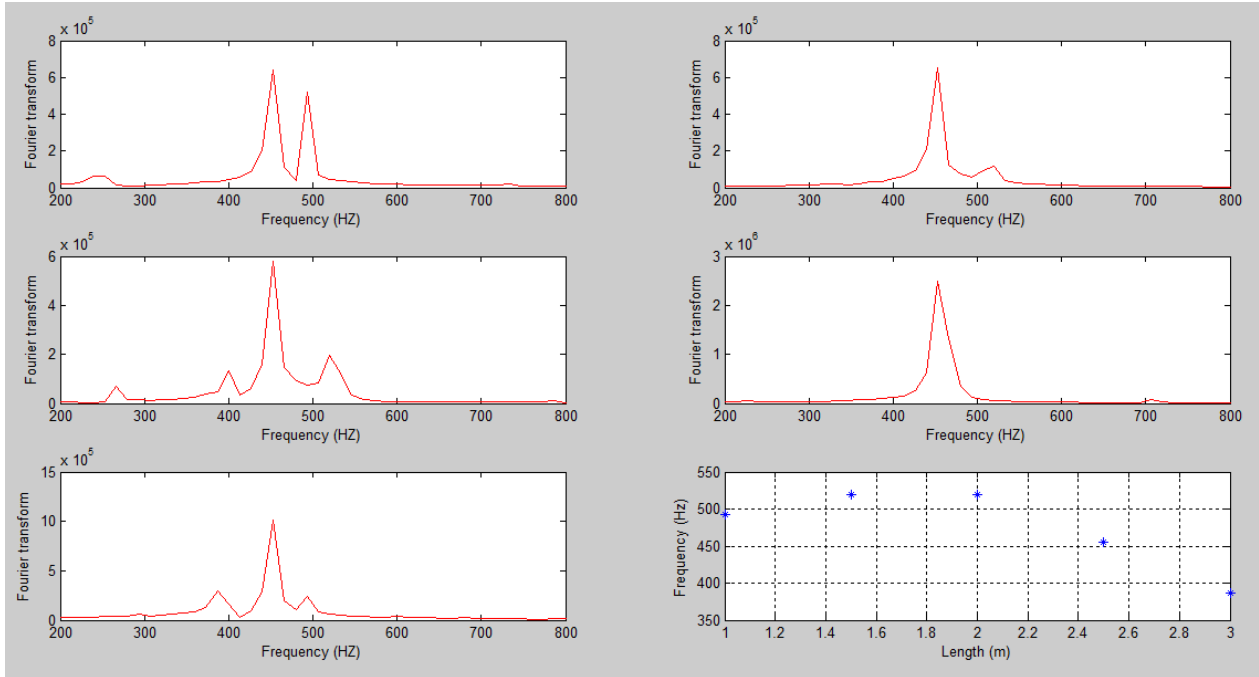

Image 6.17: Fourier transform of different waves for different values of the length of the pipe. Graph with the "second" frequency on length dependency.
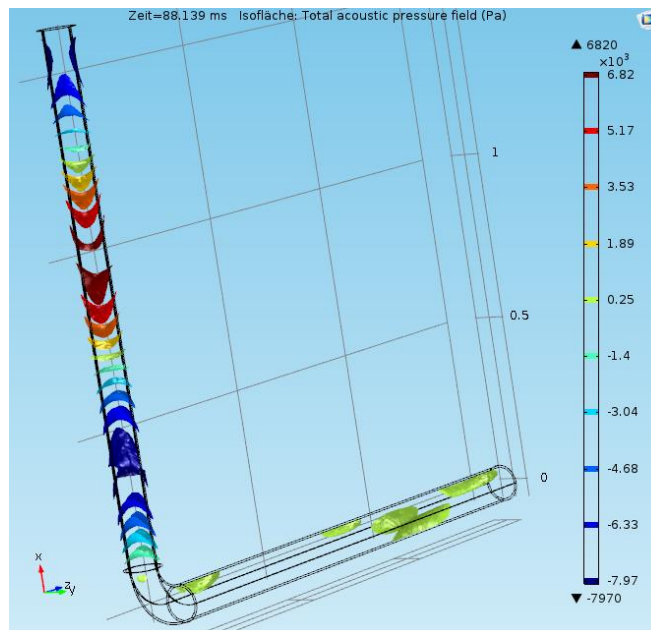
Image 6.18: Change of the orientation of the acoustic pressure isosurfaces after the bending.

An effect which is also important to notice is related to the propagation of acoustic pressure isosurfaces along the pipe. It has been seen that in a straight pipe they are perpendicular to the propagation of the sound. This effect is also possible to be appreciated before the bending of the pipe. However, after it, the isosurfaces are now parallel to the axial axis of the pipe. This effect is displayed in Image 6.18. It can be explained due to the multiple reflection that the wave suffers when

it crushes with the wall of the pipe in the bending. For further explanation about this effect in high frequencies, it can be read the reference [29].

In Image 6.19 the stress that the pipe suffers is shown. Before the bending of the pipe, it is possible to notice a torsional stress quite important that does not occur after the bending. This stress did not occur when the pipe was not bent. Therefore, an important study of the characteristics of the pipe should be taken in order to avoid any failures when the pipe is bent.
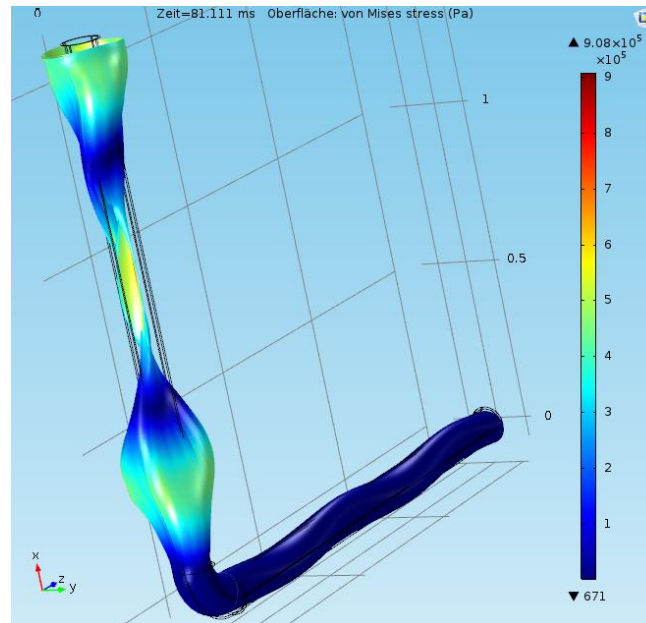
Image 6.19: Stress of the bending pipe.

7. Measurements

7.1. Selection of transducers

Before starting measuring the propagation of sound waves inside the pipe filled with water, it is necessary to select which converters are going to be used in order to produce and measure these waves. For these reasons, different transducers are going to be used and their frequency responses (transfer function) are going to be calculated in order to decide which ones are the best ones. The measurement consists of two converters pasted on a plastic plate. One of the converter plays the role of exciter and the other of transducer. Note that the accurate word to define the converters that excites the plate converting the electricity in sound is exciter, and the one for the converter that receives the sound and converts it in electricity is transducer.

The fastest way to calculate these frequency responses is to excite the medium with a chirp signal, since it contains a band of frequencies and, thus, it is possible to analyze a wide range of frequencies with just one signal. In Image 7.1 a chirp signal is shown. In this signal, the frequency changes on time dependency starting in 0Hz and finishing in 400Hz. Note that this is not the signal used to obtain the transfer functions of the converters since the converters reach higher frequencies, but an image of the real signal would be useless since it would not be clear at all. For this reason, it is better to shown an easy example of what is going to be used.

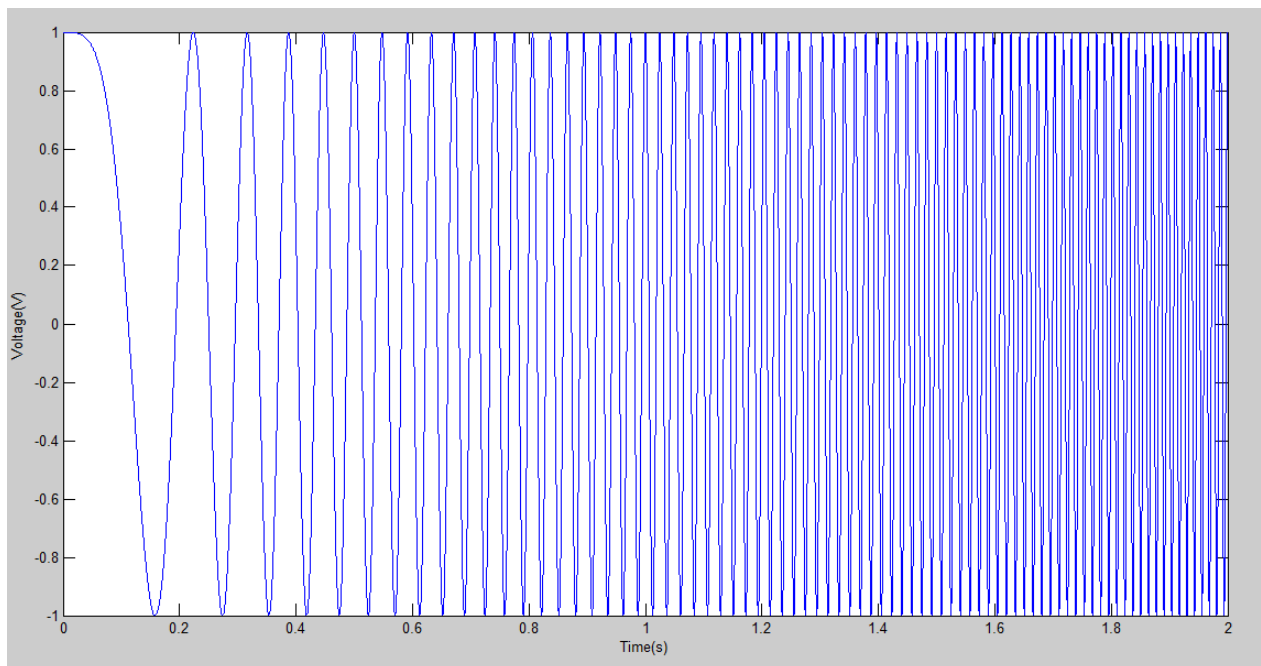**Image 7.1: Chirp signal from 0 to 400Hz**

In images from Image 7.2 to Image 7.7, the result for the different tests are shown. In every test, there are two results. The one represented with a blue line and with the label *with* represents the experiment done with a sponge under the plate, whereas the one with the red line and with the label *without* represents the experiment done without this sponge.

72

The converters that are going to be used are:

- Visaton EX 60 S - 8 Ohm (Appendix C. 2. EX 60 S - 8 Ohm)
- Visaton BS 76 S - 8 Ohm (Appendix C. 1. BS 76 S - 8 Ohm)
- Visaton EX 45 S - 8 Ohm (Appendix C. 3. EX 45 S - 8 Ohm)

One of the things that is possible to appreciate is that the transfer function when one of the converters acts as exciter and the other as transducer is not the same than the converters act on the other way round. This is easy to explain taking into account the definition of a transfer function $H_{12}(s)$ of the Laplace transform of the input $F_1(s)$ and the Laplace transform of the output $F_2(s)$:

$$F_1(s) = H_{12}(s) \cdot F_2(s)$$

Eq. 7.1

The inverse transfer function is then:

$$F_2(s) = H_{12}^{-1}(s) \cdot F_1(s) = H_{21}(s) \cdot F_1(s)$$

Eq. 7.2

So it is clear that $H_{12}(s) \neq H_{21}(s) = H_{12}^{-1}(s)$ and this is the reason why the two obtained transfer functions are different for every pair of converters.
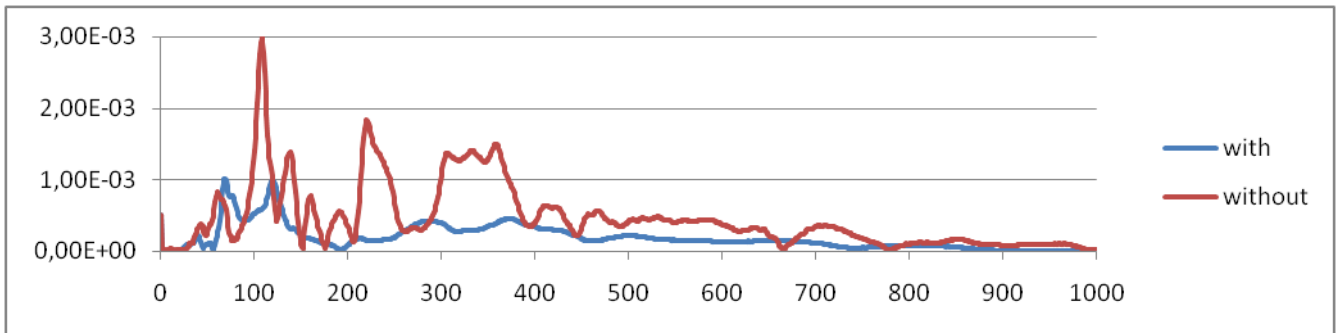
Image 7.2: Generator EX 60 S – Receiver EX 60 S
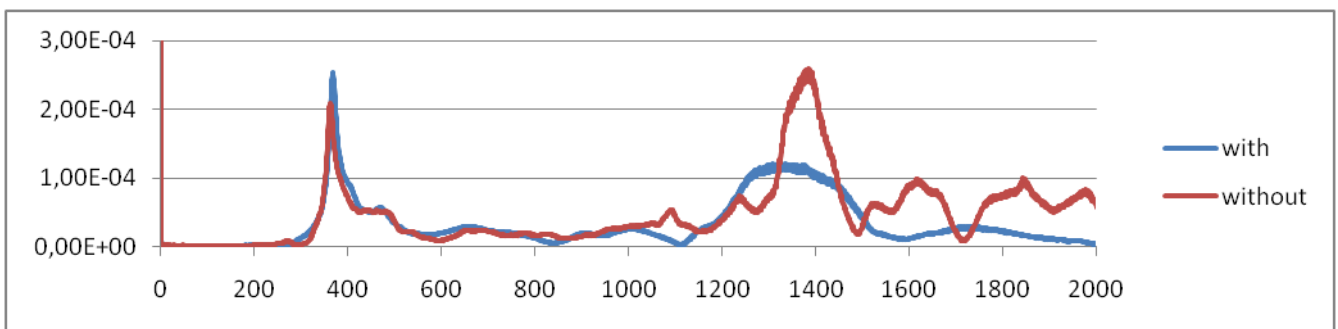
Image 7.3: Generator BS 76 – Receiver BS 76

Other thing that is possible to see when a look to the results is taken is that when the experiment is done without the sponge, the values for the Fourier transform are normally higher than with the sponge. This is possible due to absorption of sound that is done by the sponge and, thus, the sound propagation is not transmitted in such high values as just with the plate. It is possible

to appreciate that, in most of the cases, both curves have their relative maximum and minimum values in the same frequencies.

Observing the graphs, it is possible to say that using the converter BS 76 is not a good idea because in all the transfer function that it is involved, the values of the Fourier transform are lower - values of approximate 10^{-4} - than in any other case. For this reason, the converters that are going to be used are the EX 60 S and the EX 45 S, which cannot reach high frequencies though, but the thesis is focused in low frequencies.
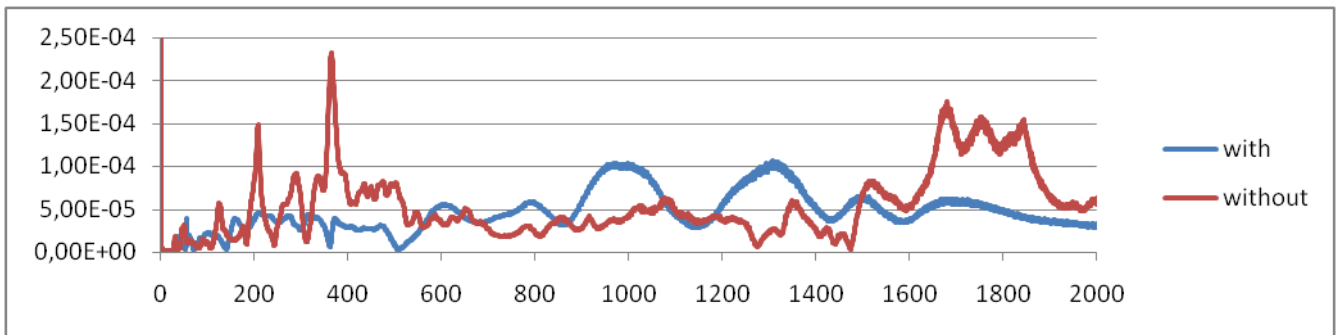
Image 7.4: Generator BS 76 – Receiver EX 60 S
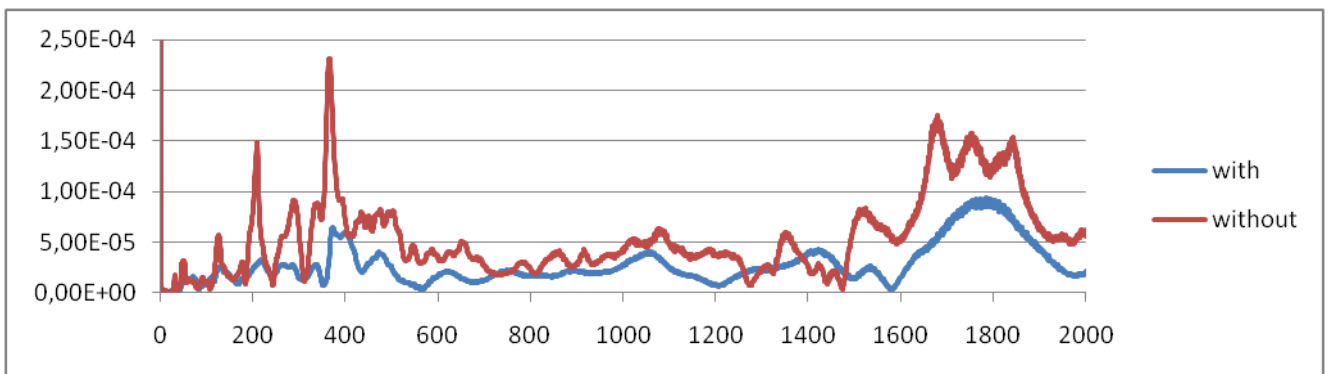
Image 7.5: Generator EX 60 S - Receiver BS 76
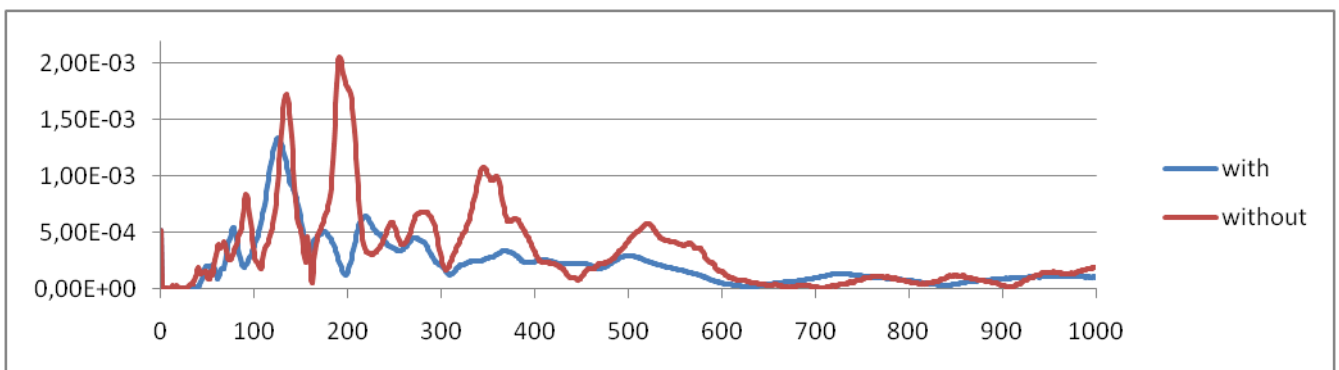
Image 7.6: Generator EX 45 S – Receiver EX 60 S
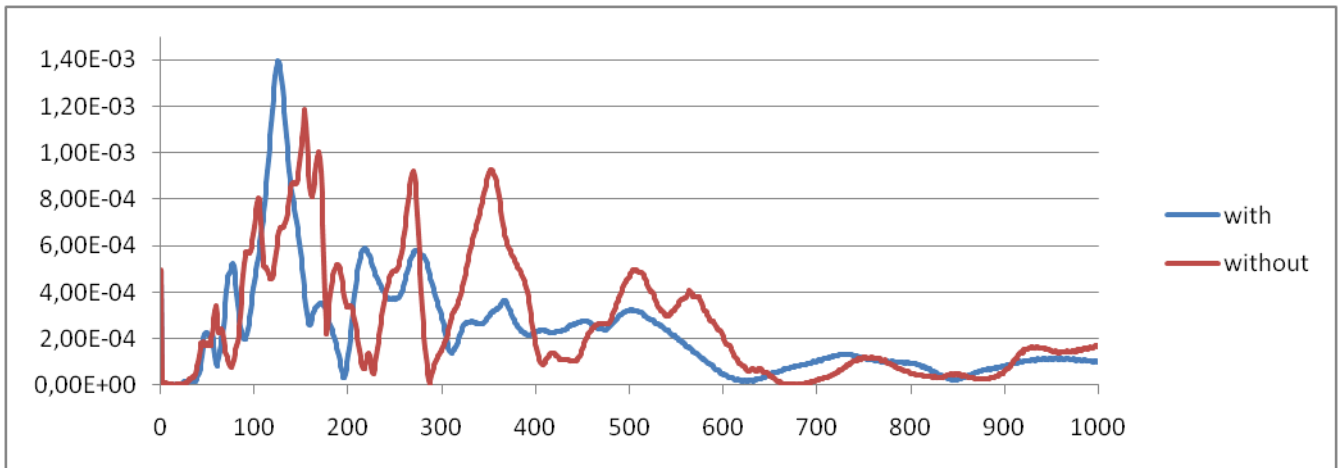
Image 7.7: Generator EX 60 S – Receiver EX 45 S
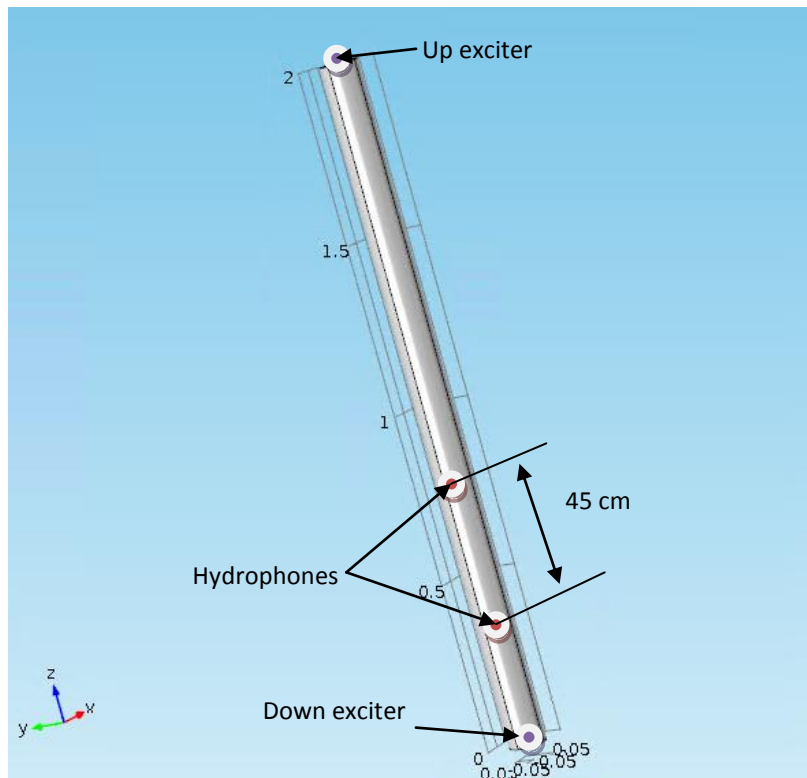
Image 7.8: Diagram of the PVC straight pipe used in the laboratory

7.2. Straight pipe

7.2.1 Up exciter

The source is going to be a sinusoidal wave, which is long enough to not take into account the transient effects. Comparing the phase of the two obtained waves in the hydrophones it is possible to calculate the phase velocity as the space between them is knows and is $d = 0,45m$. The PVC pipe which is going to be used is schematized in the Image 7.8, where the placement of the hydrophones and of the exciter is shown. It is a pipe of about 2m length.

An example of how the phase velocity is measured is shown now. The stimulating frequency in this case is $f = 700Hz$ s. In Image 7.9, the two obtained waves by the transducers are shown. It is possible to appreciate that there is a phase difference in between them. A transient effect is also easy to appreciate in the beginning of the wave, $t \approx 0s$, and in the end of it, $t \approx 0,15s$. For this reason, the part of the wave that is taken in order to measure the phase velocity is after the first transient effect and before the last one. This selected part is shown in Image 7.10, where the part selected for every wave is painted in red.
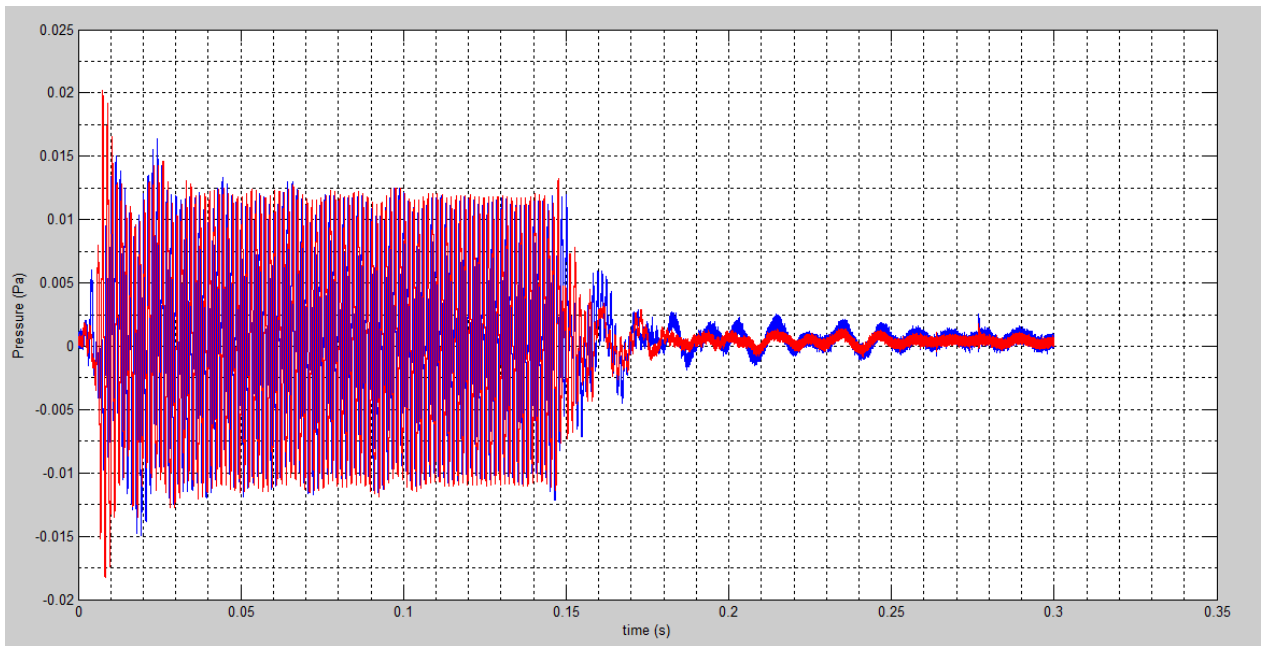
Image 7.9: Measurement results when applying a continuous sinusoidal wave for a specific time.
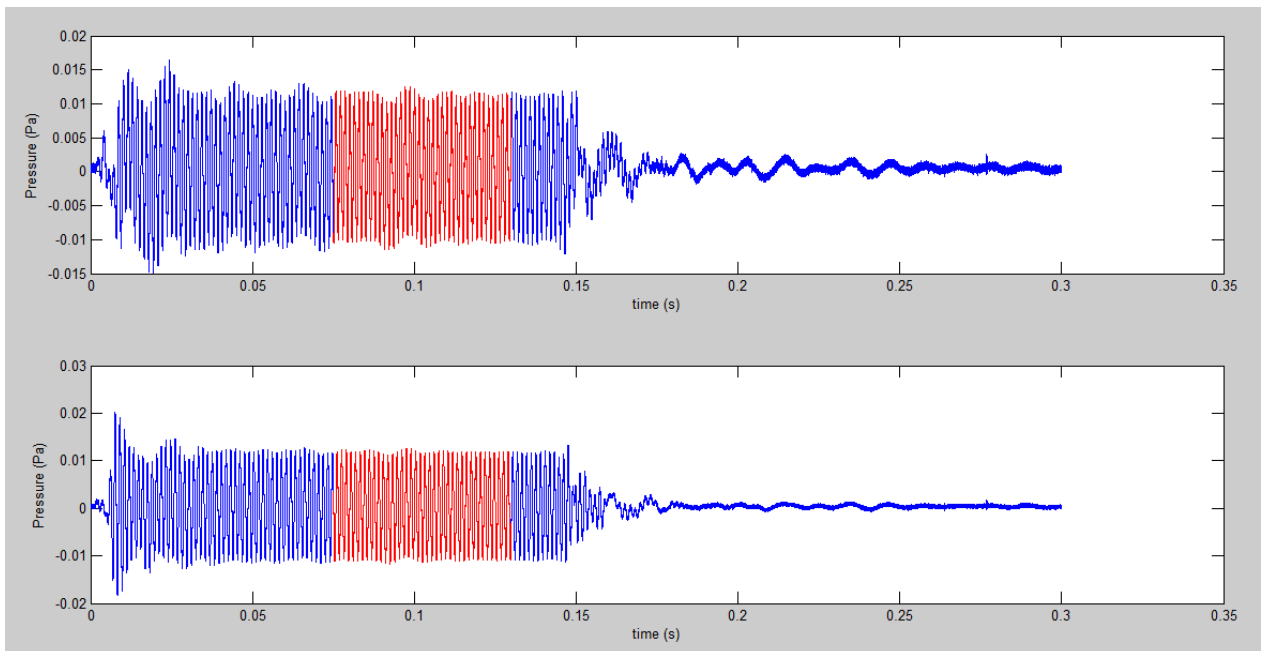
Image 7.10: Selected part of the measurement results to measure the phase velocity.

In order to eliminate the noise of the measurements, the selected parts are adjusted by the method of least squares as it was explained in the section: 5.6. The result of this adjustment is

possible to be seen in Image 7.11 and in Image 7.12 for the two hydrophones, respectively. In red the original wave is shown and in blue the adjusted wave. As the phase delay is known because the Eq. of the two adjusted waves is known, it is possible to calculate the time difference by:

$$t = \frac{\varphi}{2\pi f},$$

Eq. 7.3

where φ is the phase delay and f the frequency of the stimulating wave.

Once this time difference is known, the phase velocity is calculated by:

$$v_p = \frac{d}{t}$$

Eq. 7.4
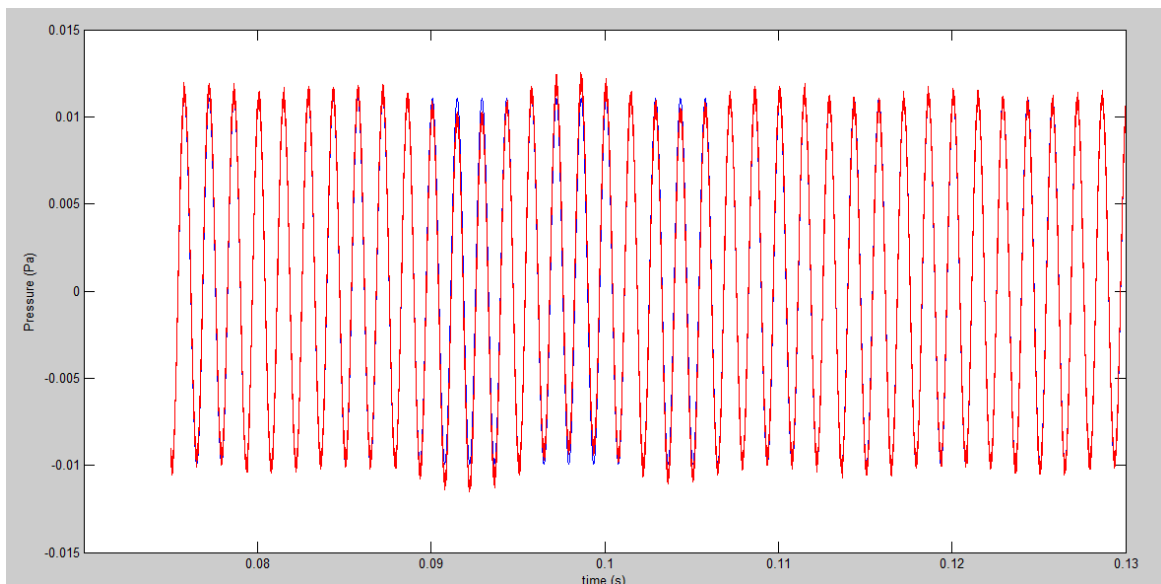
Image 7.11: Adjustment of the selected part for the first hydrophone.
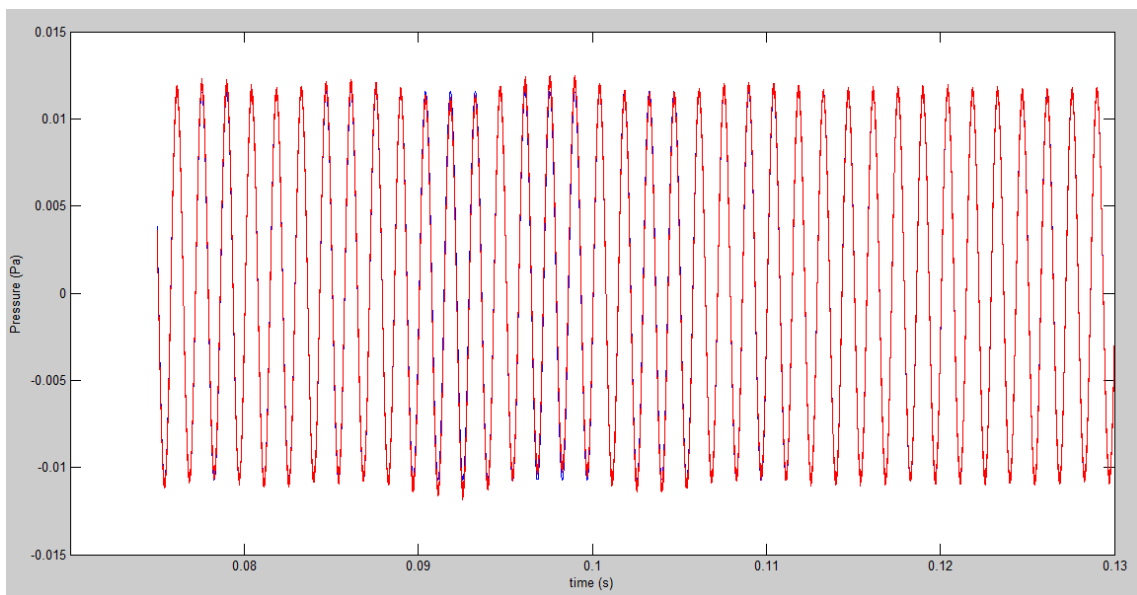
Image 7.12: Adjustment of the selected part for the second hydrophone.

The values obtained using this method are shown in Table 7.1 and are compared to the values obtained in the FEM simulation in Image 7.13. The values are close to the ones obtained in the simulation but they have a considerable deviation. They should also follow a straight line but they curve formed by these values goes up and down all the time. This deviation from the simulation results is possible to be produced due to the multiple reflection effects that make the wave be a superposed of different waves.

In order to avoid this effect, the water inside the pipe is going to be excited by a one-period-sinusoidal-gaussian pulse.

Frequency (Hz)	Phase velocity (m/s)
300	165,14
350	439,771
400	463,34
450	508,0196
500	554,595
550	406,9785
600	394,94
650	390,9645
700	416,28
715	483,1907
800	482,5313
850	586,2908
900	583,1331
950	534,6228

Table 7.1: Values for the phase velocity obtained by applying a continuous sinusoidal wave for a specif time.
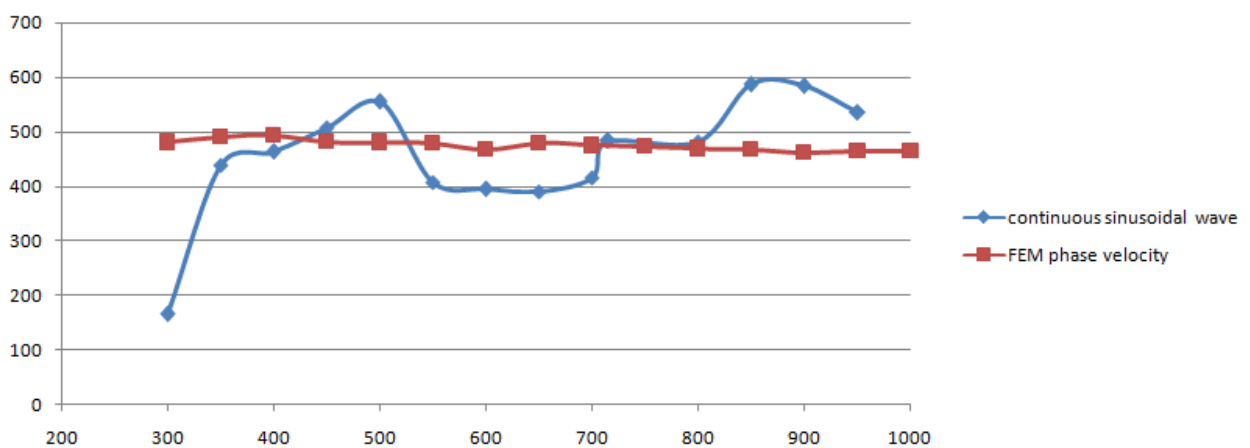
Image 7.13: Comparison of the measured phase velocity and the one obtained by FEM simulation.

7.2.2 Down exciter

7.2.2.1 Long Gaussian pulse

The pipe is going to be excited with a gaussian pulse of 100 periods from the exciter placed at the bottom. Then, the obtained waves in the hydrophones are going to look like the ones shown in Image 7.14. In this case, the pipe has been stimulated by a gaussian wave of $f = 500Hz$. In order to determine the group velocity of the transmitted signal, the obtained waves by the hydrophones are going to be processed. Firstly, the noise is going to be removed by using a low-pass filter, since the noise has higher frequencies than the one with which the pipe is stimulated. The result of the waves after been filtered can be seen in Image 7.15, where it is possible to appreciate that the signals are much clearer than before been filtered. Secondly, the envelope waves of the original ones are going to be calculated by using Hilbert transformation as it was done in 5.3.1 Calculation of the envelope wave by the Hilbert transform. However, it is known that the envelope wave has to have the shape of a gaussian bell, therefore, in order to have a better envelope wave, the calculated signal by Hilbert transform is going to be adjusted to this gaussian bell. This is to say, it is going to be adjusted by the least squares method to the following function:

$$f(t) = a \cdot exp\left(\frac{1}{2} \cdot \frac{(t-b)^2}{c^2}\right) \qquad \text{Eq. 7.5}$$

Thus, the goal is to find the parameters a, b, and c that make this function best fit to the obtained wave by Hilbert transform. The calculated envelope waves after this procedure for this specific case are shown in Image 7.16.
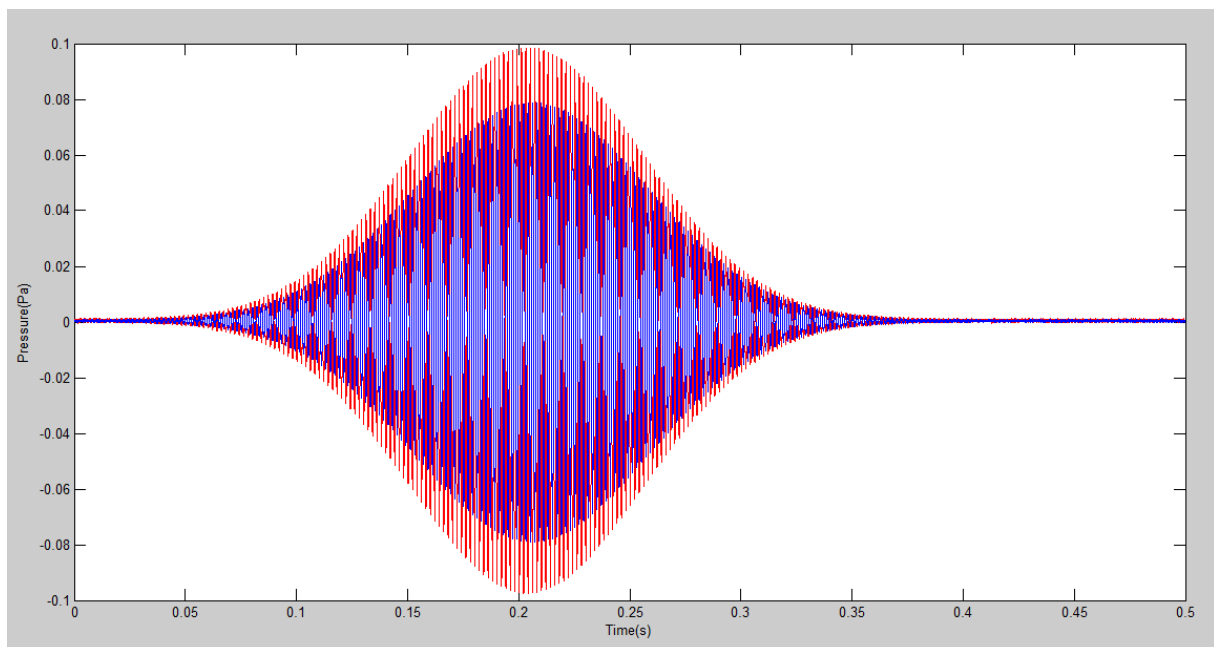
Image 7.14: Obtained waves by the two probes

When the envelope waves are found, it is possible to proceed with the method shown in 5.3. Group velocity by time delay of maximum of envelope wave.
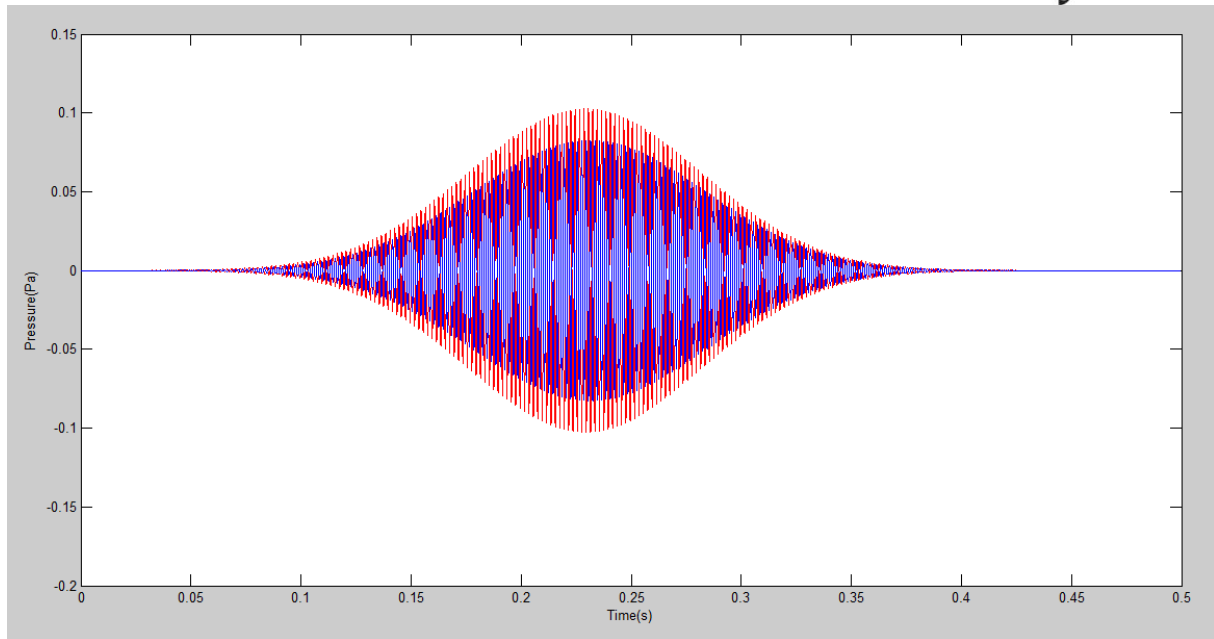
Image 7.15: Obtained waves by the two probes after been filtered
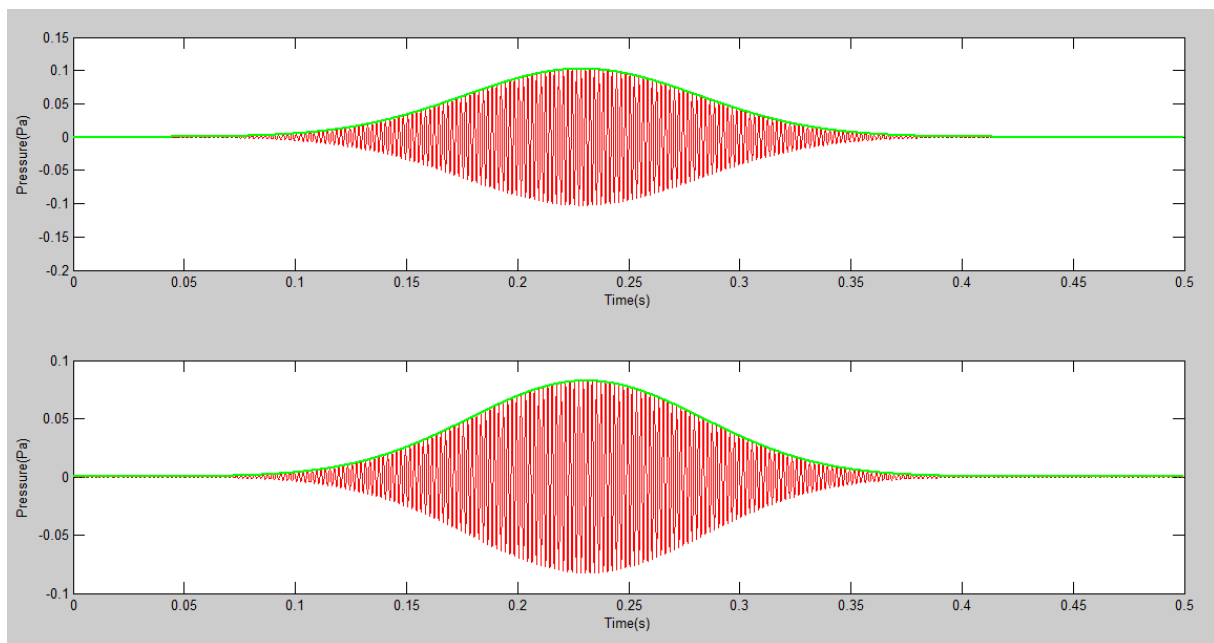
Image 7.16: Envelope wave for the two obtained waves

The results, however, using this method are quite confusing due to the reflection effects that occur inside the pipe. The transmitted wave is too long for the used pipe and it is reflected at the beginning and at the bottom of the pipe. For this reason, the waves acquired by the hydrophones are a superposition of different waves and it is not possible to calculate neither the group velocity nor the phase velocity.
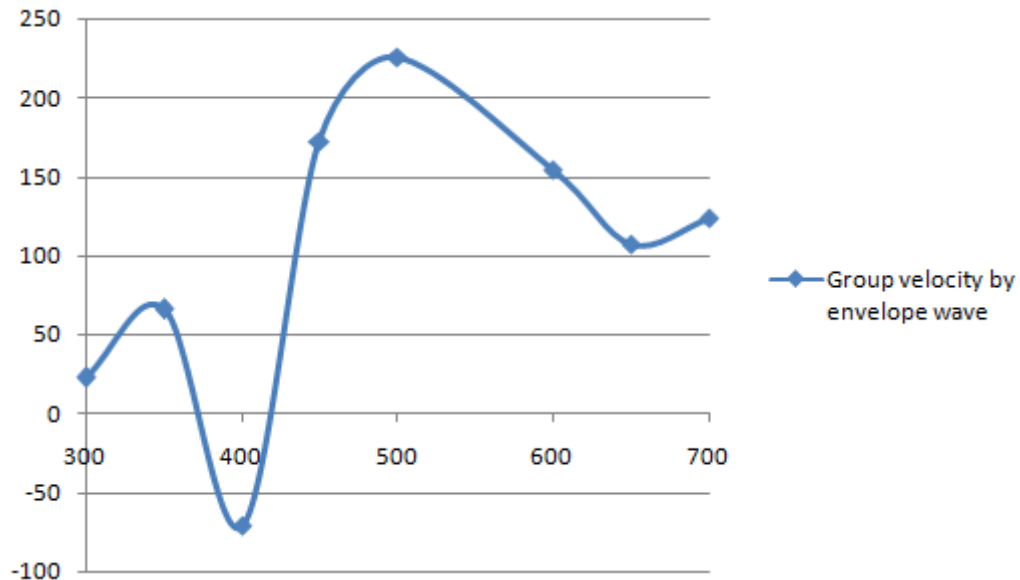
Image 7.17: Group velocity calculated by the method of the envelope wave for the straight pipe.

Therefore, what is going to be used in order to avoid these reflection effects is a short gaussian pulse of only one period, so that the reflection effects can be discarded and do not play an important role as it will be shown in 7.2.2.2 Short Gaussian pulse.

7.2.2.2 Short Gaussian pulse

The pipe is going to be excited by a one-period-sinusoidal-gaussian pulse, so the velocity that can be measured is the group velocity, as there is only one period and it is not a truly sinusoidal wave. By measuring the time difference in which the wave reaches its maximum value in every hydrophone, it will be possible to measure the group velocity since the distance between the two hydrophones is known and is $d = 0,45m$.

An example of how to proceed with this method is shown now.

In Image 7.18 the two obtained waves by the hydrophones are shown, where it is easy to see the time difference mentioned above that is to be measured. It is also possible to appreciate the transient effects both before the wave and after the wave, which are added to the reflection effects. Due to this reason, only the time of the highest point is going to be measured to calculate the group velocity.

Before measuring the time, it is a good idea to apply a low-pass filter to reduce the noise. It is not necessary to apply a band-pass filter since the noise has much higher frequencies than the stimulated signal and, therefore, it is only necessary to filter the high frequencies. The response of the filter which is going to be applied is shown in Image 7.19. In Image 7.20 the wave after been filter is shown. The noise has disappeared and the wave has been moved to bigger values in time. This effect does not affect to the measurement since both waves are moved the same distance because the same filter is applied.
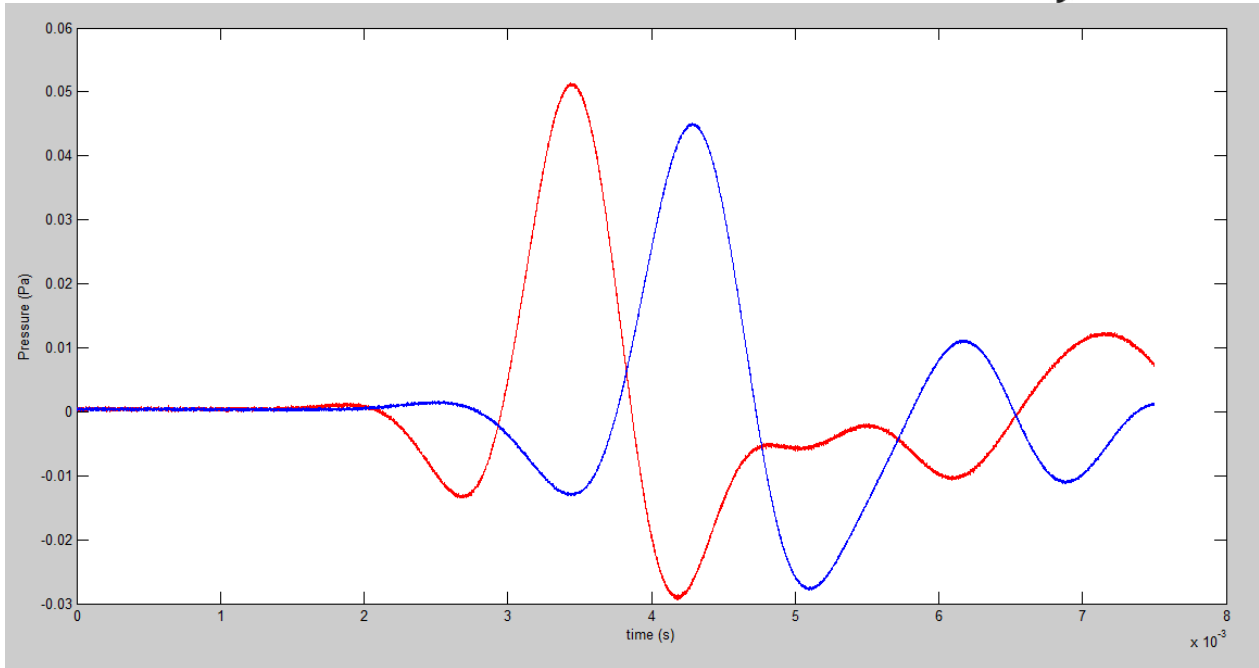
Image 7.18: Acquired waves when applying a short pulse wave.

The MATLAB script used to process the signals and calculate the group velocity is shown in the appendix A. 11. Calculate group velocity from a short Gaussian pulse.
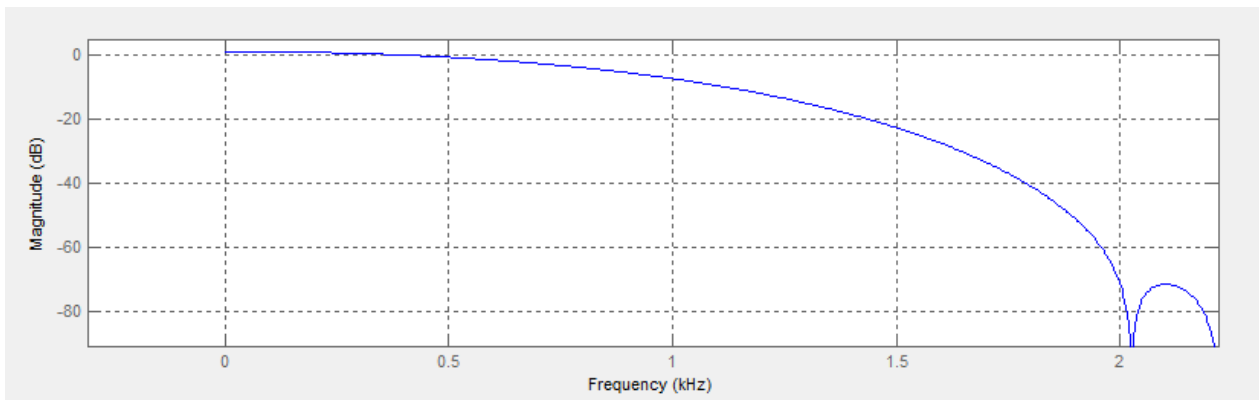
Image 7.19: Filter used to eliminate the noise of the waves obtained.

After calculating the time difference, it is possible to obtain the group velocity by:

$$v_g = \frac{d}{t},$$

Eq. 7.6

where t is the time difference.

The values obtained for the different frequencies are shown in Table 7.2.
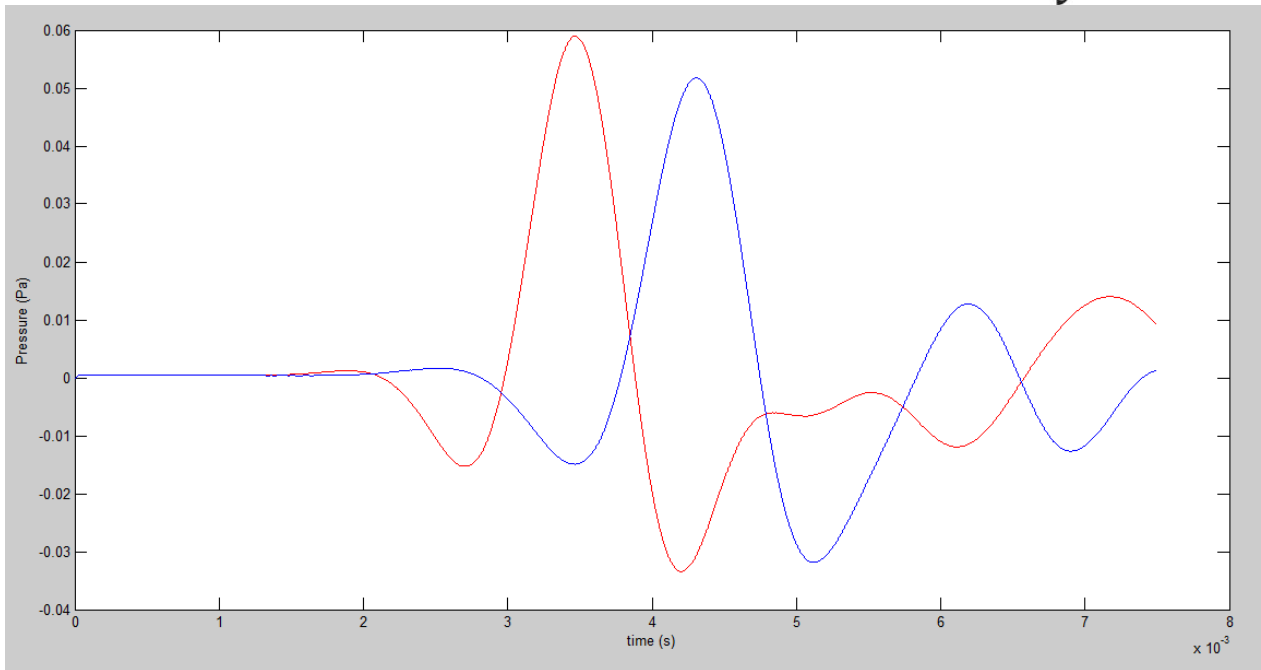
Image 7.20: Waves obtained after filtering the acquired waves.

Frequency (Hz)	Group velocity (m/s)
200	534,4418
250	545,4545
300	542,1687
350	538,9222
400	536,3528
450	535,3956
500	535,0773
550	536,9928
600	537,3134
650	537,3134
700	535,2046
750	534,188
800	531,6321
850	528,5412
900	527,7231
950	526,932
1000	528,169

Table 7.2: Measured values of the phase velocity by applying a short pulse wave.

In Image 7.21 a comparison between the results obtained in the FEM simulation for the group velocity and the measured one is shown. Both curves are quite the same, but the measured group velocity has bigger values. This effect can be due to the change of the properties of the material (PVC), which changes due to different parameters, such as temperature, humidity, stress caused by the installation and the water inside, etc. Changing these parameters and setting the

simulation with these ones, both curves should fit exactly. However, it is not possible to know a priori which values are those and the parameters set in the simulation were the ones by default for PVC.

For waves that are propagated in a specific medium, there is a relation between the angular frequency ω and the wave number k, which is known as dispersion relation. When the frequency interval $\Delta\omega$ with center in ω_m is small, it is possible to write:

$$v_g = \frac{d\omega}{dk} = \frac{d(kv_p)}{dk} = v_p + k\frac{\partial v_p}{\partial k},$$

Eq. 7.7

where v_p is the phase velocity and f is the frequency of the stimulating wave. The differentiation can be approximated to a division of differences as:

$$v_g = v_p - \frac{\Delta v_p}{\Delta f},$$

Eq. 7.8

This last equation was the one that was used to determine the group velocity in the simulation.
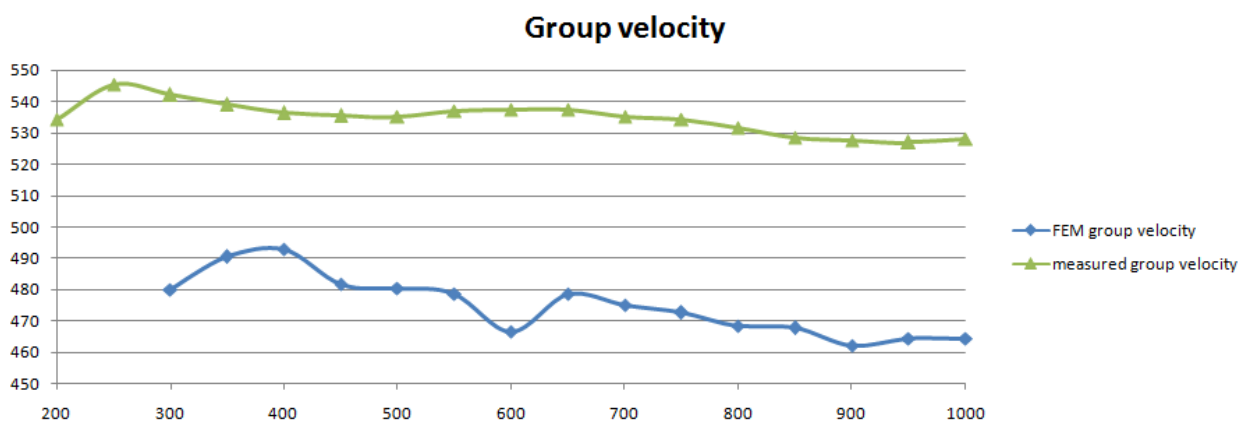
Image 7.21: Comparison between the results obtained in the FEM simulation for the group velocity and the measured.

7.3. Bent pipe

In order to investigate how the group velocity change when an acoustic pressure wave is transmitted in not a straight direction, but with different shapes, the next test is going to be formed by a bent pipe. The velocities are going to be measured both before the bending and after the bending so as to determine how the velocities change from the ones obtained in the straight pipe and if there are any changes before and after the bending.

The hydrophones are placed in just one place of the pipe to a distance of $d = 0,45m$ to each other. However, it is going to be possible to measure both before and after the bending because two converters are going to be used. The first converter is going to be placed at the top of the pipe, and

the other one at the bottom. When the first one acts as exciter, the other one acts as transducer, and vice versa. By doing so, it is possible to measure signals "after" and "before" the bending.
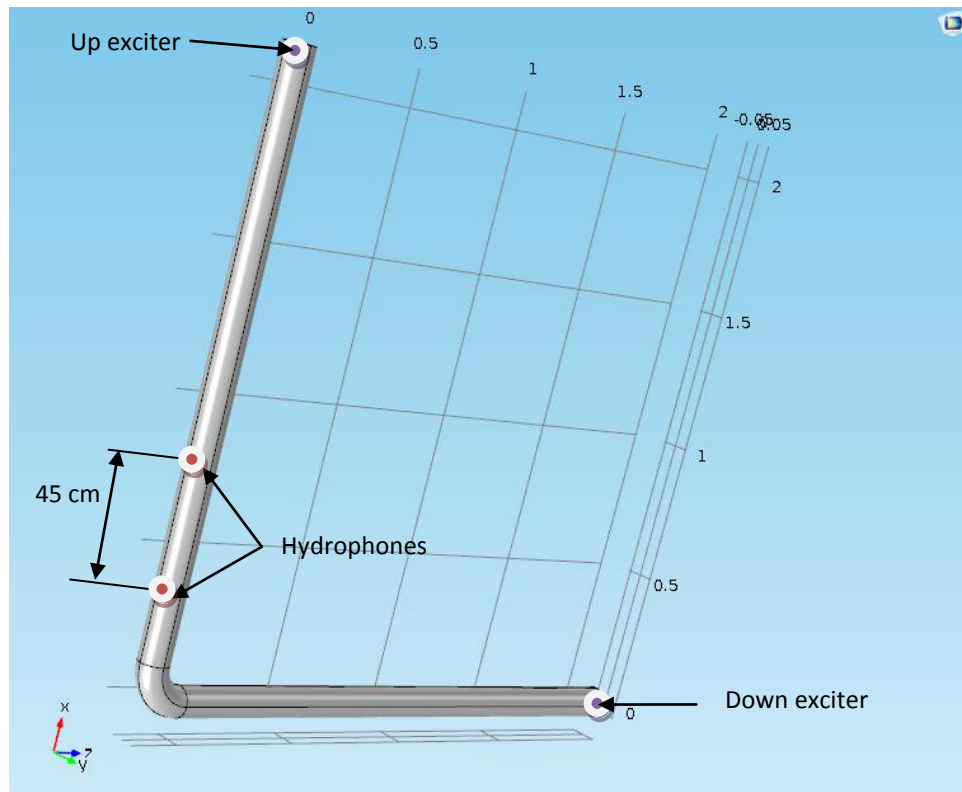
Image 7.22: Diagram of the PVC bent pipe used in the laboratory.

7.3.1 Before the bending

7.3.1.1 Short gaussian pulse

As it was done in the section 7.2.2, a gaussian sinusoidal pulse wave is going to be applied so as to measure the group velocity because it avoided the reflection effects. However, as in the section 7.3.1.2 the group velocity was calculated, now the group is velocity is going to be tried to be calculated. For this reason, a gaussian sinusoidal pulse of more than one period is going to be applied. However, in this case, due to proximity of the bending with the hydrophones, the reflection effects are very noticeable. Thus, when a pulse wave of frequency $f = 1kHz$ is applied, the result consists of a transient response and a multiple reflection, which is shown in Image 7.23. What is going to be done is split the signal in different frequencies according to its spectrum (Image 7.24) by using bandpass filters of the specific frequencies.

The first split is going to be done is in the range of frequencies of $f \in (1000, \ 1250) \ Hz$ by applying the filter whose frequency response is shown in Image 7.25. The result after filtering the original two signals is shown in Image 7.26. In Image 7.27, it is displayed the spectrum of the filtered signals, in which it is possible to see that all the frequencies out of the range of the filter are decreased and are really close to zero.

Now that two clear signals are obtained, it is possible to determine the group velocity for this pressure wave. The method that is going to be used is the calculation of the group velocity by measuring the highest point of the envelope waves calculated by Hilbert transform and measuring

the time elapse (section 5.3.) In Image 7.26 the envelope waves of the filtered signals are shown, and the highest point of waves is highlighted. The time difference between this two points let us calculate the group velocity since the distance between the two hydrophones is known. The result of the group velocity for this case is $v_g = 381,36 \, m/s$.

By doing this, using different filters, the result of the group velocity on frequency dependency is shown in Table 7.3.
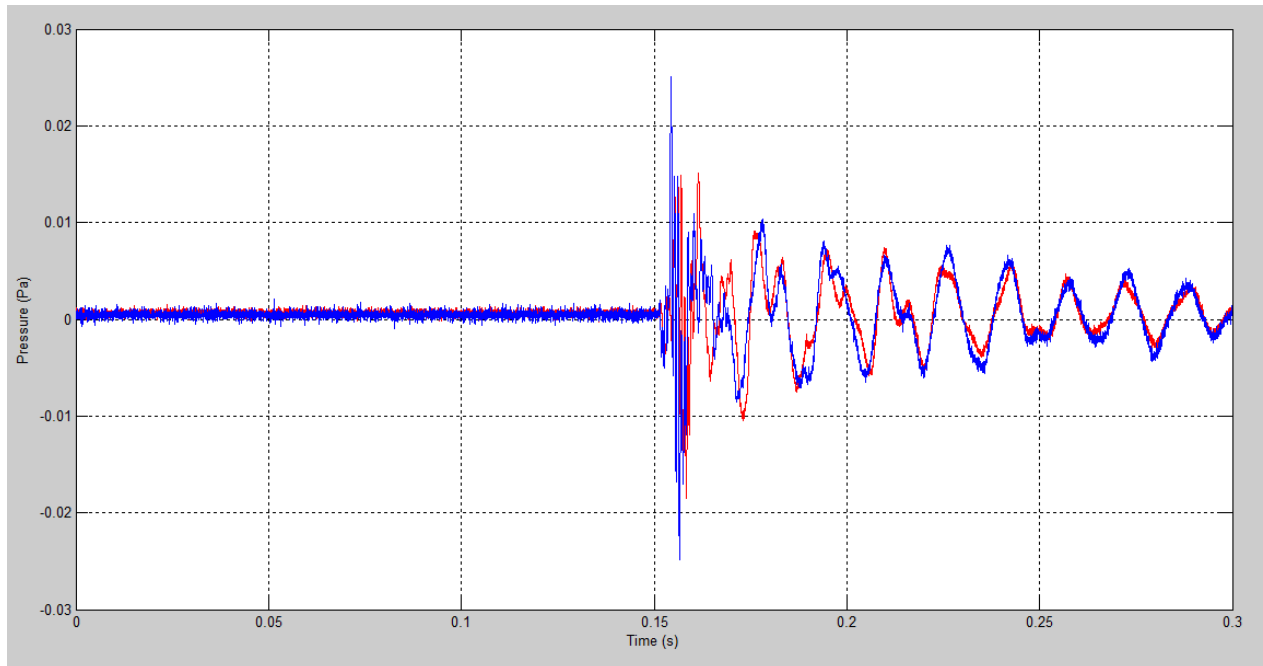
Image 7.23: Obtained signals in the hydrophones before the bending when applying a gaussian sinusoidal pulse wave of f=1kHz.
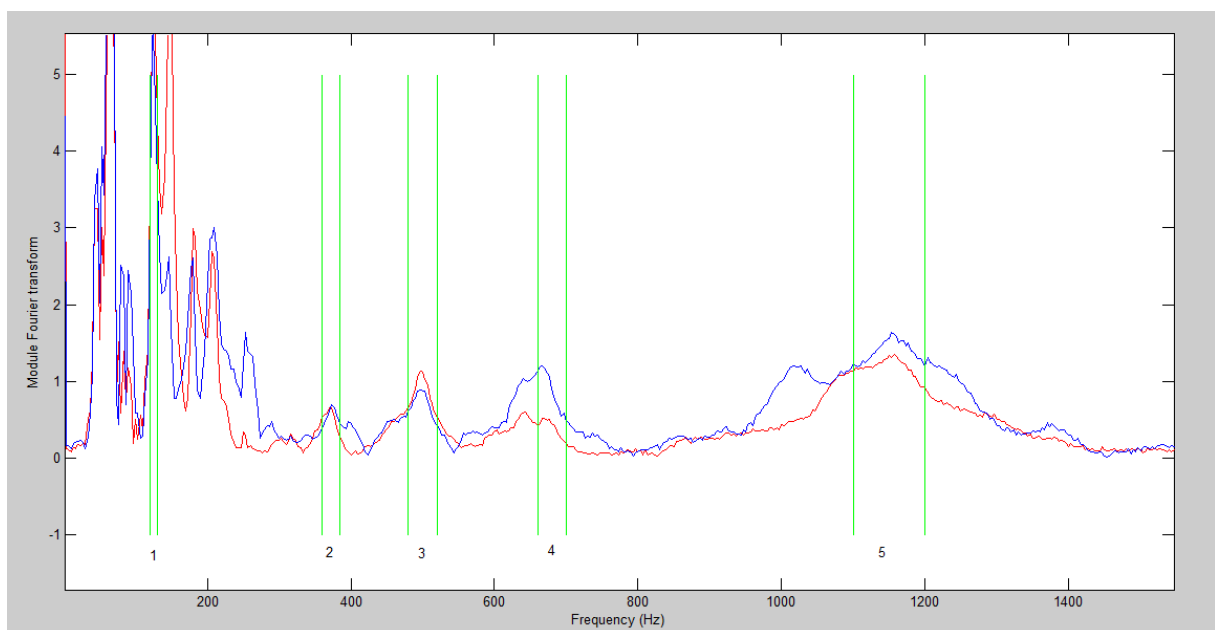
Image 7.24: Fourier transform of the obtained signals in the hydrophones before the bending when applying a gaussian sinusoidal pulse wave of f=1kHz.
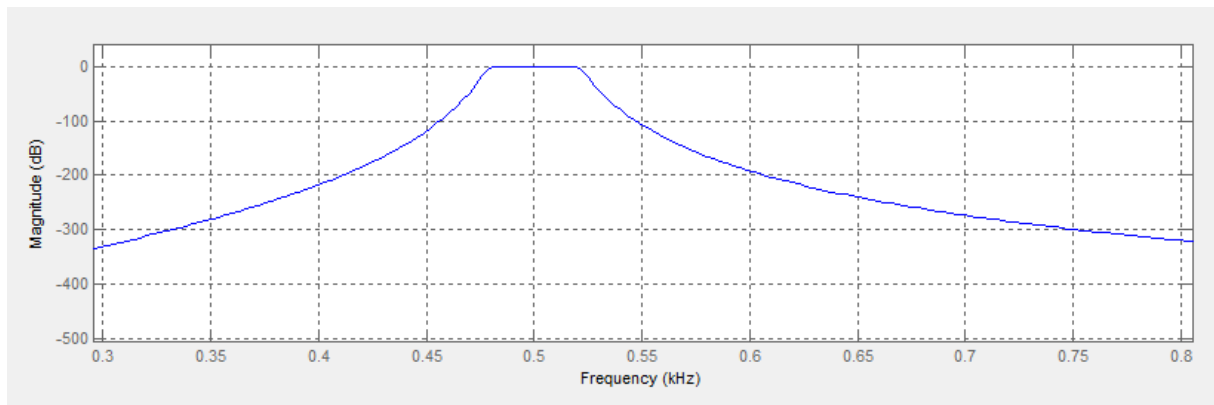
Image 7.25: Frequency response of IIR Butterwoth band-pass filter of the range 480-520Hz.
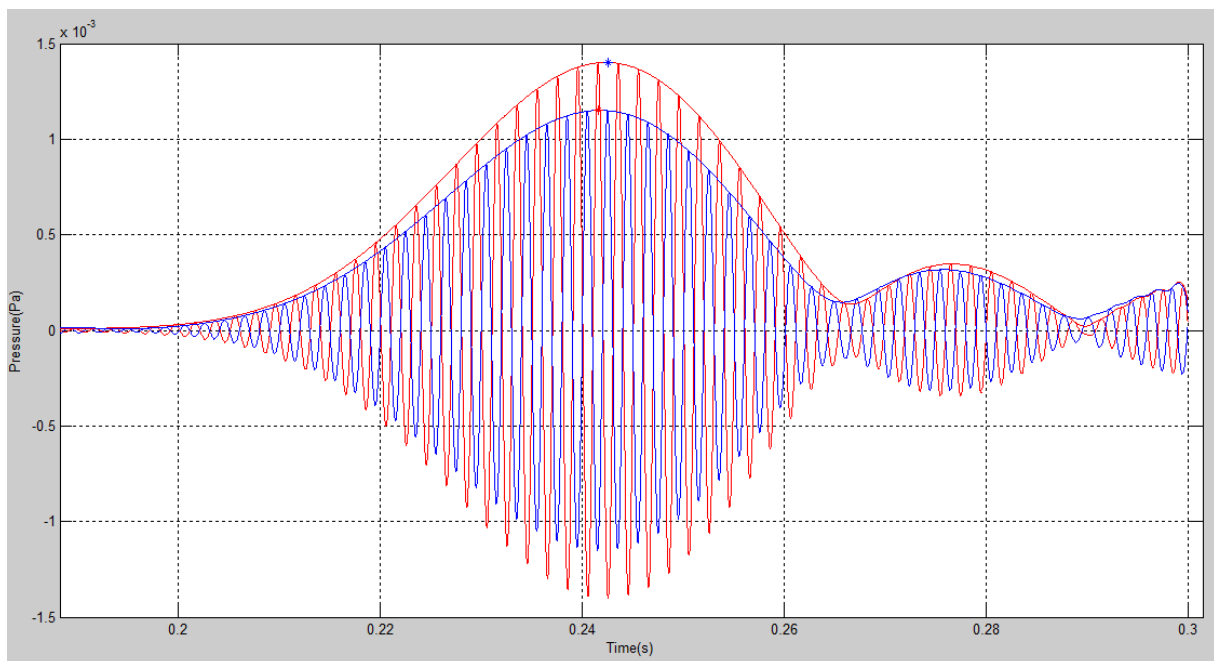
Image 7.26: Envelope waves by using Hilbert transform of two filtered signals obtained by the hydrophones before the bending.

Frequency (Hz)	120-130	360-385	480-520	660-685	1100-1200
Group velocity (m/s)	166,67	82,7206	478,7234	292,2078	576,9231

Table 7.3: Group velocity on frequency dependency.
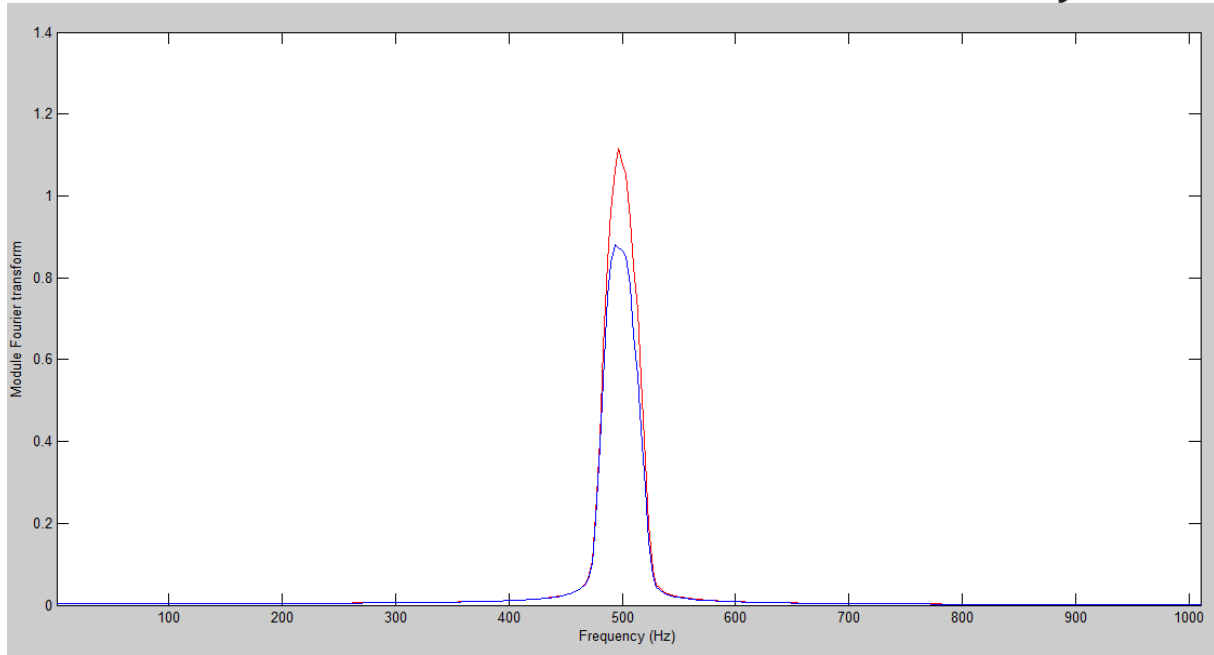
Image 7.27: Spectrum of the signal after filtering it with a band-pass filter.
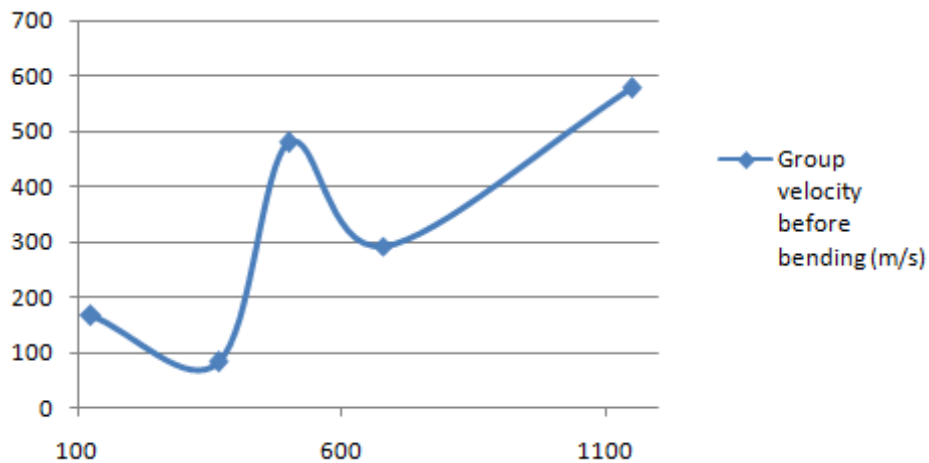
Image 7.28: Group velocity before the bending on frequency dependency.

7.3.1.2 One-period sinusoidal pulse

The stimulated signal is going to be a sinusoidal pulse which only has one period. The reason of using one only period is to avoid reflections and, thus, wrong results. Reflections play an important role within the pipe and they must be removed. When these reflections cannot be removed due to the impossibility to do so in the pipe, the other way of performing is trying to avoid its apparition and this is what is going to be tried to do in this section.

In Image 7.29, the acquired signals by the transducers are shown. It is quite interesting to notice that although the pipe has been stimulated with just one period, the response has a lot of periods. This response must be caused mainly by the multiple reflection on the bending, since it is

not a straight surface and the transmitted signal is reflected many times on this edge and produces the superposition of different waves. When the signal is reflected on the bending, multiple waves are generated in different direction due to the angle of the bending. This effect causes that the secondary waves also are reflected on the boundary edges of the pipe, creating more secondary waves. These multiple periods are also caused by the final edges of the pipe, that is to say, the top and the bottom.
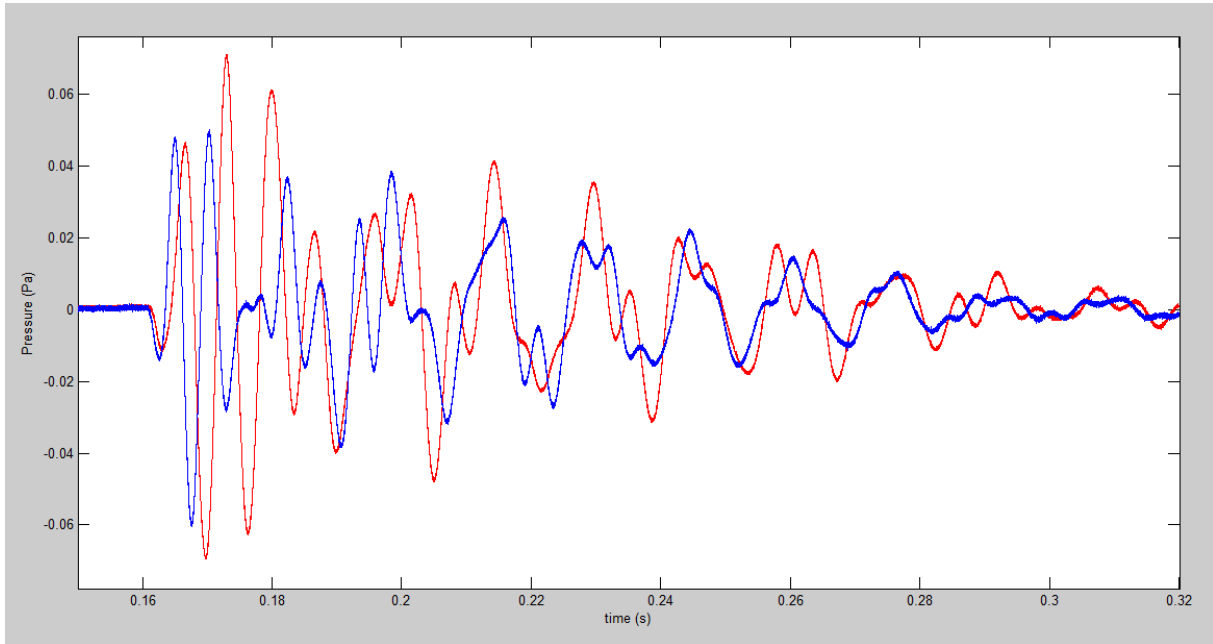
Image 7.29: Obtained waves by the hydrophones before the bending when a one-period sinusoidal pulse is applied.
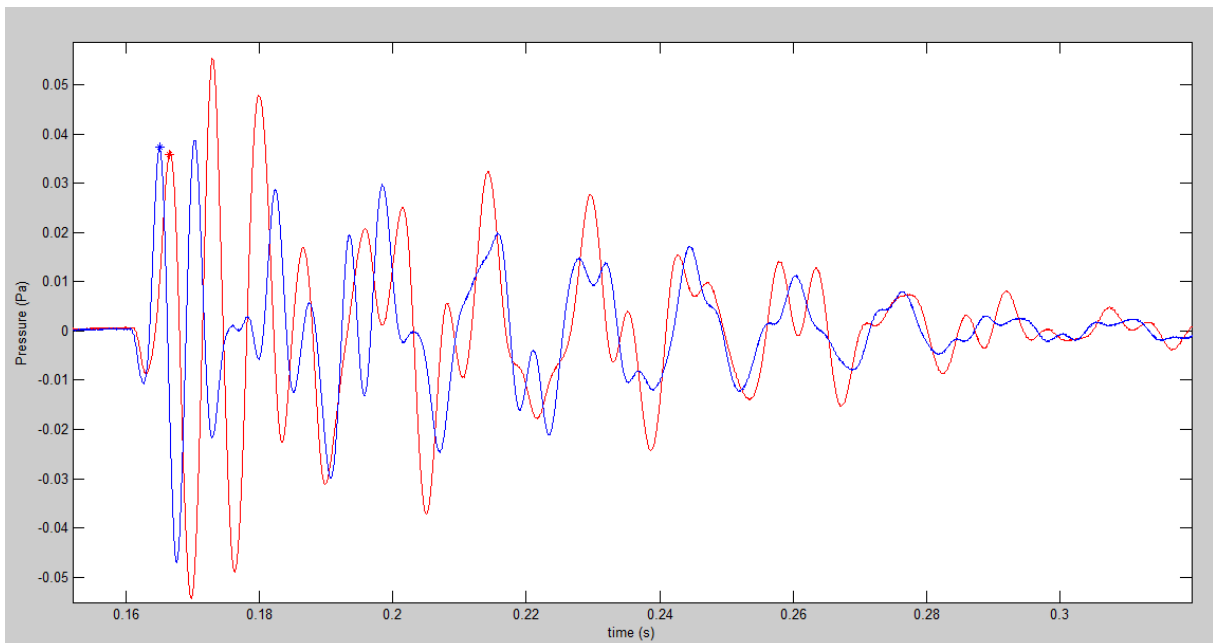
Image 7.30: Obtained signals after filtering the waves acquired by the hydrophones before the bending when a one-period sinusoidal pulse is applied.

What is going to be measured so as to calculate the group velocity is the first peak of the acquired signals. By doing so, the multiple reflection effects are discarded because the wave does not

have time to travel until the bending and reflects. However, before measuring these peaks, a low pass filter is going to be used in order to remove the noise. In Image 7.30, the signals after been filtered are shown. It is possible to appreciate that these filtered waves do not have noise and, therefore, it is easier to work with them.

In Image 7.30, the two points that are going to be used to measure for calculating the group velocity are highlighted. When these two points are known, it is easy to calculate the group velocity because the distance is known and it is done like in the straight pipe with Eq. 7.6. How to perform with MATLAB is shown in a script in the appendix A. 12. Group velocity before bending with one-period sinusoidal pulse.

The obtained group velocities on frequency dependency with this method are shown in Image 7.31 and in Table 7.4.
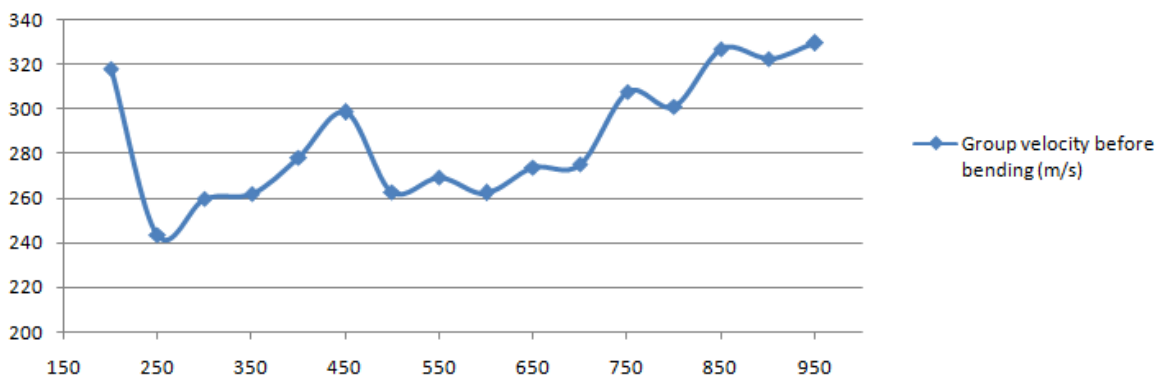
Image 7.31: Group velocity on frequency dependency before the bending.

Frequency(Hz)	Group velocity(m/s)	Frequency(Hz)	Group velocity(m/s)
200	317,7966	600	262,2378
250	243,5065	650	273,7226
300	259,5156	700	275,0611
350	261,9325	750	307,7975
400	278,1211	800	301,2048
450	298,4085	850	327,0349
500	262,8505	900	322,3496
550	269,1388	950	329,429

Table 7.4: Values for the group velocity on frequency dependency before the bending.

7.3.2 After the bending

7.3.2.1 Short gaussian pulse

The same process that was performed in the section 7.3.1.1. the converter but with the converters acting the other way round so as to measure the group velocity after the bending.

In Image 7.32 the acquired signals by the hydrophones when a gaussian sinusoidal pulse of $f = 500Hz$ is shown. In this case, it is possible to see the same multiple reflection effects that also occurred in the other experiments with the bent pipe. What is going to be done so as to remove these reflections is split the signal in different frequencies according to its spectrum Image 7.33 with a band pass filter as it was done in the section 7.3.1.1.

In Image 7.33, the spectrum of the obtained signals are shown. It is also displayed the different frequency bands in which the spectrum is going to be split so as to measure the group velocity.

In Image 7.34, the result of filtering the acquired signals with a band-pass filter for the band between 545 and 595Hz are shown. The two selected points to calculate the group velocity are highlighted.

In Image 7.35 and in Table 7.5, the calculated values for the group velocity after the bending are shown.
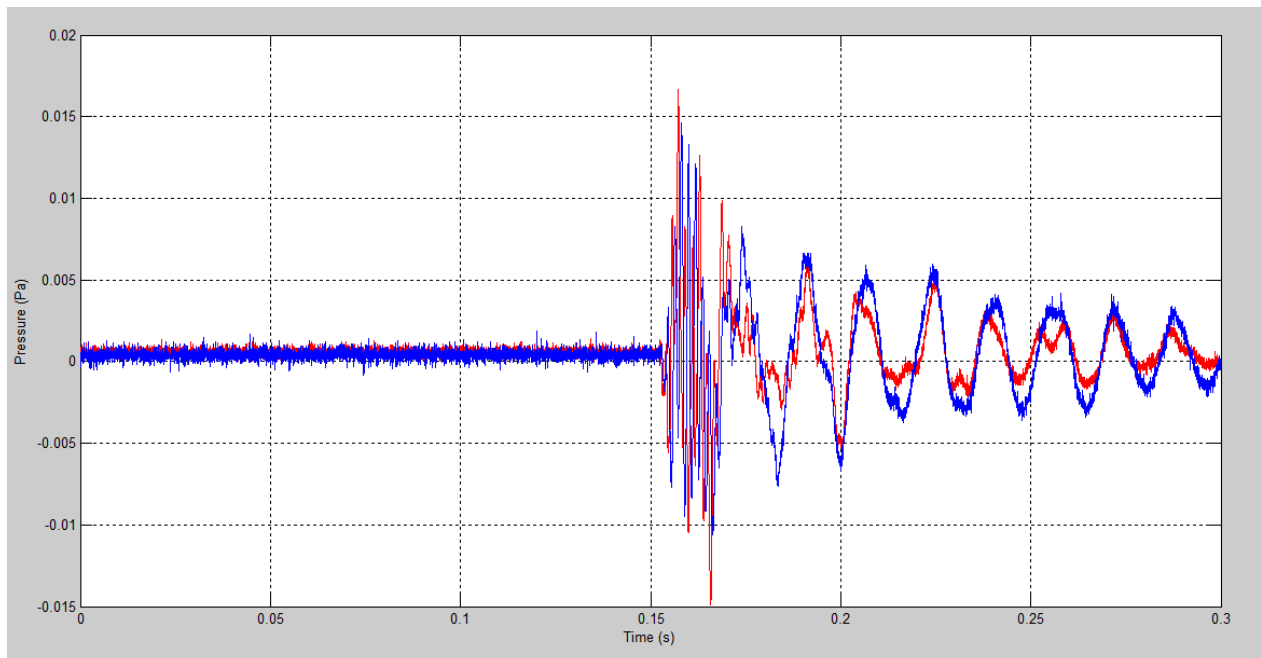
Image 7.32: Acquired signals by the transducers after the bending when a gaussian sinusoidal pulse wave of f=1kHz is applied.
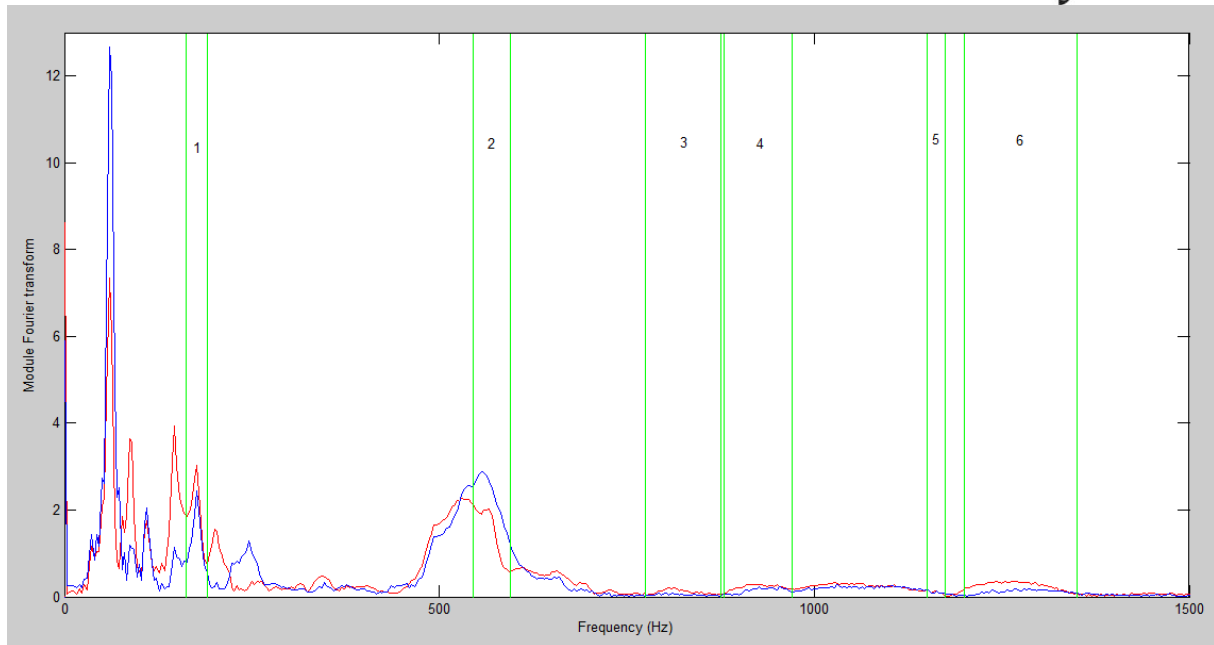
Image 7.33: Spectrum of the acquired signals after the bending when a short gaussian pulse is applied.
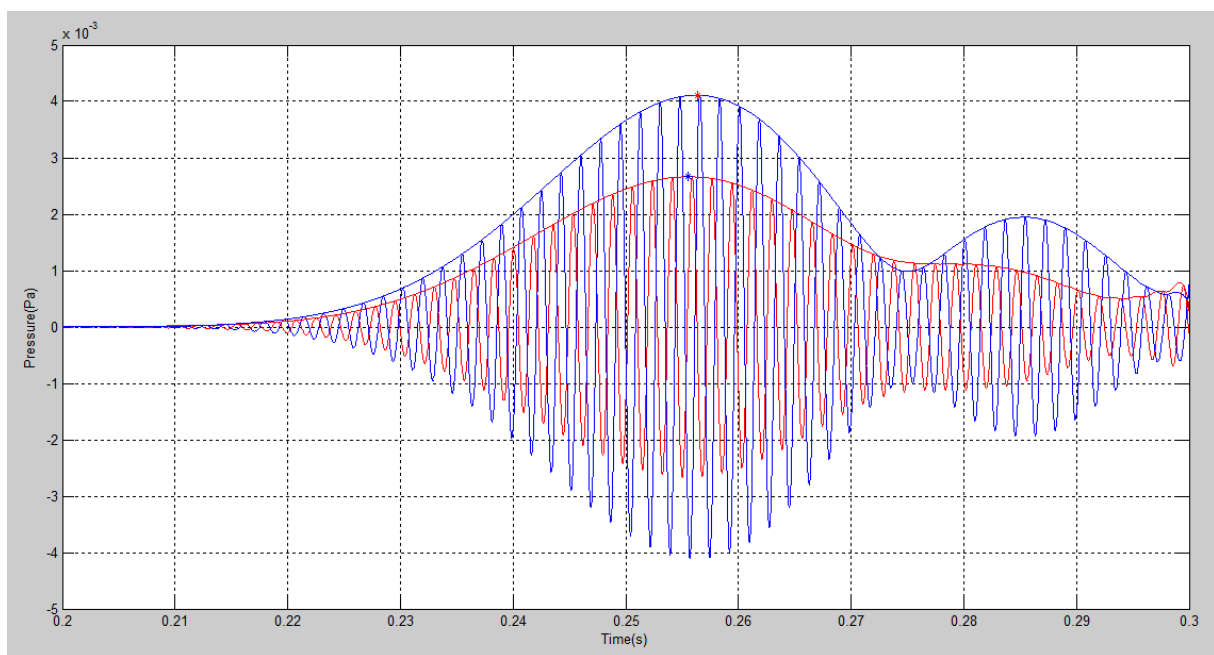
Image 7.34: Acquired signals after the bending after been filtered. Selected points to calculate the group velocity.

Frequency (Hz)	163-190	545-595	775-875	880-970	1150-1175	1200-1350
Group velocity after bending (m/s)	64,2857	548,7805	206,422	416,667	409,0909	750

Table 7.5: Exact values for the group velocity on frequency dependency after the bending.
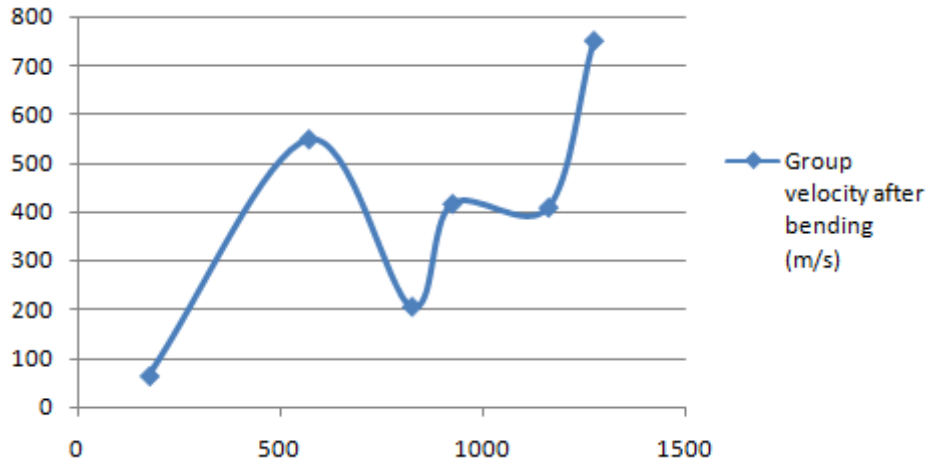
Image 7.35: Group velocity on frequency dependency after the bending.

7.3.2.2 One-period sinusoidal pulse

The same process that was performed in the section 7.3.1.2 One-period sinusoidal pulse but in this case, the converter that is going to work as exciter is the other one than in the previous section. For this reason, the hydrophones are placed "after" the bending.

In Image 7.36 the acquired signals by the hydrophones when a one-period sinusoidal wave of frequency $f = 400Hz$ is shown. It is possible to see the same multiple reflection effects that were shown and explained in the section 7.3.1.2. Therefore, what is going to be measured is also the first peak of the signal in the first transient.
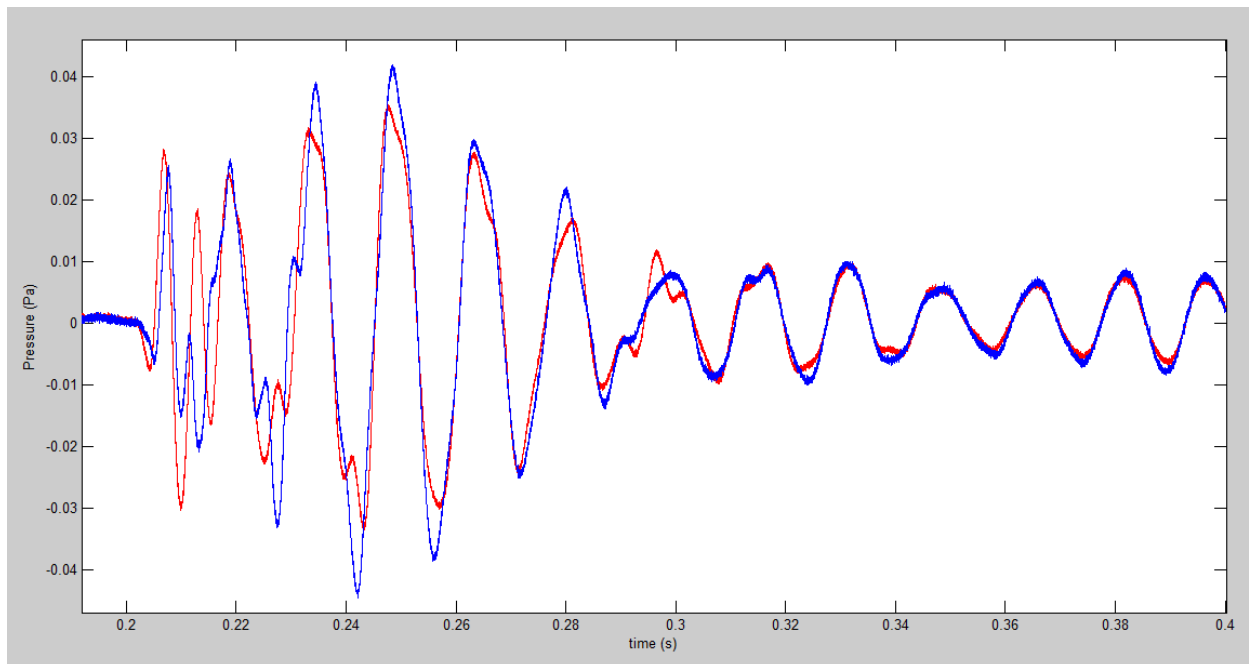
Image 7.36: Obtained waves by the hydrophones after the bending when a one-period sinusoidal pulse is applied.

In Image 7.37 the obtained waves in this case after been filtered are shown. Besides, the two points that are used to measure the group velocity are highlighted.

In Image 7.38 and in Table 7.6 the values obtained for the group velocity after the bending are displayed.
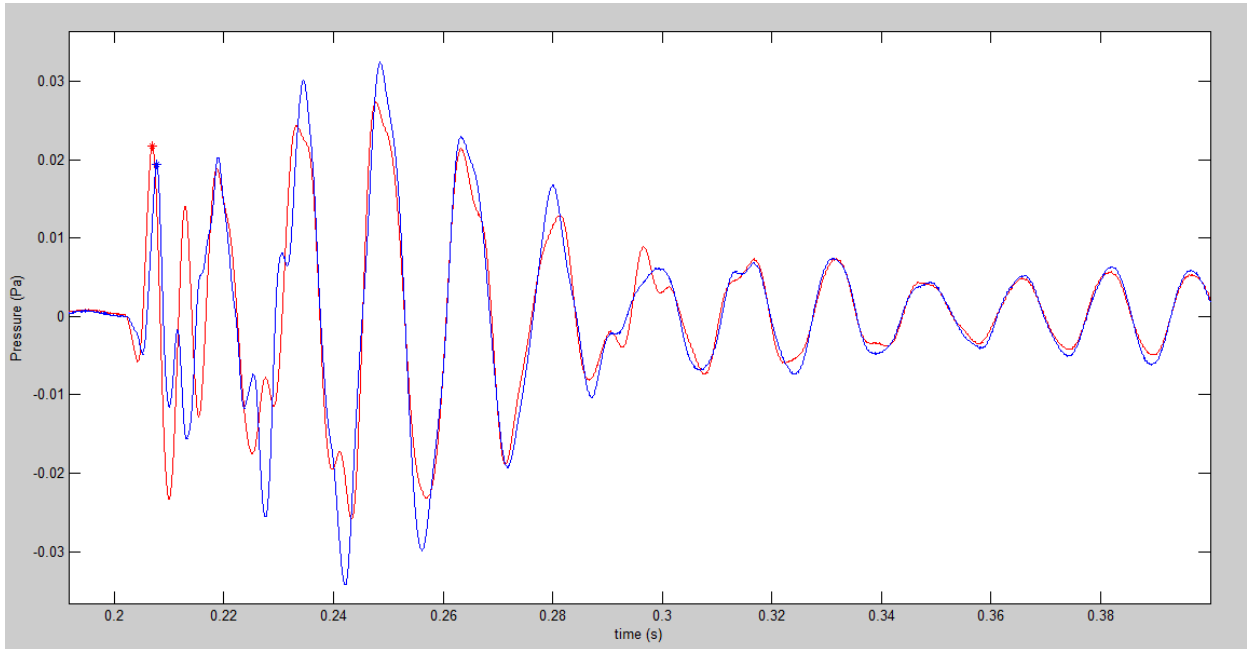


Image 7.37: Obtained signals after filtering the waves acquired by the hydrophones after the bending when a one-period sinusoidal pulse is applied.
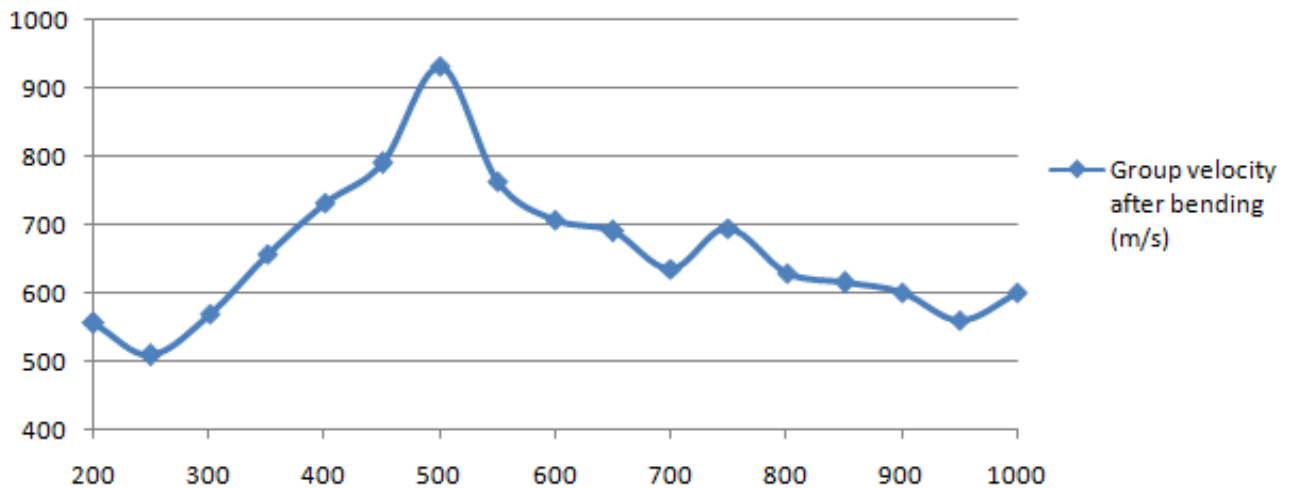
Image 7.38: Group velocity on frequency dependency after the bending

Frequency (Hz)	Group velocity (m/s)
200	555,5556
250	508,4746
300	569,6203
350	656,9343
400	731,7073
450	790,2639
500	931,9664
550	763,4753
600	707,5138

Frequency (Hz)	Group velocity (m/s)
650	689,6552
700	636,0424
750	694,9807
800	629,3706
850	614,7541
900	601,6043
950	559,7015
1000	600

Table 7.6: Exact values for the group velocity after the bending on frequency dependency.

7.4. Comparison

In Image 7.39, the group velocities before and after the bending and the group velocity in the straight pipe which have been obtained during the experiments in this thesis are shown all together in order to compare the different curves.
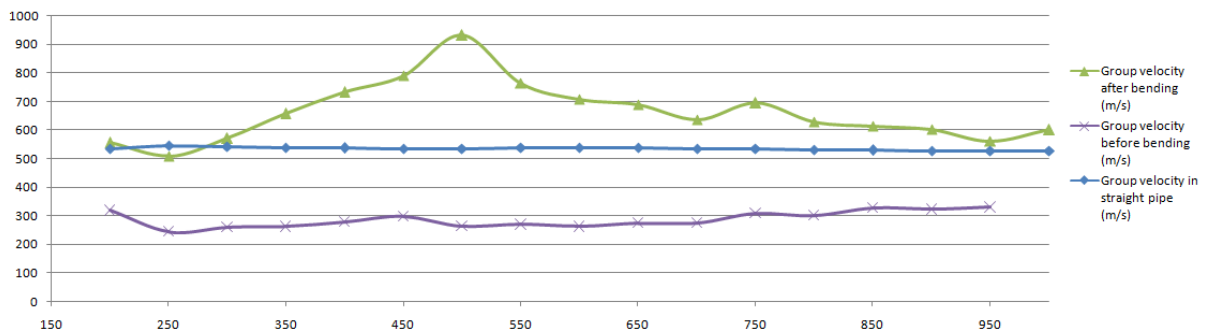
Image 7.39: Comparison among the group velocities after and before the bending of the pipe.

To start with, what is really noticeable is that the group velocity before the bending and in the straight pipe look the same because they are always close to a same value. There is a gap that is approximately the same between the group velocity before the bending and in the straight pipe, which has a value of about 200m/s. However, the velocity in the straight pipe has a negative slope, whereas the one before the bending is positive.

Comparing the velocities within the pipe, it is possible to see that the group velocity before the bending is much lower than after the bending. The two curves look quite different, since the one for the velocity after the bending starts with values of 500m/s for low frequencies, it increases until values of about 900m/s when the frequency is of 500Hz, and then it starts decreasing the velocity until the last values of the range of frequencies which has been tested. Furthermore, the first values of the group velocity after and before the bending must not be taken into account because in low frequencies the effect of the interferences with the net frequency and other noise is very noticeable.

The reason why the group velocity after the bending and the group velocity in the straight pipe have similar values could be due to the position of the pipe. The pipe tested has the same diameter in both experiments, but the sound reaches the hydrophones in the straight pipe and after the bending in the same way. That is to say, the position of this part of the pipe is vertical and the sound arrives from the bottom in both tests. Due to this fact, the velocity in both cases could have similar values. Besides, when the hydrophones are working to measure the velocity before the bending, the sound arrives from the top of the pipe and, thus, this fact could change the measured velocity.

8. Conclusions

Theoretical overview of acoustics, explanation of what group and phase velocities are and how to measure them discussing different methods and their application with MATLAB, simulations for PVC pipes with different diameters and different shapes (straight pipe and bent pipe), and validation of the obtained results by simulation by doing tests in the laboratory have been presented in this current thesis.

It has been proved that even though there are many methods to measure group and phase velocities within pipes, not all of them can be used obtaining a good result. Almost all of them have problems when there is noise in the acquired signals and it is necessary to use a filter to reduce this noise. The only presented method which does not need a filter is the adjustment by least squares, but it also works better when a filter is applied.

It has also been presented that when a short pipe is tested like the one used in this thesis, the reflection effects are very important and can make impossible to measure velocities. For this reason, in laboratory tests, it has been tried to avoid the reflection effects by measuring the velocities in the first peak of the first transient acquired by the hydrophones when a short pulse is applied. This method has resulted to be the only method that works well in every situation since it is not affected by reflection effects. When other signals were applied and phase velocity wanted to be measured, the reflection effects caused so much distortion in the acquired signals due to the interferences of different signals that the results obtained were wrong. It was tried to split the signal according to its spectrum in order to measure group velocity and phase velocity for different frequencies but it was not possible due to the mentioned fact. Therefore, the conclusion after performing the measurements in the lab is that the method that best works for measuring velocities is the one that measures the time delay between the first peak in the first transient in the two acquired signals by the hydrophones.

The reflections were much more noticeable in the case of the bent pipe due to the fact that waves were reflected on the bending producing many secondary waves that were propagated within the pipe and creating interferences with the original signal. These secondary waves were not only superposed with this original signal, but also with the other secondary waves reflected on the boundaries of the pipe. For this reason, it has been more difficult to measure velocities in the bent pipe than in the straight pipe. However, when applying the method of the first peak in the first transient everything was working properly and the reflection effects did not cause any wrong results.

8.1. Further research

In order to see if the results presented in this thesis after the measurements were affected for reflection effects, it would be a good idea to test pipes with different lengths. If the obtained velocity does not change when the length changes, it is possible to say that the reflection effects are not important in those measurements and that the obtained results are reliable. However, if these results change, it would be necessary to investigate a different method to measure velocities within a pipe. Nevertheless, it is quite likely that the results would not change when changing the length of the pipe since the tests were done in order to avoid these effects, but it is always important to verify the results with a different way.

As a pipe with a different diameter was also simulated, it would be interesting to measure velocities in a pipe with different diameters and compare the changes in order to find a law that relates the diameter of the pipe with the group and phase velocity.

As this thesis was only focused in water-filled pipes, it would be possible line of further research to fill a pipe with different liquids such as oil, which is very used in the industry, or a mix of different components. Changing the filling liquid, the obtained results for velocities may change considerably since sound propagation velocity depends on the fluid in which it is propagated.

Furthermore, this thesis has only presented the measurement of velocities at low frequencies, so it would be good to amplify the range of frequencies to higher ones and deal with the different modes that may occur in these frequencies. Besides, in the industry, many materials are used to construct pipes, so it would be also a further research to measure velocities in pipes of different materials and in non-elastic pipes to see the big change that may occur comparing this kind of pipes with the one used in this thesis.

To sum up, much work is yet to be done, but the experiments and methods developed in this thesis may offer researchers a few small stepping stones on their path toward a better understanding of the curious compounds we call waveguides.

Appendices

Appendix A. MATLAB Scripts

A. 1. Propagation of a wave in a non-dispersive medium

```matlab
%% Movie that shows the move of a wave modulated in amplitude in a non-
%dispersive medium

t=100; %time elapse that is going to be shown
x=linspace(0,100,400); %definition of the x points

for j = 1:t
    %calculate the value of the wave
    A=2*2*cos(0.25*j/10-(1/32)*x);
    y=A.*cos(7.75*j/10-(31/32)*x);
    %plot the graph in this moment
    plot(x,y,'r');
    %create the movie
    F(j)=getframe;
end
movie(F,5); %play the movie

%% Plot the envelope of an amplitude modulated wave in one specific moment

x=linspace(0,100,400); %definition of the x points

%calculate the value of the wave and plot it
A=2*2*cos(0.25*1-(1/32)*x);
y=A.*cos(7.75*1-(31/32)*x);
plot(x,y,'r')
grid on
hold on

%evaluate the envelope wave and plot it
y2=4*cos(0.25*1-(1/32)*x);
plot(x,y2,'b')
```

A. 2. Propagation of a wave in a dispersive medium

```matlab
%% Movie that shows the move of a wave modulated in amplitude in a
% dispersive medium

t=100; %time elapse that is going to be shown
x=linspace(0,100,400); %definition of the x points

for j = 1:t
    %calculate the value of the wave
    A=2*2*cos(0.25*j/10-(2/33)*x);
    y=A.*cos(7.75*j/10-(31/33)*x);
    %plot the graph in this moment
    plot(x,y,'r');
    %create the movie
    F(j)=getframe;
end
movie(F,5); %play the movie
```

A. 3. Noisy waves with which is not possible use the zero-crossing method

```matlab
%% Noisy waves with which is not possible to use the zero crossing
% method

t=0:0.001:3; %time elapse that is going to be shown
y1=cos(10*t+5)+0.1*randn(size(t)); %first wave with gaussian noise
y2=cos(10*t)+0.1*randn(size(t)); %second wave with gaussian noise

%display both waves in the same plot
plot(t,x)
grid on
hold on
plot(t,y,'r')
```

A. 4. Fourier transform

```matlab
function [Xmod, Xang] = fourier_selfmade(x)
%Function that calculates the Fourier transform of a serial of values.
%It returns the absolute value of the Fourier transform and its angle

[~,N]=size(x);
X=zeros(1,N);

for j=0:N-1
    for n=0:N-1
        if (n==0)
            X(j+1)=0+x(n+1)*exp(-2i*pi*j*n/N);
        else
            X(j+1)=X(j+1)+x(n+1)*exp(-2i*pi*j*n/N);
        end
    end
end

Xmod=abs(X);
Xang=unwrap(angle(X))*180/pi;
```

A. 5. Phase velocity with the method of phase shift

```matlab
%% Fourier transform of two waves to measure the phase velocity with the
% method of the phase shift

Fs=1000; %sample frequency
t=0:1/Fs:0.2; %time elapse

x=cos(2*pi*10*t);
y=cos(2*pi*10*t+1.5);

[Xmod, Xang] = fourier_selfmade(x);
[Ymod, Yang] = fourier_selfmade(y);

f=(0:N/2-1)*Fs/N; %range of frequencies that are going to be displayed

%plot the three graphs for the two waves
subplot(3,1,1), plot(t,x,'r'), hold on, plot(t,y,'b')
subplot(3,1,2), plot(f,Xmod(1:N/2),'r'), hold on, plot(f,Ymod(1:N/2),'b')
```

```
subplot(3,1,3), plot(f,Xang(1:N/2),'r'), hold on, plot(f,Yang(1:N/2),'b')
```

A. 6. Group velocity with two envelope waves

```
%example of two envelope waves to calculate the group velocity

t=-10:0.001:10; %time elapse
x1=1; x2=10; %two different positions

%calculation of the values
A=2*2*cos(0.25*t-(2/33)*x1); %envelope for the first wave
a=A.*cos(7.75*t-(31/33)*x1); %first wave
B=2*2*cos(0.25*t-(2/33)*x2); %envelope for the second wave
b=B.*cos(7.75*t-(31/33)*x2); %second wave

%display the waves
plot(t,a,'r')
hold on, grid on
plot(t,A,'r','linewidth',2)
plot(t,b,'b')
plot(t,B,'b','linewidth',2)
```

A. 7. Group velocity with cross-correlation

```
%calculate the cross-correlation of two waves so as to obtain the group
%velocity

m=4; %chosen m (it could be any)
w=0.25; %angular frequency
t=0:0.01:m*pi/(w*2); %time elapse
x1=1; x2=10; %two different points

%calculate the values of the waves
A=2*2*cos(0.25*t-(2/33)*x1); %envelope for the first wave
a=A.*cos(7.75*t-(31/33)*x1); %first wave
B=2*2*cos(0.25*t-(2/33)*x2); %envelope for the second wave
b=B.*cos(7.75*t-(31/33)*x2); %second wave


%calculate the cross-correlation
N=size(a);
cxy=zeros(1,1000);
p=0;
for k=1:1000
    for i=0:0.01:m*pi/(w*2)
        cxy(k)=cxy(k)+2*2*cos(w*i-(2/33)*x1)*2*2*cos(w*i-(2/33)*x2-k/100);
    end
end

[~,s]=max(cxy); %maximum value of the cross-correlation

%draw all the waves
subplot(2,1,1)
plot(t,a,'r')
hold on, grid on
plot(t,A,'r','linewidth',2)
plot(t,b,'b')
plot(t,B,'b','linewidth',2)
```

```matlab
%prove that the value in which the maximum of the cross-correlation is
%reached is the correct one. Both envelopes must be the same.
C=2*2*cos(w*t-(2/33)*x2-s/100);
%draw the calculated wave according to the result of the cross-correlation
plot(t,C,'g','linewidth',2), xlim([1 25])

%display the cross-correlation
subplot(2,1,2), stem((1:1000)/100,cxy), grid on
```

A. 8. Calculation of the relationship between the main frequency and the second one

```matlab
%Calculate and plot the relationship between the main frequency and the
second one
%Initial values
f=450; A10=500; phi10=2; A20=400; w2=490; phi2=0;
f0=[490 514 500 450 400];

x0=[56 50 44 44 56]; %probes that are going to be used

j=1; k=1;

for i=2:3201:12806

    x=a(i+500:1:i+3200,2);
    y=a(i+500:1:i+3200,x0(j));

%initial values
    w2=f0(j);
    u0=[A10 phi10 A20 w2 phi2];

%finding the function that best fits the values
    [u,f]=fminsearch(@(u) fobj(u,x,y),u0);

    f2(j)=u(4); %vector of "second" frequencies

%drawing
    z=u(1)*cos(450*2*pi*x+u(2))+u(3)*cos(u(4)*2*pi*x+u(5));
    subplot(3,2,j)
    plot(x,y,'b'), grid on, hold on, plot(x,z,'r'), title(k)
    xlabel('Time (s)'), ylabel('Pressure (Pa)');
    j=j+1;
    k=k+0.5;

end
subplot(3,2,6), plot(1:0.5:3,f2,'*'), grid on, xlabel('Length (m)'),
ylabel('Frequency (Hz)')
```

A. 8. 1. Functions used to find the adjustment

```matlab
function z=f01(u,x)
%A1*cos(w1*t+phi1)+A2*cos(w2*t+phi2);

z=u(1)*cos(450*2*pi*x+u(2))+u(3)*cos(u(4)*2*pi*x+u(5));
```

```matlab
function z=fobj(u,x,ym)
%method of least squares

ycal=f01(u,x);
z=sum((ym-ycal).^2);
```

A. 9. Fourier transform for different waves for different lengths

```matlab
%% Fourier transform for different waves for different lengths

a=xlsread('Name_of_the_file_with_results.xlsx');
j=1; %counter

for i=2:3201:12806
    Fs=1/(a(4,2)-a(3,2)); %sample frequency
    t=a(i+500:1:i+3200,2);%row that has the time values
    x=a(i+500:1:i+3200,x0(j));%row that has the values of the wave

    [N,~]=size(x);

    %calculate Fourier transform
    [Xmod, Xang] = fourier_selfmade(x);

    f=(0:N/2-1)*Fs/N; %range of frequencies that are going to be shown

    %display the graph in every loop
    subplot(3,2,j), plot(f,Xmod(1:N/2),'r'), hold on,xlim([0 1000])
    xlabel('Frequency (HZ)'), ylabel('Fourier transform')

    j=j+1;
end
```

A. 9. Calculate the phase velocity from the measurements

```matlab
%%Calculate the phase velocity from the results obtained in measurement

data_400=xlsread('Name_of_the_file_with_results.xlsx');
freq=700; %frequency of the exciter

t=data_400(:,3); %row for the time
x1=data_400(:,1); %row for the data of the first point
x2=data_400(:,2); %row for the data of the second pint
Fs=data_400(3,6); %sample frequency

%draw the two obtained waves
plot(t,x1,'b'), hold on, plot(t,x2,'r'), grid on, grid minor
xlabel('time (s)'), ylabel('Pressure (Pa)')

%open a different window to draw the two obtained waves in different plots
%and the selected part to measure the phase velocity
figure
subplot(2,1,1), plot(t,x1,'b'), xlabel('time (s)'), ylabel('Pressure
(Pa)')
```

```matlab
subplot(2,1,2), plot(t,x2,'b'), xlabel('time (s)'), ylabel('Pressure (Pa)')

%select the data after the first transient part and before the second one
t=data_400(75000:1:130000,3);
x1=data_400(75000:1:130000,1);
x2=data_400(75000:1:130000,2);

%draw the selected part of the waves
subplot(2,1,1), hold on, plot(t,x1,'r')
xlabel('time (s)'), ylabel('Pressure (Pa)')
subplot(2,1,2), hold on, plot(t,x2,'r')
xlabel('time (s)'), ylabel('Pressure (Pa)')

%adjust the selected part to sinusoidal waves
u0=[0    0.01  freq   -pi/2]; %initial value

u1=adjust2sinus(u0,t,x1);

u0=[0    0.015   freq pi];

u2=adjust2sinus(u0,t,x2);


%calculate the waves that best fit to the obtained waves with the found
%results

x1adj=f01(u1,t);
x2adj=f01(u2,t);

%open two different windows to see how good the adjustment is
figure
plot(t,x1adj,'b'), hold on, plot(t,x1,'r')
xlabel('time (s)'), ylabel('Pressure (Pa)')

figure
plot(t,x2adj,'b'), hold on, plot(t,x2,'r')
xlabel('time (s)'), ylabel('Pressure (Pa)')

%calculate the phase velocity
phase_delay = u2(4)+2*pi-u1(4);
time = phase_delay/(2*pi*freq);
phase_velocity=0.45/time;

%open a different window to draw the two adjusted waves and prove that
%the results given are OK
figure, plot(t,x1adj,'r'), hold on, grid on, grid minor
plot(t,x2adj,'b'), xlabel('time (s)'), ylabel('Pressure (Pa)')
```

A. 9. 1. Functions used to calculate the adjustment

```matlab
function u1=adjust2sinus(u0,t,x)
%return the values of the sinusoidal wave that best fits to the given wave

[u1,~]=fminsearch(@(u) fobj(u,t,x),u0); %find the values
```

```matlab
%the angle has to be between -pi and +pi
while (u1(4)>pi || u1(4)<-pi)
    if (u1(4)>pi)
        u1(4)=u1(4)-2*pi;
    end
    if (u1(4)<-pi)
        u1(4)=u1(4)+2*pi;
    end
    u1(4);
end
```

```matlab
function y=f01(u,t)
%A+B*cos(2pi*f*t+phi)

y = u(1)+u(2)*cos(2*pi*u(3)*t+u(4));
```

```matlab
function z=fobj(u,t,ym)
%method of least squares

ycal=f01(u,t);
z=sum((ym-ycal).^2);
```

A. 10. Calculate group velocity from a long Gaussian pulse

```matlab
%Calculate group velocity from the results obtained stimulating the pipe
% with a long Gaussian pulse

results=xlsread('Name_of_the_file.xlsx');

x1=results(:,1); %column for the first probe
x2=results(:,2); %column for the second probe
t=results(:,3); %column for the time
Fs=1/(t(3)-t(2)); %sample frequency

%draw the two obtained waves
figure,plot(t,x1,'r'), hold on, plot(t,x2,'b')
xlabel('Time(s)'), ylabel('Pressure(Pa)')

%filter the obtained waves to reduce the noise and display this result
x1=filter(filter500,x1);
x2=filter(filter500,x2);
figure,plot(t,x1,'r'), hold on, plot(t,x2,'b')
xlabel('Time(s)'), ylabel('Pressure(Pa)')

%calculate the envelope of the filtered waves
xan = hilbert(x1); %analytical signal for the first wave
env1 = abs(xan); %envelope signal for the first wave
xan2 = hilbert(x2); %analytical signal for the second wave
env2 = abs(xan2); %envelope signal for the second wave

%calculate the functions that best fit the envelope waves
```

```matlab
u0=[0.08    0.2    0.05]; %initial values
[u1,~]=fminsearch(@(u) fobj(u,t,env1),u0);
u0=[1 1 1];
[u2,~]=fminsearch(@(u) fobj(u,t,env2),u0);


f1=f01(u1,t);
f2=f01(u2,t);


%obtain the maximum values of the envelope to determine the group velocity
[~,t1]=max(f1);
[~,t2]=max(f2);
t1=t(t1);
t2=t(t2);
time = t2-t1;
group_velocity=0.45/time;


%display the envelope waves and the filtered waves to see how good the
%adjustment is
figure
subplot(2,1,1), plot(t,env1,'b'), hold on, plot(t,x1,'r')
plot(t,f1,'LineWidth',2,'Color','g')
xlabel('Time(s)'), ylabel('Pressure(Pa)')

subplot(2,1,2), plot(t,env2,'b'), hold on, plot(t,x2,'r')
plot(t,f2,'LineWidth',2,'Color','g')
xlabel('Time(s)'), ylabel('Pressure(Pa)')
```

A. 11. Calculate group velocity from a short Gaussian pulse

```matlab
%%Calculate group velocity from the results obtained stimulating the pipe
% with a short Gaussian pulse

results=xlsread('Name_of_the_file_with_results.xlsx');
x1=results(:,1); %column for the first probe
x2=results(:,2); %column for the second probe
t=results(:,3); %column for the time

Fs=1/results(3,6); %sample frequency

%draw the original signals
figure, plot(t,x1,'r'), hold on, plot(t,x2,'b')
xlabel('time (s)'),ylabel('Pressure (Pa)')

%filter the original signals and display them
x1=filter(filter500,x1);
x2=filter(filter500,x2);
figure, plot(t,x1,'r'), hold on, plot(t,x2,'b')
xlabel('time (s)'),ylabel('Pressure (Pa)')

%find the maximum values of the filtered signals
[~,t1]=max(x1);
t1=t(t1);


[~,t2]=max(x2);
t2=t(t2);

%calculate the time delay between the maximum values
time_delay=t2-t1;
```

```
%calculate the group velocity
group_velocity=0.45/time_delay;
```

A. 12. Group velocity before bending with one-period sinusoidal pulse

```
%%Calculate phase velocity from the results obtained stimulating the pipe
% with a one-period sinusoidal pulse

results=xlsread('Name_of_the_file_with_results.xlsx');
x1=results(:,1); %column for the first probe
x2=results(:,2); %column for the second probe
t=results(:,3); %column for the time

Fs=1/results(3,6); %sample frequency

%draw the original signals
figure, plot(t,x1,'r'), hold on, plot(t,x2,'b')
xlabel('time (s)'),ylabel('Pressure (Pa)')

%filter the original signals and display them
x11=filter(filter_lowpass,x1);
x22=filter(filter_lowpass,x2);
figure, plot(t,x11,'r'), hold on, plot(t,x22,'b')
xlabel('time (s)'),ylabel('Pressure (Pa)')

%select the range in which the first transient is
p=find(t>0.205 & t<0.21);
p1=x11(p);
p2=x22(p);

%find the maximum values of the filtered signals
[~,s1]=max(p1);
t1=t(s1+p(1))

[~,s2]=max(p2);
t2=t(s2+p(1))

%print the selected points
plot(t1,x11(s1+p(1)),'r*')
plot(t2,x22(s2+p(2)),'b*')

%calculate the time delay between the maximum values
time_delay=t1-t2

%calculate the phase velocity
phase_velocity=0.45/time_delay
```

Appendix B. Filters

B. 1. FIR Equiripple

The Equiripple method approaches filter design as an optimization problem in which the coefficient values are adjusted to create an optimal filter with ripples that are of equal height. This method uses the most efficient optimization procedure to minimize the transition width along with the stopband and passband ripple.

The Equiripple method uses the Parks-McClellan algorithm to compute the filter such that its response $H(e^{j2\pi f})$ represents the best approximation to the ideal frequency response $H_d(j2\pi f)$ in a manner that minimizes the maximum weighted approximation error (where Q() is the weighting function):

$$\varepsilon(j2\pi f) = \max_{f \in [-0,5; \, 0,5]} \left| Q(j2\pi f) \left[H_d(j2\pi f) - H(e^{j2\pi f}) \right] \right| \qquad \text{Eq. 0.1}$$

In Image 0.1, the filter specifications for a bandpass filter are shown. It is necessary to specify different characteristics to obtain the filter with the MATLAB tool of filter design. In Image 0.2 the frequency response in magnitude is displayed for a bandpass filter for the frequencies between 500 and 600 Hz. It is possible to appreciate that all the frequencies out of that band are removed with a factor of 80dB, and that there are ripples of equal height at it was said above. In Image 0.3 the frequency response in phase is shown and it is also possible to see these ripples out of the band selected. It is also possible to notice the linear response within the selected band.
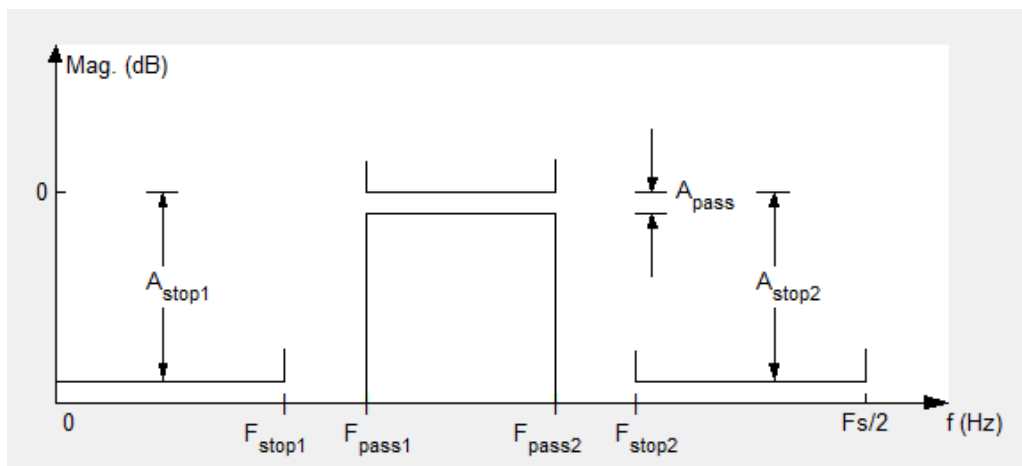

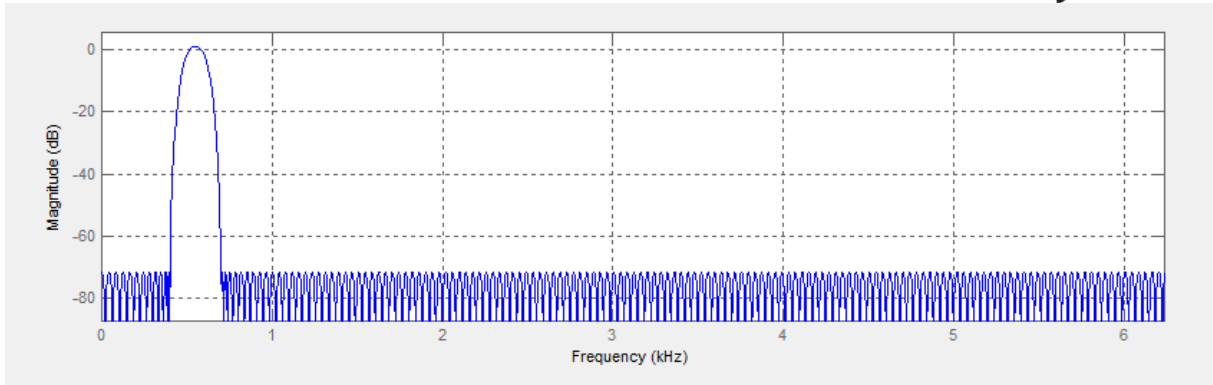Image 0.1: Filter specifications for a bandpass filter.

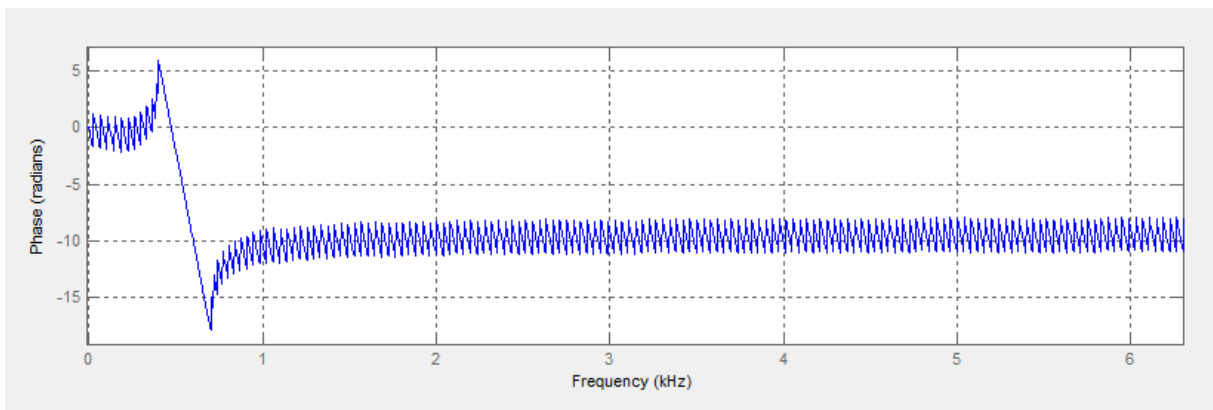**Image 0.2: Magnitude diagram for a Equiripple bandpass filter between 500 and 600 Hz.**

Image 0.3: Phase diagram for a Equiripple bandpass filter between 500 and 600 Hz.
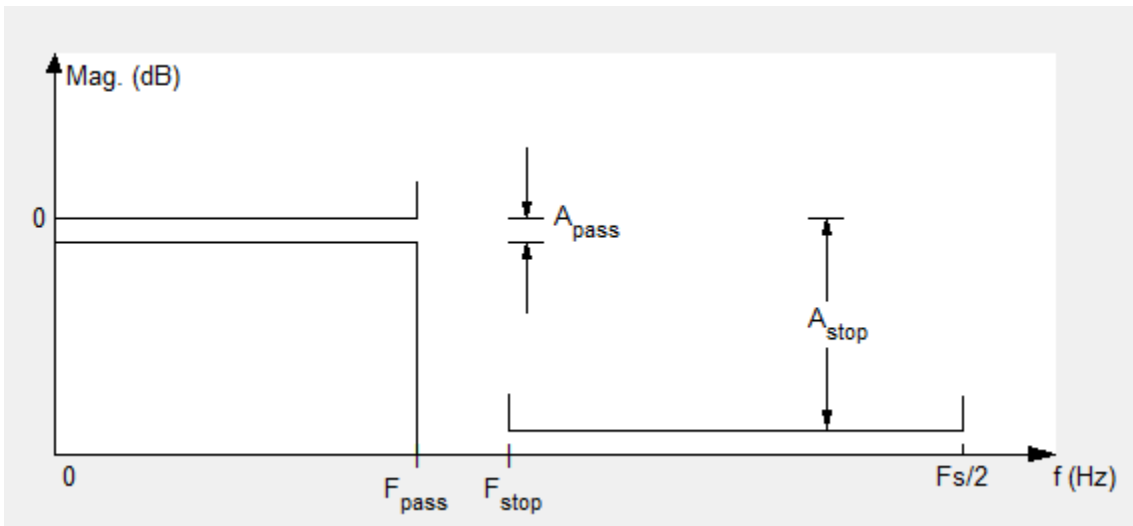

Image 0.4: Filter specifications for a lowpass filter.

In Image 0.4 the specifications needed to obtain a lowpass filter with the MATLAB too fdatool are displayed. It is necessary to specify the cutoff frequency and the magnitude of the factor in charge of removing the components out of the specified band. In Image 0.5 the frequency

response in magnitude is shown and in Image 0.6 the frequency response in phase is displayed. It is also possible to see the same characteristics than in the bandpass filter, but, in this case, the low frequencies are not going to be removed.
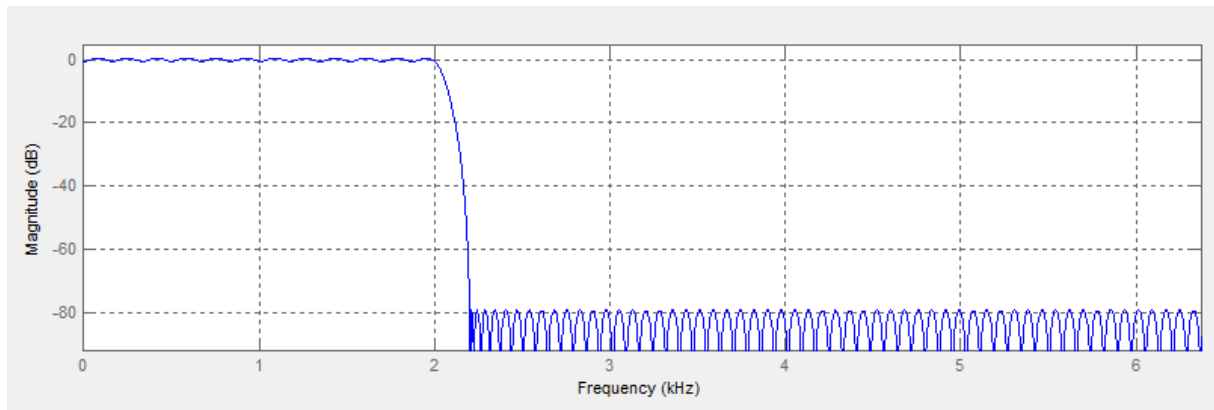

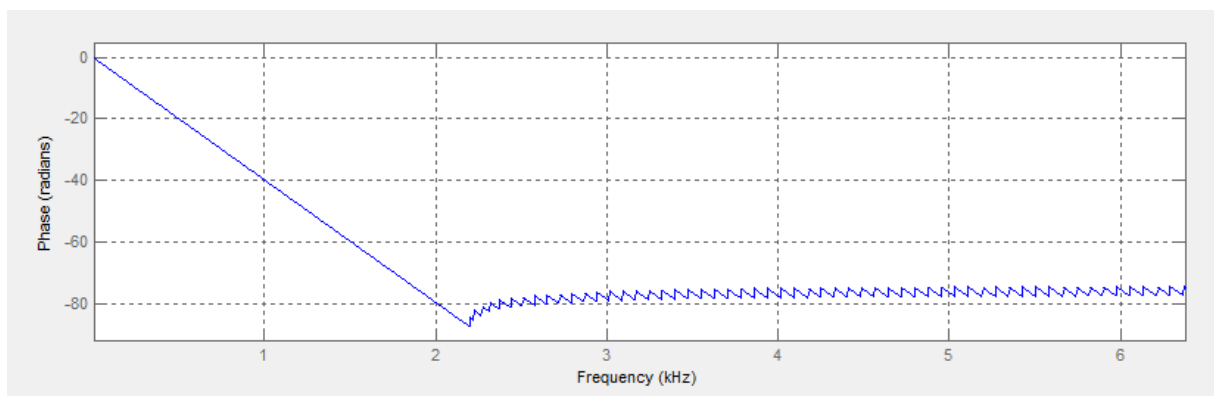**Image 0.5: Magnitude diagram for a Equiripple lowpass filter for 2000 Hz.**

Image 0.6: Phase diagram for a Equiripple lowpass filter for 2000 Hz.

B. 2. IIR Butterworth

The Butterworth method of approximation provides a monotonic performance in the passband and the stopband. As the filter order is increased, the passband and stopband performance improves, with the transition from passband to stopband becoming sharper. The Butterworth method is best suited for design problems that focus on controlling passband and stopband ripple.

A Butterworth lowpass filter with cutoff frequency f_c and order n is specified using the following equation:

$$A_n(f^2) = \frac{1}{1 + \left(\frac{f}{f_c}\right)^{2n}}$$

Eq. 0.2

In Image 0.7 and in Image 0.8 the frequency response in magnitude and in phase for a bandpass filter are displayed. It is important to notice that the factor of removal components is much bigger than in Equiripple. Also, the phase diagram is not linear.
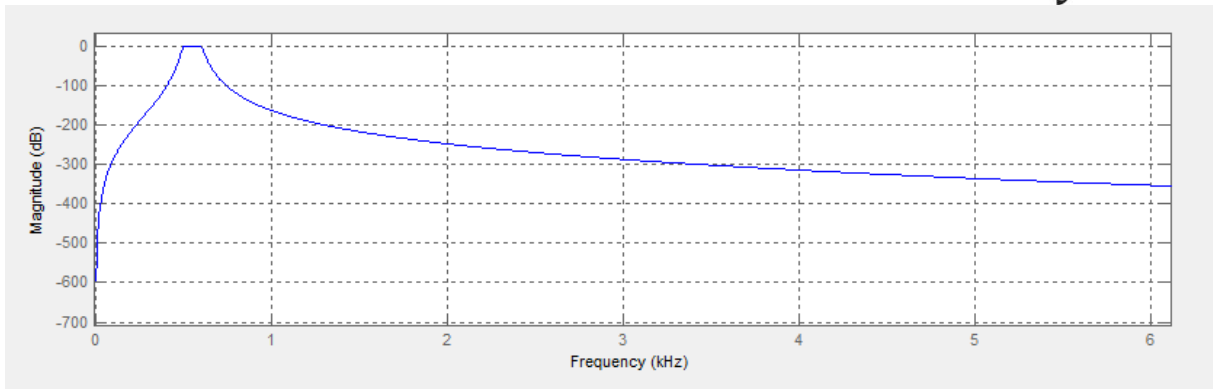
Image 0.7: Magnitude diagram for a Butterworth bandpass filter between 500 and 600 Hz.
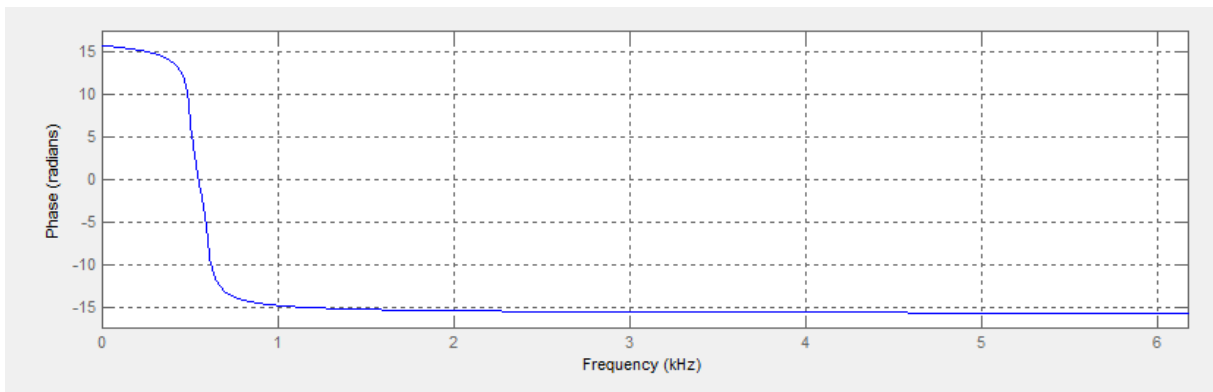

Image 0.8: Phase diagram for a Butterworth bandpass filter between 500 and 600 Hz.

In Image 0.9 and in Image 0.10 the frequency response in magnitude and in phase for a lowpass filter are displayed. The same characteristics than in the bandpass filter can be appreciated.
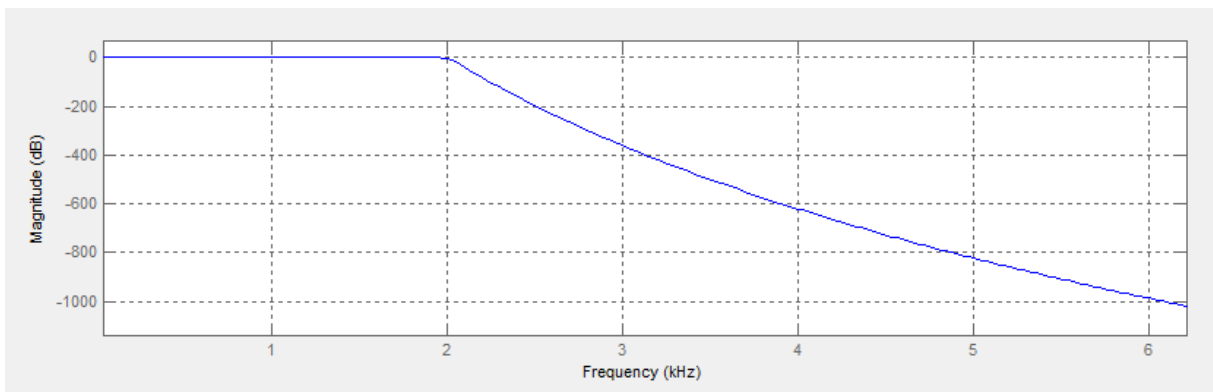

Image 0.9: Magnitude diagram for a Butterworth lowpass filter for 2000 Hz.
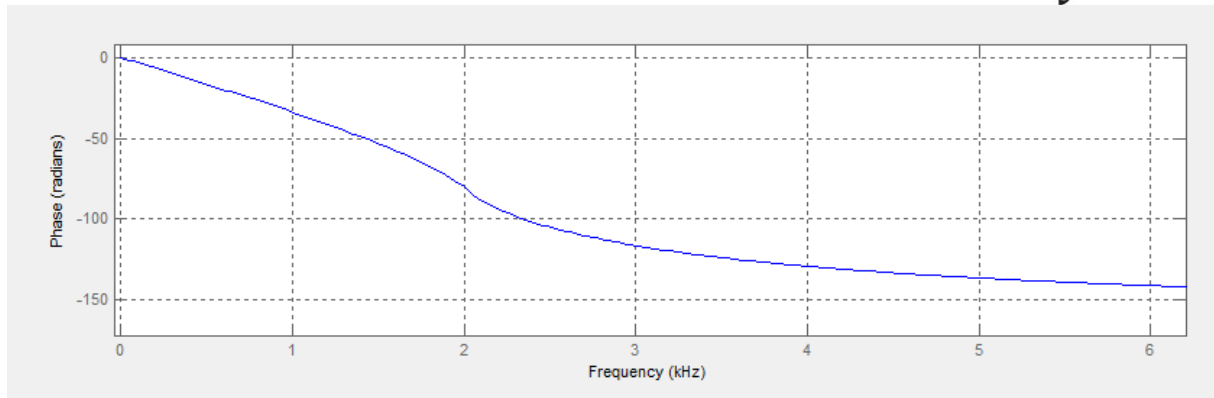
Image 0.10: Phase diagram for a Butterworth lowpass filter for 2000 Hz.

B. 3. IIR Elliptic

The Elliptic method of approximation provides an Equiripple response in both the passband and the stopband. This method uses the smallest filter order for a transition from passband to stopband, but it does so at the cost of some ripple in both bands. As a result, when phase linearity is not an issue, the elliptic method results in a filter with the lowest-order and therefore the least computation overhead.

An Elliptic filter is based on a mapping of the following function:

$$T^2(\omega) = \frac{1}{1 + \varepsilon^2 sn^2(\omega, k)}$$

Eq. 0.3

In Image 0.11 and in Image 0.12 the frequency response for the magnitude is shown. It is clear that the ripple that appears is not the same as the one in Equiripple, as it only appears in the proximity of the cutoff frequencies. In Image 0.14 the frequency response for the phase is displayed. There is a clear non-linearity in this diagram. However, the values for the phase are smaller than in any other case.
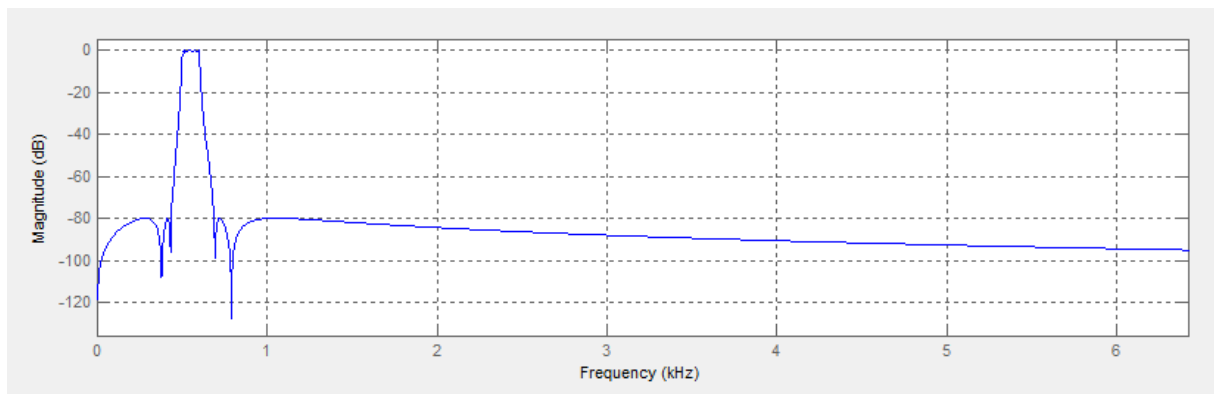

Image 0.11: Magnitude diagram for an Elliptic bandpass filter between 500 and 600 Hz.

113
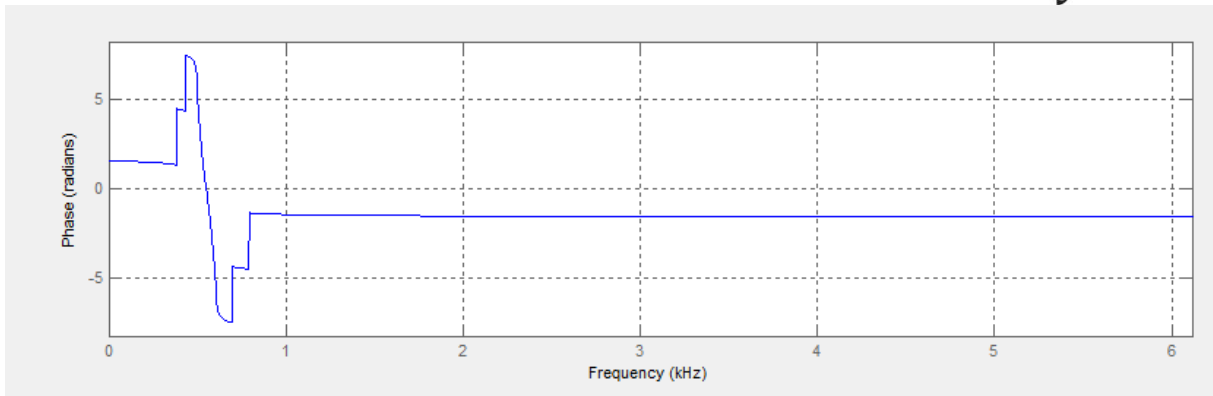
Image 0.12: Phase diagram for an Elliptic bandpass filter between 500 and 600 Hz.

In Image 0.13 the frequency response for the magnitude for a lowpass filter is shown. There are ripples out of the band, which are not the same to each other. In Image 0.14 the frequency response for the phase is displayed. The values for this diagram are also much lower than in the rest of the cases and it could be possible to use this filter when a small phase shift is needed.

Image 0.13: Magnitude diagram for an Elliptic lowpass filter for 2000 Hz.
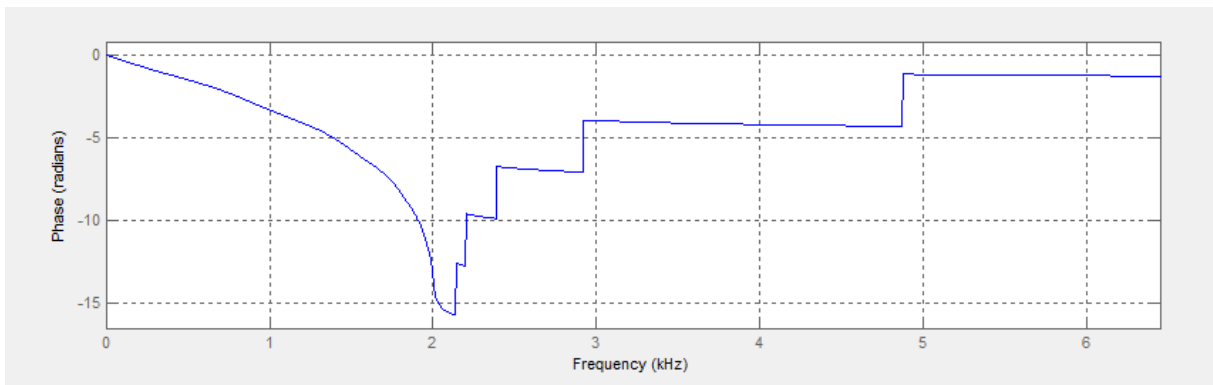
Image 0.14: Phase diagram for an Elliptic lowpass filter for 2000 Hz.

Appendix C. Datasheets

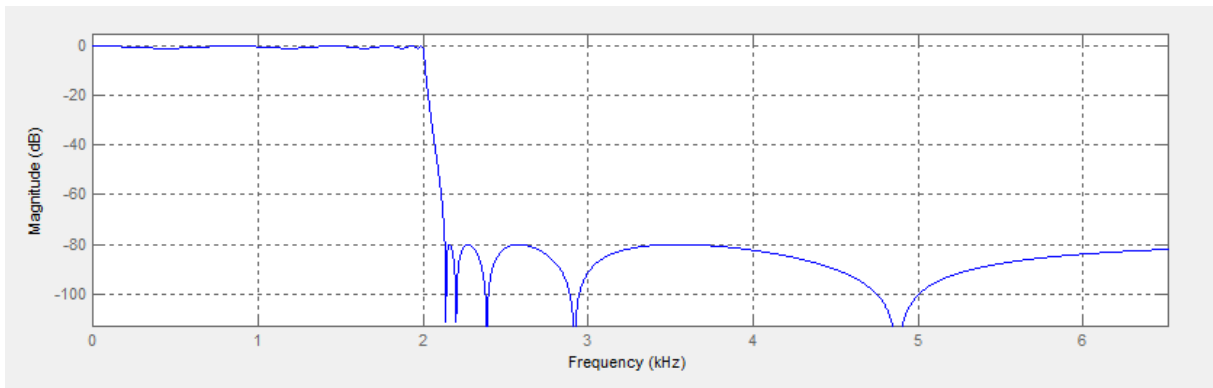**VISATON** GERMANY

BS 76 - 8 Ohm

Art. No . 4511

Körperschallwandler für die Mittel- und Hochtonwiedergabe. Die Montage (mit Schraube M5) erfolgt auf einer schwingfähigen Fläche, die dadurch direkt zum Schwingen angeregt wird. Ein geschlossenes Gehäuse ist nicht notwendig.

Weitere Informationen zu Excitern finden Sie hier: Grundlagen der Exciter-Technologie (PDF; 349 KB)

Structure-borne sound converter for midrange- and high frequencies. The units are attached (with screw M5) to a surface which is able to resonate, which causes it to oscillate. No enclosed cabinet is required.

Please find further information on exciters here: Basic principles of exciter-technology (PDF; 388 KB)

06.05.2013

VISATON
GERMANY

BS 76 - 8 Ohm

Art. No. 4511

Nennbelastbarkeit Rated power	20 W
Musikbelastbarkeit Maximum power	30 W
Nennimpedanz Z Nominal Impedance Z	8 Ohm
Resonanzfrequenz fs Resonance frequency fs	200 Hz
Gewicht netto Net weight	0,41 kg
Länge des Anschlusskabels Length of cable	3 m
Schutzklasse Protective system	IP 68
Temperaturbereich Temperature range	−25 ... 80 °C

06.05.2013

EX 60 S - 8 Ohm

Art. No

. 4506

Elektrodynamischer Exciter zur Anregung von Platten zu Biegewellenschwingungen. Die Befestigung des Exciters auf der Oberfläche der

anzuregenden Platte kann durch Kleben oder Schrauben erfolgen.

Weitere Informationen zu Excitern finden Sie hier: Grundlagen der Exciter-Technologie (PDF; 349 KB)

*) Maximale Langzeit-Eingangsleistung nach DIN EN 60268-5

or screwing.

Electro dynamical exciter for stimulating bending waves on plates. The unit can be attached to the surface of the plate by gluing

Please find further information on exciters here: Basic principles of exciter-technology (PDF; 388 KB)

*) Maximum long term power according to DIN EN 60268-5

Anwendungsmöglichkeiten / **Typical applications**

- Signalausgabe in Anwendungen aller Art, bei denen aus Designgründen oder zum Schutz vor Umwelteinflüssen oder Vandalismus keine sichtbaren Lautsprecher verbaut werden können.

  reasons or for protection against environment

- Signal output in every application where normal speakers can not be installed for optical conditions or vandalism.

06.05.2013

VISATON
GERMANY

EX 60 S - 8 Ohm

Art. No. 4506

Technische Daten / **Technical data**

Musikbelastbarkeit Maximum power	25 W *)
Nennimpedanz Z Nominal Impedance Z	8 Ohm
Schwingspulendurchmesser Voice coil diameter	32,5 mm
Gewicht netto Net weight	0,12 kg
Anschlüsse Connections	4,8 x 0,8 mm (+) 2,8 x 0,8 mm (−)
Temperaturbereich Temperature range	−25 ... 70 °C

06.05.2013

VISATON GERMANY

EX 45 S - 8 Ohm

Art. No
. 4501

Elektrodynamischer Exciter zur Anregung von Platten zu Biegewellenschwingungen. Die Befestigung des Exciters auf der Oberfläche der

anzuregenden Platte kann durch Kleben oder Schrauben erfolgen.

Weitere Informationen zu Excitern finden Sie hier: Grundlagen der Exciter-Technologie (PDF; 349 KB)

*) Maximale Langzeit-Eingangsleistung nach DIN EN 60268-5

Electro dynamical exciter for stimulating bending waves on plates. The unit can be attached to the surface of the plate by gluing or screwing.

Please find further information on exciters here: Basic principles of exciter-technology (PDF; 388 KB)

*) Maximum long term power according to DIN EN 60268-5

Anwendungsmöglichkeiten **/ Typical applications**

- Signalausgabe in Anwendungen aller Art, bei denen aus Designgründen oder zum Schutz vor Umwelteinflüssen oder Vandalismus keine sichtbaren Lautsprecher verbaut werden können.
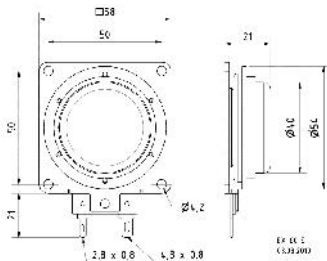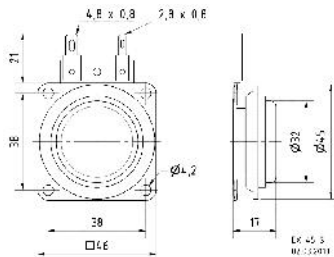
- Signal output in every application where normal speakers can not be installed for optical reasons or for protection against environment conditions or vandalism.

06.05.2013

GERMANY
VISAT**O**N®

EX 45 S - 8 Ohm

Art. No. 4501

Musikbelastbarkeit Maximum power	10 W *)
Nennimpedanz Z Nominal Impedance Z	8 Ohm
Schwingspulendurchmesser Voice coil diameter	25,4 mm
Gewicht netto Net weight	0,06 kg
Anschlüsse Connections	4,8 x 0,8 mm (+) 2,8 x 0,8 mm (−)
Temperaturbereich Temperature range	−25 ... 70 °C

06.05.2013

References

[1] Robert Novelline,.: Harvard University Press, 1997, pp. 34-35.

[2] J. F. Corso, "Bone-conduction thresholds for sonic and ultrasonic frequencies," in *Journal of the Acoustical Society of America 35*., 1963, ch. 11, pp. 1738–1743.

[3] N. J. Hangiandreou, "Physics Tutorial for Residents: Topics in US: B-mode US: Basic Concepts and New Technology – Hangiandreou," in *Radiographics 23*., 2003, ch. 4.

[4] Western Electric Company Co.,., 1969, ch. 2.

[5] Rıza Atav, *The Use of New Technologies in Dyeing of Proteinous Fibers*. Turkey: Namık Kemal University, Textile Engineering Department.

[6] Robert Bruce Lindsay, *What is acoustics?*, 2010.

[7] E.W. Weisstein, *Wave velocity*.: ScienceWorld, 2009.

[8] A.E.H. Love, *A Treatise on The Mathematical Theory of Elasticity*. New York: Dover.

[9] T. H. Ellison, *The propagation of sound waves through a medium with very small random*. Cambridge.

[10] Douglas D. Reynolds, *Engineering Principles in Acoustics*. Boston: Allyn and Bacon Inc., 1981.

[11] Boyce/ Di Prima, *Ecuaciones diferenciales y problemas con valores en la frontera*. México: Editorial Limus, 1981, p. 585.

[12] Chr. Huygens, *Traitė de la Lumiere*. Leyden, 1690.

[13] Diffraction physics, *John M. Cowley*. Amsterdam, 1975.

[14] A. Fresnel, "Ann Chim et Phys," in *Oeuvres*., 1816, vol. 1, ch. 89, p. 129.

[15] Julius Adams Stratton, *Electromagnetic Theory*.: McGraw-Hill, 1941.

[16] John Lekner, *Theory of Reflection, of Electromagnetic and Partivle Waves*.: Springer, 1987.

[17] Ibn Sahl, *On Burning Mirrors and Lenses*. Baghdad, 984.

[18] V.A. del Grosso, "Analysis of multimode acoustic propagation in liquid cylinders with realistic boundary conditions – Application to sound speed and absorption measurements," in *Acustica*.: S. Hirzel Verlag, 1971, vol. 24, p. 299.

[19] Joseph Fourier, *Théorie analytique de la chaleur*. Paris: Firmin Didot Père et Fils, 1822.

[20] James W. Cooley and John W. Tukey, "An Algorithm for the Machine Calculation of Complex Fourier series," in *Mathematics of Computation*.: American Mathematical Society, 1965, vol. 19, ch. 90, pp. 297-301.

[21] David Hilbert, *Grundzüge einer allgemeinen Theorie der linearen Integralgleichungen*.: Chelsea Pub. Co., 1953.

[22] Subhash Kak, "The discrete Hilbert transform," in *The discrete Hilbert transform*.: IEEE, 1970, pp. 585-586.

[23] S. L. Marple, "IEEE Transactions on Signal Processing," in *Computing the Discrete-Time Analytic Signal via FFT*., 1999, vol. 47, pp. 2600-2603.

[24] Inc Agilent Technologies, "Digital Filter Designer," in *Advanced Design System 1.5*., 2000, ch. 4. [Online]. http://cp.literature.agilent.com/litweb/pdf/ads15/dfilter/df044.html

[25] Elena Punskaya. Design of FIR Filters. [Online]. http://www.vyssotski.ch/BasicsOfInstrumentation/SpikeSorting/Design_of_FIR_Filters.pdf

[26] University of Colorado. College of Engineering & Applied Science. FIR Filters. [Online]. http://www.eas.uccs.edu/wickert/ece2610/lecture_notes/ece2610_chap5.pdf

[27] University of Colorado. College of Engineering & Applied Science. IIR Filters. [Online]. http://www.eas.uccs.edu/wickert/ece2610/lecture_notes/ece2610_chap8.pdf

[28] Elena Punskaya. Design of IIR Filters. [Online]. http://www.fisika.ub.ac.id/web/sites/default/files/L08-Design%20of%20IIR%20Filter.pdf

[29] Joseph L. Rose, "Appendix D," in *Ultrasonic Guided Waves in Solid Media*. New York: Cambridge University Press, 2014.